DISSERTATION

PHYSIOLOGICAL AND BIOCHEMICAL MECHANISMS BEHIND THE FAST ACTION

OF GLUFOSINATE

Submitted by

Hudson Kagueyama Takano

Department of Bioagricultural Sciences and Pest Management

In partial fulfillment of the requirements

For the Degree of Doctor of Philosophy

Colorado State University

Fort Collins, Colorado

Fall 2019

Doctoral Committee:

      Advisor: Franck E. Dayan
      Co-advisor: Philip Westra

      Anireddy Reddy
      Christopher Preston
      Todd Gaines

ABSTRACT

PHYSIOLOGICAL AND BIOCHEMICAL MECHANISMS BEHIND THE FAST ACTION

OF GLUFOSINATE

Glufosinate is one of the few herbicides that are still effective for controlling herbicide resistant weeds, but its performance is often inconsistent and affected by environmental conditions. It inhibits glutamine synthetase (GS) by competing with glutamate for the active binding site. Unlike other amino acid biosynthesis inhibitors, glufosinate is a fast-acting herbicide and susceptible plants develop visual symptoms within a few hours after treatment. Inhibition of GS leads to ammonia accumulation and photosynthesis inhibition, which have traditionally been proposed as the causes of the rapid phytotoxicity. This dissertation presents a new understanding of the mechanism(s) of action of glufosinate and a biochemical approach to improve its herbicidal efficacy. Glufosinate uptake is inhibited by glutamine levels in the plant, and translocation is not affected by the rapid phytotoxicity. Glufosinate translocates primarily through the apoplast (xylem) rather than the symplast (phloem) probably due to its physicochemical properties and the absence of an effective membrane transporter. Glufosinate efficacy is proportional to the herbicide concentration in leaf tissues. Neither ammonia accumulation nor carbon assimilation inhibition are directly associated with the fast action of glufosinate. Instead, rapid phytotoxicity results from a massive light-dependent accumulation of reactive oxygen species (ROS). Inhibition of GS blocks the photorespiration pathway leading to a massive photooxidation damage. Under full sunlight, the excess of electrons is accepted by molecular oxygen leading to ROS generation. These free radicals cause lipid peroxidation, which

ultimately leads to rapid cell death. The addition of protoporphyrinogen oxidase (PPO) inhibitors to glufosinate enhances ROS accumulation and herbicidal activity. This enhanced activity results from protoporphyrin formation at high levels due to a transient accumulation of glutamate, the precursor for chlorophyll biosynthesis. The herbicide combination also showed enhanced activity in the field and may help to overcome the lack of glufosinate efficacy under certain environmental conditions.

ACKNOWLEDGEMENTS

TABLE OF CONTENTS

LIST OF TABLES

BACKGROUND INFORMATION

Discovery and Commercialization

Glufosinate was discovered as a bioactive metabolite from the actinomycetes *Streptomyces hygroscopis* and *S. viridochromogenes* (Bayer et al., 1972; Kondo, 1973). A tripeptide called bialaphos (4-[hydroxy(methyl)phosphinoyl]-L-homoalanyl-L-alanyl-L-alanine) is produced and released by fermentation culture of these microorganisms (Figure B.1). Bialaphos is commercialized in eastern Asia as a broad-spectrum and non-selective herbicide. The tripeptide is actually a pro-herbicide that requires metabolic bioactivation inside plants via a conversion into L-phosphinothricin, the actual phytotoxic molecule (Dayan et al., 2009; Duke et al., 2010).

Glufosinate was first commercialized in the USA and Canada by Bayer CropScience in 1993-1994 as non-selective herbicide with a broad spectrum of weed control. In 2018, BASF Corporation purchased Bayer's global business of Liberty Link® (LL) traits (glufosinate resistance) in multiple crops and glufosinate non-selective herbicide, commercialized under the Liberty®, Basta®, and Finale® brands. The area treated with glufosinate is approximately 12 million ha per year (Busi et al., 2018), with a significant increase in the last decade to manage glyphosate-resistant weeds in LL soybean and LL cotton (Figure B.2). Glufosinate usage is more intense in the Midwest and Southern US where the majority of soybean and cotton are planted. In the Western US, glufosinate is used for weed management in perennial crops such as vineyards and orchards.

Physicochemical Properties

Glufosinate or 2-amino-4-(hydroxymethylphosphinyl)butanoic acid ($C_5H_{12}NO_4P$,

molecular weight: 181.13 g mol^{-1}) belongs to the organophosphorus chemical family. It is

commercialized as a racemic mixture of D,L-phosphinothricin but only the L-isomer has

herbicidal activity (Beriault et al., 1999) (Figure B.3). Glufosinate is highly water soluble (Log

K_{ow}: -4.0) with different ionization constant values (pKa: 2, 2.9, and 9.8). It is not volatile (vapor

pressure: 1.0 x 10^{-4} Pa) and commercial formulations are typically sold as an ammonium salt,

which dissociates once in solution (Shaner, 2014).

Glutamine Synthetase, the Target for Glufosinate

Glufosinate targets glutamine synthetase (GS), the second most abundant protein in plant

leaves (Carvalho et al., 1992; Bernard and Habash, 2009). This enzyme is essential for nitrogen

metabolism by catalyzing the ATP-dependent incorporation of ammonia into glutamate to yield

glutamine (Miflin and Lea, 1976) (Figure B.4). It is a two-step reaction in which glutamate is

phosphorylated in the first step followed by the assimilation of ammonia (Gill and Eisenberg,

2001). Glufosinate is an irreversible inhibitor and competes with glutamate for the active site in

GS (Ridley and McNally, 1985).

Glutamine and α-ketoglutarate are then converted into two glutamate molecules by

glutamine 2-oxoglutarate aminotransferase (GOGAT) (Figure B.5). Thus, in most angiosperm

plant species, ammonia assimilation into nitrogen organic compounds occurs via the

GS/GOGAT cycle. Two main isoforms have been reported in plants, GS1 is located in the

cytoplasm and GS2 functions in the chloroplast (Ishiyama et al., 2004). Because glutamine is a

central amino group donor, GS1 is important for nitrogen export throughout the plant in the form

of glutamine (Bernard and Habash, 2009). In contrast, GS2 plays a key role recycling ammonia

from the photorespiration pathway (Edwards and Coruzzi, 1989). In addition to photorespiration,

ammonia can also come from the activity of nitrate/nitrite reductase to a smaller extent (Weber and Flügge, 2002).

In green leaves of C3 species, GS2 is the predominant isoenzyme but in some C4 and CAM plants, the contribution of GS1 to the total enzyme activity can reach up to 80% (McNally et al., 1983). Loss of function mutants have been described in *Arabidopsis* and barley for GS2 and GOGAT (Blackwell et al., 1987; Somerville and Ogren, 1980). These mutants are unable to grow in normal atmosphere but develop normally under non-photorespiratory conditions, demonstrating the importance of the GS/GOGAT system for the photorespiration pathway. In C4 species, while GS2 has a greater contribution to the total GS activity in bundle sheath cells, GS1 is predominant in mesophyll cells (González-Moro et al., 2000). In addition, both isoforms seem to be slightly more tolerant to glufosinate in the bundle sheath cells than in the mesophyll and GS2 is less sensitive than GS1 (González-Moro et al., 2000).

Genetically Engineered Crops for Glufosinate Resistance

Glufosinate-resistant crops (Liberty Link®) are genetically engineered to metabolize glufosinate by expressing the *phosphinothricin acetyltransferase* (*pat*) gene (also known as the *bar* gene) (Dröge et al., 1992). These plants rapidly convert L-phosphinothricin into *N*-acetyl-L-phosphinothricin, a non-phytotoxic compound (Figure B.6). Overexpression of pat in high levels allows the post-emergence application of glufosinate in LL crops, which have been developed in soybean, cotton, corn and canola (Carbonari et al., 2016).

Evolution of Glufosinate Resistance in Weeds

To date, only two weed species have evolved resistance to glufosinate in the world. Glufosinate resistance was first documented in a goosegrass (*Eleusine indica*) population from Malaysia (Jalaludin et al., 2010). The resistance mechanisms in this population are not associated

with target site alterations, nor herbicide metabolism or reduced uptake and translocation (Jalaludin et al., 2017). A *Lolium rigidum* population from Oregon showed increased levels of glufosinate metabolism compared to susceptible plants (Brunharo et al., 2019). These populations did not show reduced enzyme sensitivity as stated elsewhere (Avila-Garcia et al., 2012), suggesting target site mutations are unlikely. However, the metabolites and enzymes involved are yet to be determined. In contrast, other *L. rigidum* populations have been identified as glufosinate-resistant but their resistance mechanisms remain unknown. More recently, Palmer amaranth (*Amaranthus palmeri*) populations have shown reduced sensitivity to glufosinate along with increased expression of detoxification enzymes such as glutathione-*S*-transferases and cytochrome P_{450} monooxygenases (Salas-Perez et al., 2018).

Inconsistent Performance in the Field

Glufosinate is a contact herbicide with limited translocation making it effective primarily on annual species (Steckel et al., 1997). It also tends to exhibit lower activity on grasses than broadleaf species and is less effective on larger than smaller weeds (Tharp et al., 1999). There are some evidences suggesting glufosinate metabolism in weeds but the parent molecule is fairly stable in most species (Everman et al., 2009). In a study with 20 different weed species, the main metabolite observed with all species was 3-hydroxymethylphosphinyl)propionic acid, along with low amounts of 2-hydroxy-4-(hydroxymethylphosphinyl)butanoic acid found in 14 species (Jansen et al., 2000). While glufosinate can be an effective herbicide, its field performance can be highly affected by environmental conditions. In particular low temperature and low humidity conditions around application reduce herbicide efficacy.

There has been research attempting to determine the reasons for the variable responses of plant species to glufosinate. While differences in leaf cuticular structure probably play a role in

the differential response of different species to this herbicide, different amounts of translocation out of the treated leaf are also important. Rigid ryegrass (*Lolium rigidum*) was much more tolerant to glufosinate compared to sterile oats (*Avena fatua*). The difference in tolerance was consistent with a significant reduction in translocation of glufosinate from treated leaves to the rest of the plant (Kumaratilake et al., 2002).

Studies on the impact of relative humidity on glufosinate activity show that control is greater at higher relative humidity. Control levels of three *Amaranthus* species was higher at 90% humidity than it was at 35% humidity. This was correlated with a large difference in translocation of glufosinate out of treated leaves (Coetzer et al., 2001). Studies on temperature effects on control of weeds with glufosinate have consistently shown lower control under low temperatures. Wild radish (*Raphanus raphanistrum*) control was greatly affected by temperature. Complete control could be achieved with 500 g ha^{-1} at 25/20 C, but this rate of glufosinate provided less than 20% control at 10/5 C. This difference in survival was correlated with an increase in the amount of glufosinate translocated out of the treated leaf at the higher temperature (Kumaratilake and Preston, 2005).

Herbicidal efficacy also depends on the time of day when glufosinate is applied. Early morning and late afternoon applications usually provide lower levels of weed control than midday applications. Glufosinate treatment at 12 pm provided, on average, 40% higher levels of weed control compared to applications performed at 4 hours after sunlight or before sunset (Martinson et al., 2005; Sellers et al., 2003). For these reasons, glufosinate applications are typically recommended under full sunlight, warm temperatures, and high humidity.

Mechanism of Action Is Controversial

While glufosinate inhibits chloroplast glutamine synthetase (GS2), its rapid phytotoxicity may not be a direct consequence of a reduction in glutamine synthesis. If phytotoxicity resulted from amino acid depletion, plants would show slow response to the herbicide, similar to glyphosate and acetolactate synthase inhibitors (Kishore and Shah, 1988). In contrast, susceptible plants show rapid development of symptoms following glufosinate treatment. When GS is inhibited, plants accumulate ammonia at high levels which could be phytotoxic, and this has been proposed to explain the fast response to glutamine synthetase inhibition (Platt and Anthon, 1981). Studies have shown that more than 60% of the total accumulated ammonia comes from the photorespiration pathway (Wild et al., 1987). In fact, there is evidence showing that the catastrophic consequences of the inhibition of glutamine synthetase by glufosinate is associated with reduced capacity to cope with photorespiration (Wendler et al., 1990).

Increasing O_2 concentration in the air when plants are treated with glufosinate enhances inhibition of photosynthesis. Under these conditions, plants cannot reach the compensation point because Rubisco (ribulose-1,5-bisphosphate carboxylase/oxygenase) uses a significant amount of oxygen. This suggests that photorespiration is essential for glufosinate inhibition of glutamine synthetase activity and lead to inhibition of photosynthesis (Wendler et al., 1992). Similarly, differential photosynthetic response of C3 and C4 plants to glufosinate is further evidence that the toxic consequences of the inhibition of glutamine synthetase is also associated with photorespiration (Wendler et al., 1990). The inhibition of photosynthesis by glufosinate is greater in C3 plants because C4 plants have a modified leaf structure that prevents the accumulation of O_2 under photorespiratory conditions (Pearcy and Ehleringer, 1984).

Dissertation Content

In response to the uncertain mechanism(s) of action and the inconsistent field performance, this PhD research focuses on elucidating the biochemical basis for the herbicidal activity of glufosinate. The first chapter explains the physiological factors affecting glufosinate uptake and translocation. The second chapter shows that glufosinate is primarily toxic to plants due to a massive light-dependent generation of reactive oxygen species (ROS) rather than ammonia accumulation or carbon assimilation inhibition. The relationship between glutamine synthetase, photorespiration and ROS generation is investigated in the third chapter. Finally, the last chapter demonstrates how herbicidal activity can be improved by manipulating changes in amino acid fluxomic and biosynthetic pathways by glufosinate and other inhibitors.
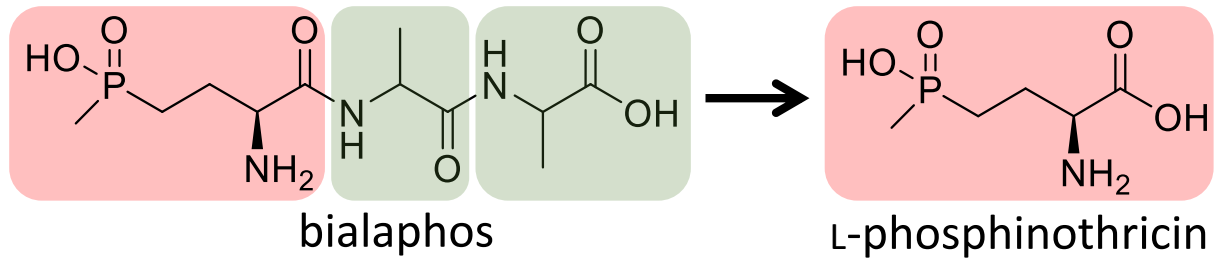
Figure B.1: Bialaphos, a tripeptide (L-phosphinothricin + two alanine), is naturally produced by *Streptomyces* sp. and metabolically bioactivated by plants into L-phosphinothricin.
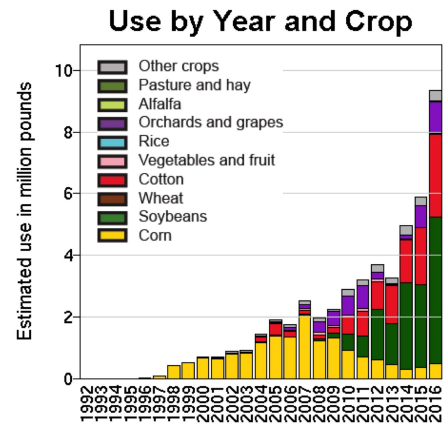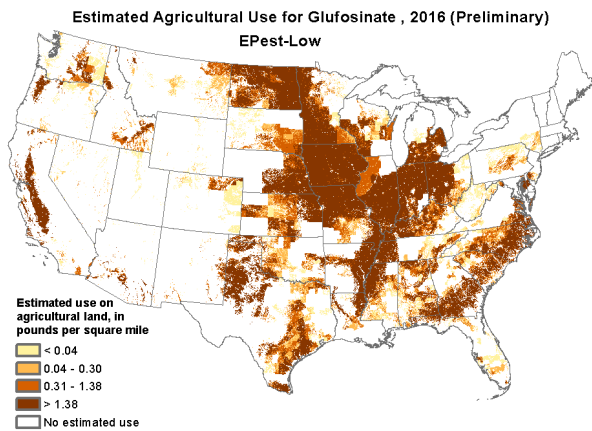
Figure B.2: Estimated agricultural use for glufosinate across the USA in 2016 (A). Estimated use by year and crop from 1992 to 2016 (B). Source: United States Geological Survey – USGS. Accessed in August 16th, 2019. Available at: <https://water.usgs.gov>.
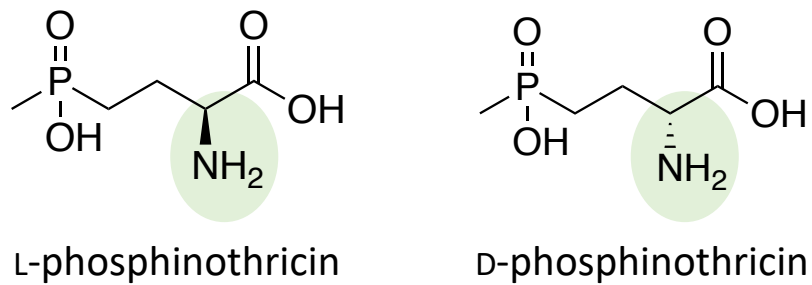
Figure B.3: Chemical structure of D- and L-phosphinothricin, which differ only by the special orientation of the amino group attached to the β-carbon (highlighted in green circles). Glufosinate is a racemic mixture of both isomers but only L-phosphinothricin is phytotoxic.
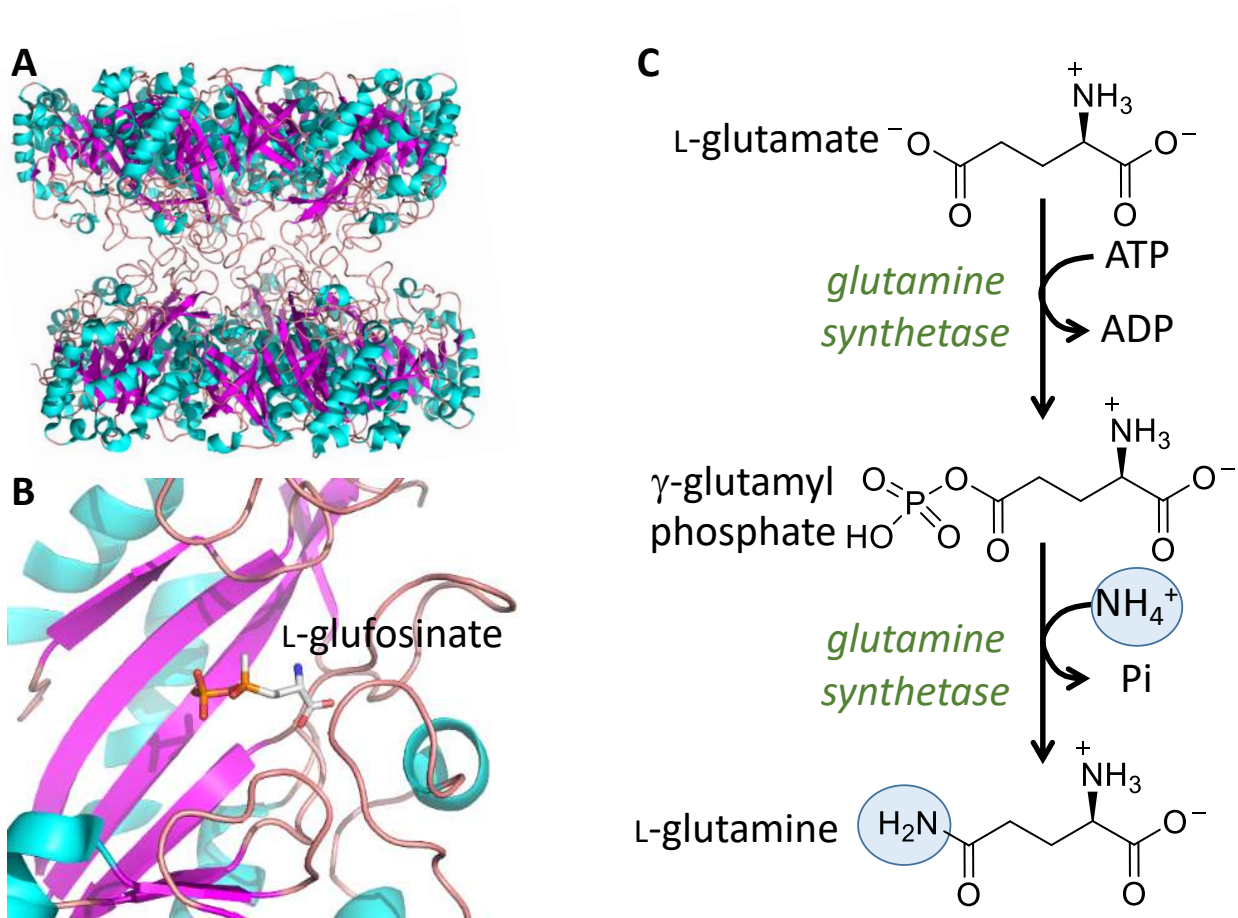
Figure B.4: Glutamine synthetase (GS) three-dimensional structure (A) and active site with glufosinate bound (B). The two-step reaction catalyzed by GS (C). Three-dimensional structures are adapted from the GS crystal structure of maize (Unno et al., 2006).
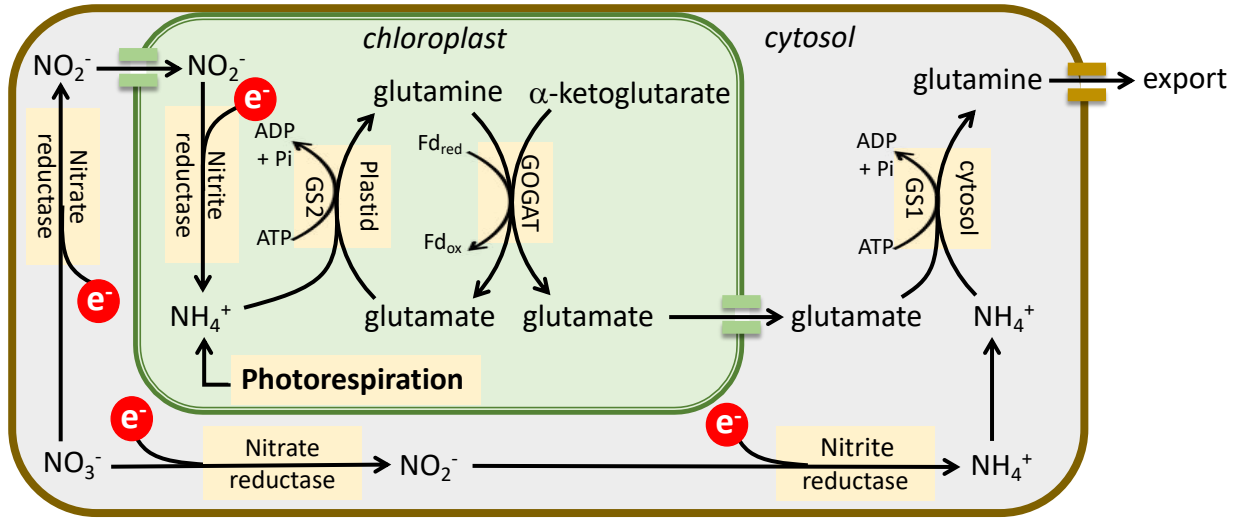
Figure B.5: The two isoforms of glutamine synthetase (GS) and their function. GS1 is involved in nitrogen export throughout the plant in form of glutamine. GS2 plays a central role in recycling ammonia from photorespiration.
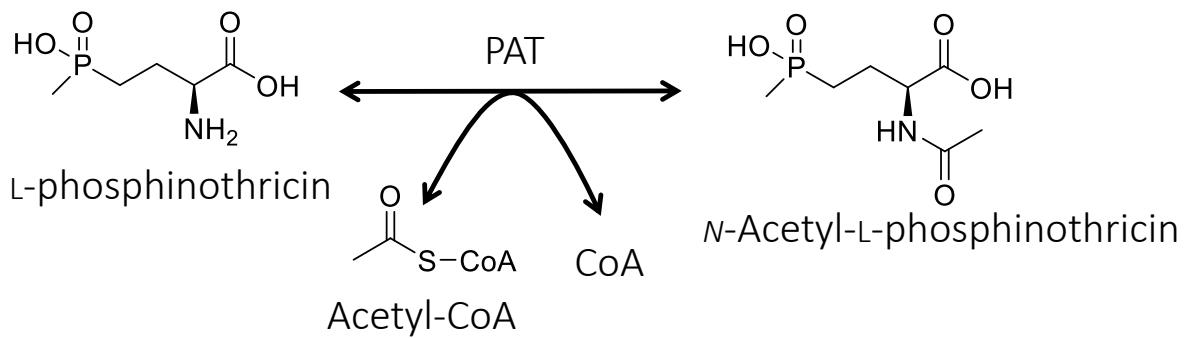
Figure B.6: Metabolism of L-phosphinothricin into *N*-acetyl-L-phosphinothricin by phosphinothricin acetyltransferase (PAT).

References

Avila-Garcia, W.V.; Sanchez-Olguin, E.; Hulting, A.G.; Mallory-Smith, C., 2012. Target-site mutation associated with glufosinate resistance in Italian ryegrass (*Lolium perenne* L. ssp. *multiflorum*). Pest Management Science 68: 1248-1254.

Bayer, E.; Gugel, K.H.; Hägele, K.; Hagenmaier, H.; Jessipow, S.; König, W.A.; Zähner, H., 1972. Stoffwechselprodukte von Mikroorganismen. 98. Mitteilung. Phosphinothricin und phosphinothricyl-alanyl-alanin. Helvetica Chimica Acta 55: 224-239.

Beriault, J.N.; Horsman, G.P.; Devine, M.D., 1999. Phloem transport of D,L-glufosinate and acetyl-L-glufosinate in glufosinate-resistant and -susceptible *Brassica napus*. Plant Physiology 121: 619-627.

Bernard, S.M.; Habash, D.Z., 2009. The importance of cytosolic glutamine synthetase in nitrogen assimilation and recycling. New Phytologist 182: 608-620.

Blackwell, R.D.; Murray, A.J.S.; Lea, P.J., 1987. Inhibition of photosynthesis in barley with decreased levels of chloroplastic glutamine synthetase activity. Journal of Experimental Botany 38: 1799-1809.

Brunharo, C.A.C.G.; Takano, H.K.; Mallory-Smith, C.A.; Dayan, F.E.; Hanson, B.D., 2019. Role of glutamine synthetase isogenes and herbicide metabolism in the mechanism of resistance to glufosinate in *Lolium perenne* L. spp. *multiflorum* biotypes from Oregon. Journal of Agricultural and Food Chemistry 67: 8431-8440.

Busi, R.; Goggin, D.E.; Heap, I.M.; Horak, M.J.; Jugulam, M.; Masters, R.A.; Napier, R.M.; Riar, D.S.; Satchivi, N.M.; Torra, J., 2018. Weed resistance to synthetic auxin herbicides. Pest Management Science 74: 2265-2276.

Carbonari, C.A.; Latorre, D.O.; Gomes, G.L.G.C.; Velini, E.D.; Owens, D.K.; Pan, Z.; Dayan, F.E., 2016. Resistance to glufosinate is proportional to phosphinothricin acetyltransferase expression and activity in LibertyLink® and WideStrike® cotton. Planta 243: 925-933.

Carvalho, H.; Pereira, S.; Sunkel, C.; Salema, R., 1992. Detection of a cytosolic glutamine synthetase in leaves of *Nicotiana tabacum* L. by immunocytochemical methods. Plant Physiology 100: 1591-1594.

Coetzer, E.; Al-Khatib, K.; Loughin, T.M., 2001. Glufosinate efficacy, absorption, and translocation in amaranth as affected by relative humidity and temperature. Weed Science 49: 8-13.

Dayan, F.E.; Cantrell, C.L.; Duke, S.O., 2009. Natural products in crop protection. Bioorganic & Medicinal Chemistry 17: 4022-4034.

Dröge, W.; Broer, I.; Pühler, A., 1992. Transgenic plants containing the phosphinothricin-N-acetyltransferase gene metabolize the herbicide L-phosphinothricin (glufosinate) differently from untransformed plants. Planta 187: 142-151.

Duke, S.O.; Cantrell, C.L.; Meepagala, K.M.; Wedge, D.E.; Tabanca, N.; Schrader, K.K., 2010. Natural toxins for use in pest management. Toxins 2: 1943-1962.

Edwards, J.W.; Coruzzi, G.M., 1989. Photorespiration and light act in concert to regulate the expression of the nuclear gene for chloroplast glutamine synthetase. The Plant Cell 1: 241.

Everman, W.J.; Mayhew, C.R.; Burton, J.D.; York, A.C.; Wilcut, J.W., 2009. Absorption, translocation, and metabolism of ^{14}C-glufosinate in glufosinate-resistant corn, goosegrass (*Eleusine indica*), large crabgrass (*Digitaria sanguinalis*), and sicklepod (*Senna obtusifolia*). Weed Science 57: 1-5.

Gill, H.S.; Eisenberg, D., 2001. The crystal structure of phosphinothricin in the active site of glutamine synthetase illuminates the mechanism of enzymatic inhibition. Biochemistry 40: 1903-1912.

González-Moro, B.; Mena-Petite, A.; Lacuesta, M.; González-Murua, C.; Muñoz-Rueda, A., 2000. Glutamine synthetase from mesophyll and bundle sheath maize cells: isoenzyme complements and different sensitivities to phosphinothricin. Plant Cell Reports 19: 1127-1134.

Ishiyama, K.; Inoue, E.; Watanabe-Takahashi, A.; Obara, M.; Yamaya, T.; Takahashi, H., 2004. Kinetic properties and ammonium-dependent regulation of cytosolic isoenzymes of glutamine synthetase in *Arabidopsis*. Journal of Biological Chemistry 279: 16598-16605.

Jalaludin, A.; Ngim, J.; Bakar, B.H.; Alias, Z., 2010. Preliminary findings of potentially resistant goosegrass (*Eleusine indica*) to glufosinate-ammonium in Malaysia. Weed Biology and Management 10: 256-260.

Jalaludin, A.; Yu, Q.; Zoellner, P.; Beffa, R.; Powles, S.B., 2017. Characterisation of glufosinate resistance mechanisms in *Eleusine indica*. Pest Management Science 73: 1091-1100.

Jansen, C.; Schuphan, I.; Schmidt, B., 2000. Glufosinate metabolism in excised shoots and leaves of twenty plant species. Weed Science 48: 319-326.

Kishore, G.M.; Shah, D.M., 1988. Amino acid biosynthesis inhibitors as herbicides. Annual Review of Biochemistry 57: 627-663.

Kondo, Y., 1973. Studies on a new antibiotic SF-1293. I. Isolation and physico-chemical and biological characterization of SF-1293 substance. Scientific Reports of Meijiseika 13: 34-41.

Kumaratilake, A.R.; Lorraine-Colwill, D.F.; Preston, C., 2002. A comparative study of glufosinate efficacy in rigid ryegrass (*Lolium rigidum*) and sterile oat (*Avena sterilis*). Weed Science 50: 560-566.

Kumaratilake, A.R.; Preston, C., 2005. Low temperature reduces glufosinate activity and translocation in wild radish (*Raphanus raphanistrum*). Weed Science 53: 10-16.

Martinson, K.B.; Durgan, B.R.; Gunsolus, J.L.; Sothern, R.B., 2005. Time of day of application effect on glyphosate and glufosinate efficacy. Crop Management 4: 1-6.

McNally, S.F.; Hirel, B.; Gadal, P.; Mann, A.F.; Stewart, G.R., 1983. Glutamine synthetases of higher plants. Plant Physiology 72: 22-25.

Miflin, B.J.; Lea, P.J., 1976. The pathway of nitrogen assimilation in plants. Phytochemistry 15: 873-885.

Pearcy, R.W.; Ehleringer, J., 1984. Comparative ecophysiology of C3 and C4 plants. Plant, Cell & Environment 7: 1-13.

Platt, S.G.; Anthon, G.E., 1981. Ammonia accumulation and inhibition of photosynthesis in methionine sulfoximine treated spinach. Plant Physiology 67: 509-513.

Ridley, S.M.; McNally, S.F., 1985. Effects of phosphinothricin on the isoenzymes of glutamine synthetase isolated from plant species which exhibit varying degrees of susceptibility to the herbicide. Plant Science 39: 31-36.

Salas-Perez, R.A.; Saski, C.A.; Noorai, R.E.; Srivastava, S.K.; Lawton-Rauh, A.L.; Nichols, R.L.; Roma-Burgos, N., 2018. RNA-Seq transcriptome analysis of *Amaranthus palmeri* with differential tolerance to glufosinate herbicide. PloS One 13: e0195488.

Sellers, B.A.; Smeda, R.J.; Johnson, W.G., 2003. Diurnal fluctuations and leaf angle reduce glufosinate efficacy. Weed Technology 17: 302-306.

Shaner, D.L. (2014) Herbicide handbook. Vol 10th. Weed Science Society of America, Champaign

Somerville, C.R.; Ogren, W.L., 1980. Inhibition of photosynthesis in *Arabidopsis* mutants lacking leaf glutamate synthase activity. Nature 286: 257-259.

Steckel, G.J.; Wax, L.M.; Simmons, F.W.; Phillips, W.H., 1997. Glufosinate efficacy on annual weeds is influenced by rate and growth stage. Weed Technology 11: 484-488.

Tharp, B.E.; Schabenberger, O.; Kells, J.J., 1999. Response of annual weed species to glufosinate and glyphosate. Weed Technology 13: 542-547.

Unno, H.; Uchida, T.; Sugawara, H.; Kurisu, G.; Sugiyama, T.; Yamaya, T.; Sakakibara, H.; Hase, T.; Kusunoki, M., 2006. Atomic structure of plant glutamine synthetase a key enzyme for plant productivity. Journal of Biological Chemistry 281: 29287-29296.

Weber, A.; Flügge, U.I., 2002. Interaction of cytosolic and plastidic nitrogen metabolism in plants. Journal of Experimental Botany 53: 865-874.

Wendler, C.; Barniske, M.; Wild, A., 1990. Effect of phosphinothricin (glufosinate) on photosynthesis and photorespiration of C3 and C4 plants. Photosynthesis Research 24: 55-61.

Wendler, C.; Putzer, A.; Wild, A., 1992. Effect of glufosinate (phosphinothricin) and inhibitors of photorespiration on photosynthesis and ribulose-1,5-bisphosphate carboxylase activity. Journal of Plant Physiology 139: 666-671.

Wild, A.; Sauer, H.; Rühle, W., 1987. The effect of phosphinothricin (glufosinate) on photosynthesis I. Inhibition of photosynthesis and accumulation of ammonia. Zeitschrift für Naturforschung C 42: 263-269.

Chapter 1: Physiological Factors Affecting Uptake and Translocation of Glufosinate

INTRODUCTION

Glufosinate is a synthetic isomeric mixture of D,L-phosphinothricin, a microbial phytotoxin discovered in bacteria of the genus *Streptomyces* (Bayer et al., 1972; Kondo, 1973). It is a broad-spectrum non-selective herbicide used for post emergence control of grass and broadleaf weeds in both non-crop and agricultural systems (Dayan et al., 2009). Current estimates are over 12 million ha per year are treated with this herbicide (Busi et al., 2018), with a significant increase in the last decade due to the evolution of glyphosate-resistant weeds. Glufosinate is an alternative option for post emergence control of multiple herbicide resistant weeds in Liberty Link crops, which are genetically-engineered by the insertion of the *bar* or *pat* genes that rapidly metabolize L-phosphinothricin into the inactive *N*-acetyl-L-phosphinothricin (Thompson et al., 1987; Carbonari et al., 2016). Glufosinate has been commercialized for over 25 years, but only two weed species (*Lolium perenne* and *Eleusine indica*) have evolved resistance to the herbicide (Avila-Garcia and Mallory-Smith, 2011; Jalaludin et al., 2015; Brunharo et al., 2019).

Glufosinate inhibits glutamine synthetase (GS), an important enzyme responsible for incorporating ammonia into glutamate to yield glutamine (McNally et al., 1983). It competes with glutamate for the enzyme active site and binds irreversibly to the enzyme (Leason et al., 1982). This inhibition is only possible due to the high levels of structural similarity between glufosinate and glutamate/glutamine. The inhibition of GS causes accumulation of ammonia, but the activity of glufosinate is due to rapid light-dependent formation of reactive oxygen species (ROS) (Takano et al., 2019a). Because injury symptoms appear within a few hours after

17

treatment in sensitive species, glufosinate could potentially limit its own translocation due to the rapid cell damage (Beriault et al., 1999). Glufosinate is able to translocate through the xylem of grass species, probably due to its high hydrophilicity (log k_{ow}: -3.9), but has lower translocation in the phloem (Shaner, 2014; Kumaratilake et al., 2002).

Glufosinate concentration in leaves is proportional to GS inhibition, ROS accumulation, and phytotoxicity (Takano et al., 2019a). Herbicide efficacy is also positively correlated with glufosinate translocation, which is affected by temperature and relative humidity (Anderson et al., 1993; Coetzer et al., 2001; Kumaratilake and Preston, 2005). The effects of temperature and humidity on glufosinate translocation have been widely studied in the past. However, little is known about physiological factors affecting glufosinate uptake and translocation. For instance, glyphosate easily translocates throughout the plant even though it is hydrophilic (Barker and Dayan, 2019). This could indicate that an active transporter is involved in glyphosate movement across cellular membranes (Shaner, 2009; Takano et al., 2019b). To date, there has been no research attempting to determine whether glufosinate translocates through an active transporter or just by passive movement. Therefore, understanding the interaction between plant physiology and glufosinate uptake and translocation is essential to improve herbicidal activity. In this work, we provide new insights on glufosinate uptake and translocation and the main factors modulating its movement in plants.

MATERIAL AND METHODS

Plant Material and Growth

Palmer amaranth (*Amaranthus palmeri*) was used as a model species to evaluate glufosinate uptake and translocation. Plants were grown in 0.2 L pots with potting soil under

greenhouse conditions (25/20 C day/night, 16 h photoperiod, 70% relative humidity) until the desired growth stage (12-cm-tall and 8-9 leaves).

Glufosinate and Amino Acid Detection

Glufosinate, glutamate and glutamine contents in leaves were measured with liquid chromatography - tandem mass spectrometry (LC-MS/MS). Leaf tissue (200 mg) was washed with distilled water, dried, ground in liquid nitrogen, and homogenized in 5 mL methanol:water (75:25, v/v). The solution was vigorously mixed for one min, incubated in an ultrasonic bath for 30 min and centrifuged at 4,000 × g for 10 min. A 1 mL aliquot of the supernatant was filtered through a 0.2 μm nylon filter into an UHPLC vial, and 1 μL of this solution was used for injection. The LC–MS/MS system (Shimadzu Scientific Instruments, Columbia, MD, USA) consisted of a Nexera X2 UPLC with 2 LC-30 AD pumps, an SIL-30 AC MP autosampler, a DGU-20A5 Prominence degasser, a CTO-30A column oven, and SPD-M30A diode array detector coupled to an 8040-quadrupole mass-spectrometer. Metabolites were separated on an iHilic-Fusion column (100 × 2.1 mm, 3.5 μm; Silica) at a flow rate of 0.2 mL min^{-1} using a linear gradient of acetonitrile (B) and 25 mM ammonium acetate (A): 2 min, 80% B; 8 min, 30% B; 12 min, 30% B; 12.1 min, 80% B. The MRMs (multiple reaction monitoring) for glufosinate, glutamate and glutamine were optimized to 181.95>136.05 (CE: -15, Q1: -19, Q3: -14), 147.95>130.10 (CE: -15, Q1: -16, Q3: -23), and 147.10>130.00 (CE: -16, Q1: -15, Q3: -13), respectively. Quantification was performed based on external standard curves from serial dilutions of the analytical standard.

Effect of Glutamine on Glufosinate Uptake

Three experiments were conducted incubating 50 leaf discs (5-mm diam taken from the first fully expanded leaf) in 50-mL glass tubes containing different solutions. First, glufosinate

uptake was measured after 1, 3, 6, 12, 24, 36 and 48 h of incubation in 10 mM glufosinate or 10

mM glufosinate + 10 mM glutamine. Second, glufosinate uptake was quantified at 24 h after

incubation in 0, 125, 250, 500 and 1000 μM glufosinate with or without 500 μM glutamine. In a

third experiment, glufosinate uptake was evaluated at 24 h after incubation of the leaf discs in 0,

5, 10, 25 and 50 mM glufosinate with or without 25 mM glutamine. After the incubation period,

the leaf discs were washed three times with distilled water and dried before glufosinate

extraction and quantification.

Effect of Glutamine on Whole Plant Glufosinate Uptake

Three experiments were conducted. First, plants were sprayed with glufosinate (560 g

ha^{-1}) alone or in a tank mix with 50 mM glutamine using a commercial chamber track sprayer

equipped with an 8002EVS single even flat-fan nozzle (TeeJet; Spraying Systems Co., Wheaton,

IL, USA) and calibrated for 187 L ha^{-1}. Second, plants were carefully removed from the soil,

washed with tap water and transferred to 200 mL glass tubes containing 50 mM glutamine or

distilled water only. Glufosinate was applied as a foliar spray at 560 g ha^{-1} immediately after

transferring the plants to either solutions. A third experiment was conducted comparing

glufosinate uptake in plants using the same method, but plants were supplied with 1, 10, 25, and

50 mM glutamine compared to 50 mM of glutamate, asparagine or aspartate. Glufosinate uptake

was measured in the leaf tissue at 8 h after treatment (HAT).

Effect of Light on Glufosinate Uptake

Plants were grown in the greenhouse as previously described until the desired growth

stage. Before glufosinate application (at 560 g ha^{-1}) three plants were placed in the dark for 24 h,

while the other three were kept in the greenhouse under light. Glutamine levels were determined

in one excised leaf of these plants as described above prior to glufosinate application. Glufosinate uptake was quantified at 24 HAT as described above.

Glufosinate Translocation Between Leaves

To examine glufosinate translocation from treated leaves to other leaves, two fully expanded leaves per plant were covered with aluminum foil prior to glufosinate application at 560 g ha^{-1}. The aluminum foil was then removed and plants were placed in the greenhouse. Leaf samples were collected from protected and treated leaves 24 HAT, and evaluated for glufosinate content, glutamine and glutamate levels, glutamine synthetase (GS) activity, ammonia accumulation, and reactive oxygen species (ROS).

Glutamine Synthetase Activity

Glutamine synthetase activity was quantified *in planta* by the GS-dependent formation of γ-glutamyl hydroxamate by measuring the transferase activity (Dayan et al., 2015; Forlani, 2000). Leaf tissue (2 g) was homogenized in chilled mortar with 3 mL of extraction buffer (50 mM Tris base, pH 8, 1 mM EDTA, 2 mM DTT, 10 mM MgCl$_2$, and 50% (w/v) PVP10). The extract was filtered through miracloth layered on top of cheesecloth after washing the mortar with an additional 1 mL extraction buffer. The filtered extract was centrifuged at 12,000 × *g* for 10 min at 4 C. The reaction consisted of 0.9 mL of assay buffer (25 mM imidazole-HCl at pH 7.5, 4 mM MnCl$_2$, 5 mM ADP, 50 mM L-glutamine, 40 mM sodium arsenate, and 25 mM hydroxylamine) and 0.1 mL of crude enzyme extract, incubated for 30 min at 30 C. To stop the reaction, 0.5 mL ferric chloride reagent was added, and the mixture was incubated for 10 min at room temperature, followed by centrifugation at 12,000 × *g* for 10 min. The ferric chloride reagent consisted of 32% (w/v) anhydrous ferric chloride dissolved in 0.5 M HCl. The

concentration of γ-glutamyl hydroxamate was determined by absorbance at 540 nm on a spectrophotometer (Synergy™ 2 Multi-Mode Microplate Reader; BioTek, Winooski, VT).

Ammonia Accumulation

Ammonia accumulation in treated leaves was measured by excising leaf discs (Dayan et al., 2015). One 5-mm-diam leaf disc was placed into each well of a 96-well microtiter plate containing 100 µL of distilled water. The plate was then sealed and frozen at -80 C for 15 min, and the cell membranes lysed with two freeze-thaw cycles. An aliquot of 50 µL from each well was transferred to a new plate. Ammonia was determined by adding 150 µL water, 100 µL phenol nitroprusside solution, and 50 µL alkaline hypochlorite solution (Molin and Khan, 1995). After 30 min incubation at room temperature, absorbance was measured at 540 nm as described above.

Reactive Oxygen Species

The generation of hydrogen peroxide (H_2O_2) and superoxide (O_2^-) within treated leaves was measured by staining leaf discs in solutions containing 3,3'-diaminobendizine (DAB) and nitro blue tetrazolium chloride (NBT), respectively. The DAB solution contained 0.1 g DAB solubilized in 200 mL water with pH 3.8. The NBT solution was composed by 0.1 g NBT, 13.6 g potassium phosphate monobasic and 1.3 g sodium azide in 200 mL water. Sixteen leaf discs (5-mm diam) from control and treated (560 g ha^{-1} glufosinate) leaves were placed in 20 mL glass tubes containing each staining solution. The samples were then shaken under 20 Hg vacuum for 1 h. Leaf discs were washed in distilled water and boiled in 70% ethanol solution, having the solution replaced every 20 min for four cycles. Leaf discs were then stored in 70% ethanol solution for 12 h and scanned (Brother DCP-L2550DW; Bridgewater, NJ, USA). The levels of H_2O_2 or O_2^- were quantified using CS3 Photoshop (Adobe Systems, San Jose, CA, USA),

measuring the color intensity in each leaf disc, removing background levels. Data was calculated

as the relative intensity of treated samples compared to control samples (treated intensity –

control intensity).

Glufosinate Translocation Within a Leaf

Two fully expanded leaves per plant were used to measure glufosinate movement from

the base towards the tip and from the tip towards the base of the leaf. Glufosinate was applied on

the adaxial surface of the leaf at 5.6 µg cm^{-2}, which is equivalent to 560 g ha^{-1}. Half of the plants

(n = 3) received the treatment only on the base while others only on the tip of the leaf. The leaf

was divided in two (base and tip) 8 HAT and used for glufosinate quantification as described

above.

Glufosinate Translocation from Covered Source Leaves to Young Sink Leaves

Plants were grown in the greenhouse until the 12-leaf stage. The four oldest leaves

(source leaves) in each plant were treated with glufosinate (5.6 µg cm^{-2}) using an electronic

pipet. Half of the plants had their treated leaves immediately covered with aluminum foil to

prevent light exposure. Plants with covered and non-covered leaves were compared for

glufosinate translocation at 1, 2, 4 and 8 days after treatment. Three replications per time point

were used and aluminum foil was removed from leaves prior to analysis. Source and sink leaves

were washed and used for glufosinate quantification as described above.

Data Analysis

Data were combined from two repetitions of each experiment with three replications (n =

6), and analyzed with Prism 8 (GraphPad Software, 7825 Fay Ave, La Jolla, CA). Means were

compared by t-test (p<0.05) and presented with their standard error. An exponential one phase

equation was fitted for glufosinate uptake over time data. A four-parameter non-linear regression

was used for glufosinate uptake over μM doses and linear regression for glufosinate uptake over mM doses of glufosinate and translocation from source to sink leaves over time.

RESULTS

Glufosinate Uptake by Leaf Discs in the Presence of Glutamine

Glufosinate uptake increased over time and reached a maximum value 24 h after incubation (Figure 1.1A). The addition of glutamine to glufosinate reduced the uptake of glufosinate. Maximum uptake for glufosinate alone was 13.3 μg g FW^{-1}, compared to 8.1 μg g FW^{-1} with glufosinate + glutamine. Glufosinate uptake at low glufosinate concentrations (up to 1000 μM) increased exponentially until 250-260 μM. At concentrations greater than that, uptake saturates (Figure 1.1B) with maximum uptake values of 5.9 and 4.6 μg g^{-1} for glufosinate alone and glufosinate + glutamine, respectively. The addition of glutamine only significantly reduced glufosinate uptake at glufosinate concentrations equal to or higher than 500 μM. When leaf discs were incubated at high glufosinate concentrations (up to 50 mM), herbicide uptake increased linearly for both treatments, but glufosinate alone had a higher slope (0.7) compared to glufosinate + glutamine (0.3) (Figure 1.1C).

Effect of Glutamine on Glufosinate Uptake by Whole Plants

The addition of 50 mM glutamine into the glufosinate spraying solution decreased herbicide uptake by 39% (Figure 1.2A) and visual injury by 49% (Figure 1.2B). When 50 mM glutamine was supplied to the plant roots, reductions in glufosinate uptake (Figure 1.2C) and visual injury (Figure 1.2D) were even greater at 87 and 95%, respectively. The impact on glufosinate uptake of other amino acids with similar side chains (e.g. glutamate, asparagine and aspartate) was compared to glutamine (Figure 1.3). A linear dose response occurred with

increasing glutamine doses; however, inhibition of glufosinate uptake was specific to glutamine and did not occur with glutamate, asparagine and aspartate.

Effect of Light on Glufosinate Uptake

Higher glutamine concentrations were found in plants in the light (33 µg g^{-1}) compared to plants in the dark (8 µg g^{-1}) prior to glufosinate application (Figure 1.4A). Glufosinate uptake was lower for plants growing under light (13 µg g^{-1}) compared to those under dark (19 µg g^{-1}) (Figure 1.4B). While plants in the light were greatly injured by glufosinate (80% visual injury), those under light were not (3%) (Figure 1.4C).

Glufosinate Translocation Among Leaves

The amount of glufosinate detected in leaves protected from glufosinate application by foil was very low (0.4 µg g^{-1}), while treated leaves had 14.1 µg g^{-1} (Figure 1.5A). This represents 2.8% of the herbicide translocating from treated to protected leaves 24 HAT. Glutamine synthetase activity was 91% lower (Figure 1.5B) and ammonia accumulation was 85% higher in treated leaves compared to those that were covered with aluminum foil (Figure 1.5C). Glutamine (Figure 1.5D) and glutamate (Figure 1.5E) levels decreased and reactive oxygen species (ROS) increased in treated leaves (Figure 1.5F).

Glufosinate Translocation Within a Leaf

Under normal light conditions, when glufosinate was applied only on the basal half of the leaf, 42% of the total applied herbicide moved towards the leaf tip (Figure 1.6A). In contrast, when glufosinate was applied only on the leaf tip, most of the herbicide stayed in the leaf tip, with a very small amount (4%) translocating to the base (Figure 1.6B). Both leaf base and leaf tip were injured when glufosinate was applied to the leaf base, but only the leaf tip was injured when the herbicide was applied on the leaf tip (Figure 1.6C). In the dark there was less

translocation of glufosinate (21%) from leaf base to leaf tip (Figure 1.6D), but a slight increase in translocation from leaf tip to leaf base (8%) (Figure 1.6E). No visual injury was observed under dark conditions (Figure 1.6F).

Glufosinate Translocation from Covered Source Leaves to Young Sink Leaves

Young sink leaves developed some injury symptoms 24 HAT even though they were not treated, indicating that the herbicide translocated a little from source treated leaves (Figure 1.7A). Glufosinate concentration in source leaves decreased over time for both covered and non-covered leaves. A small difference (9%) was observed in the amount of glufosinate remaining between covered and non-covered leaves at 8 d after treatment (Figure 1.7B). The amount of glufosinate translocating was higher when source leaves were covered compared to non-covered by 5% (Figure 1.7C).

DISCUSSION

Possible Role of Active Transporters *vs* Passive Movement in Glufosinate Uptake

Glufosinate efficacy is proportional to uptake and translocation levels (Steckel et al., 1997; Pline et al., 1999; Mersey et al., 1990; Takano et al., 2019a). The hydrophilicity of glufosinate (log K_{ow} -3.9) (Shaner, 2014) may negatively affect its capacity to cross lipophilic membranes (Hsu and Kleier, 1996; Takano et al., 2019b). Glyphosate is also a hydrophilic molecule (Shaner, 2014) but is highly mobile in plants, moving along with photosynthates from source to sink tissues (Shaner, 2009; Barker and Dayan, 2019; Corrêa et al., 2016). It has been suggested the role of an active transporter in glyphosate movement across membranes due to its structural similarities with both glycine and phosphate (Shaner, 2009; Hetherington et al., 1998).

Therefore, low glufosinate translocation may result from the absence of an effective active transporter.

Glufosinate shares structure elements with glutamate and glutamine, and to some degree aspartate and asparagine. These amino acids were tested as potential competitors for glufosinate uptake. Glutamine alone reduced glufosinate foliar uptake in Palmer amaranth (Figure 1.3), and the effect was stronger when glutamine was supplied through the roots compared to foliar application in tank mix with the herbicide (Figure 1.2). When glutamine was present, glufosinate uptake was not only lower but also slower (Figure 1.1A). A comparable phenomenon was observed with 2,4-D competing for uptake with indole acetic acid (Sterling, 1994).

Glufosinate uptake saturates at low concentrations of up to 1 mM (Figure 1.1B) but there is a linear response at high concentrations (Figure 1.1C). This suggests uptake of glufosinate may be mediated by a membrane transporter at low herbicide concentrations and a diffusion process at higher concentrations. The glufosinate uptake pattern is similar to glyphosate under low concentrations and with bentazon under high concentrations (Sterling, 1994). Glufosinate is normally applied in the range of 400-1000 g ha^{-1}, which is roughly equivalent to 15-40 mM, depending on the spray volume. Therefore, under field conditions, glufosinate uptake would be driven mostly by diffusion, and a membrane transporter would provide only a small contribution. The inhibitory effect of glutamine on glufosinate uptake only occurred under high herbicide concentrations, suggesting that glutamine is more likely to compete for the diffusion process rather than an active transporter.

Plants growing under light had higher levels of glutamine in leaves than those under dark conditions (Figure 1.4). This is probably because glutamine synthetase is mostly active in the presence of light (Oliveira et al., 2002). In contrast to light-grown plants, plants in the dark had

higher levels of glufosinate uptake and no visual injury. Higher levels of uptake in the dark were associated with both absence of injury and lower glutamine levels. Increased glufosinate uptake also occurred when the herbicide solution was acidified to pH 4 (Figure A1.4). Glufosinate has multiple acid dissociation constants (pKa: 2, 2.6 and 9.8) (Shaner, 2014), therefore, greater protonation of the molecule increases with the acidity of the spray solution. The higher uptake rates at pH 4 and 4.5 suggests that glufosinate protonation could neutralize negative charges, making the molecule less hydrophilic, and consequently, better able to cross lipophilic membranes (Takano et al., 2019b). Once inside the cell, where the cytoplasm pH is closer to neutral, the protonated molecule would become dissociated, more hydrophilic, and less able to cross membranes. This phenomenon is defined as acid trapping (Hsu and Kleier, 1996), and has been described for other weak acid herbicides, such as bentazon (Sterling, 1994), 2,4-D (Rubery, 1977), clopyralid and chlorsulfuron (Devine et al., 1987), imidazolinones (van Ellis and Shaner, 1988), and sethoxydim (Struve et al., 1987).

Does the Fast Action of Glufosinate Limits Its Own Translocation?

The limited translocation of glufosinate in plants has been sometimes attributed to its fast action (Beriault et al., 1999). Consistent with field observations, low levels of glufosinate translocation were found from one leaf to another (Figure 1.5). Previous research reported less than 2% ^{14}C-glufosinate translocation from leaves to roots of Palmer amaranth (Coetzer et al., 2001), and lower glufosinate efficacy on weed species whose leaves intercept less herbicide droplets due to their vertical leaf angle and narrow morphology (Sellers et al., 2003). Consequently, spray coverage becomes a key factor for glufosinate efficacy. These observations emphasize the importance of spraying small weeds and low infestation density to achieve high leaf coverage (Womac et al., 2016).

Because the fast action of glufosinate is light dependent, we conducted translocation experiments under light and dark conditions to evaluate the self-limitation effect. Glufosinate translocation from the leaf base towards the leaf tip was higher in light than dark conditions (Figure 1.6). In the absence of light, leaf stomata are mostly closed to reduce transpiration rates (Snyder et al., 2003) which could explain lower xylem movement of glufosinate in the dark. In contrast, translocation of glufosinate from the tip to the base of leaves was limited regardless of light conditions. Therefore, limited translocation of glufosinate is probably related to its physiochemical characteristics, rather than its fast action.

Phloem *vs* Xylem Movement

Glufosinate translocation from source leaves to young sink leaves when the source leaves were covered compared to non-covered was evaluated. Covered leaves should have no tissue injury because they are protected from light exposure. Less than 10% of the total applied glufosinate translocated under both situations. Covering treated leaves increased translocation only 4% compared to those that were not covered. As previously stated, glufosinate was highly mobile from the leaf base to the leaf tip (Figure 1.6), as well as from roots to the apical meristem (Figure A1.2). Thus, translocation mainly occurs through the apoplast, indicating that glufosinate movement is dependent on the transpiration flow. This is consistent with the analysis of the xylem sap from new leaves *vs* old leaves (Figure A1.3), demonstrating that glufosinate accumulates in old leaves, possibly due to the higher transpiration rates of these leaves, compared to younger leaves. Low levels of glufosinate translocation against the transpiration flow (e.g. from leaf tip towards the leaf base) limits herbicide movement toward the apical meristem following foliar application. On the other hand, a significant amount of glufosinate translocates to the apical meristem when the herbicide is supplied through the roots, although

most of the herbicide accumulates in the apoplast of older leaves. The limited phloem translocation of glufosinate explains the observed the lack of control on meristematic tissues following foliar application of glufosinate.

In conclusion, glufosinate uptake may be driven by an active transporter under low concentrations, but at normal field rates, absorption occurs mostly by cell diffusion and is strongly affected by the presence of glutamine. Glufosinate translocation throughout the plant relies mostly on apoplastic translocation, which is affected by transpiration. Consequently, glufosinate tends to accumulate in old leaves with higher transpiration rates instead of young leaves and the apical meristem. The fast action of glufosinate does not limit its own translocation. Instead, low translocation rates result from the absence of an efficient active transporter and the physicochemical characteristics of the herbicide.
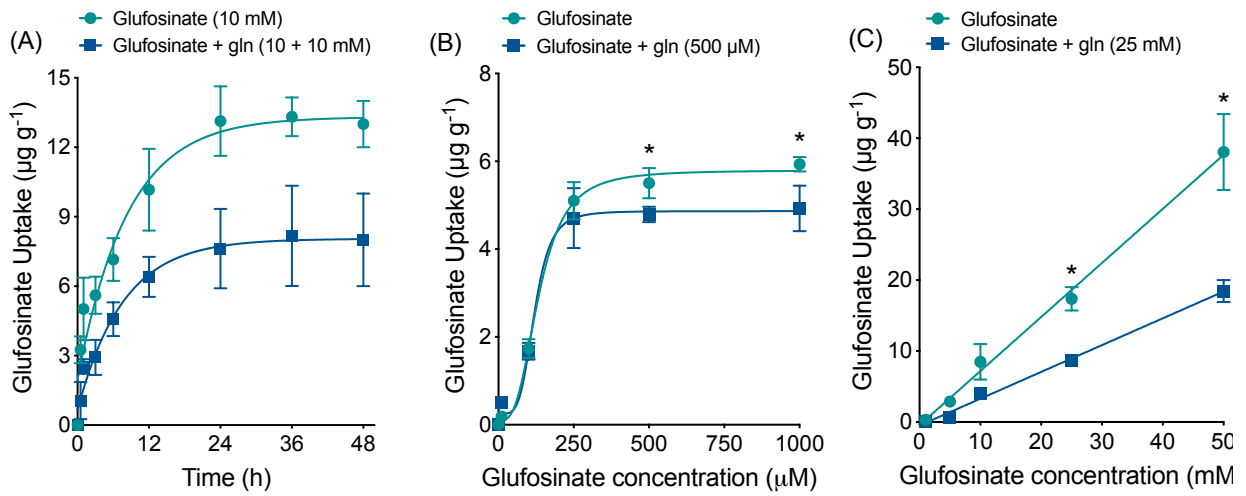
Figure 1.1: Glufosinate uptake in Palmer amaranth leaf discs over time (A) and increasing μM concentrations of glufosinate (B), or mM concentrations of glufosinate (C) in the presence or absence of a fixed glutamine concentration. Data was pooled from two experiments with three replications (n = 6). *means are significantly different by t-test (p<0.05). Gln: glutamine.
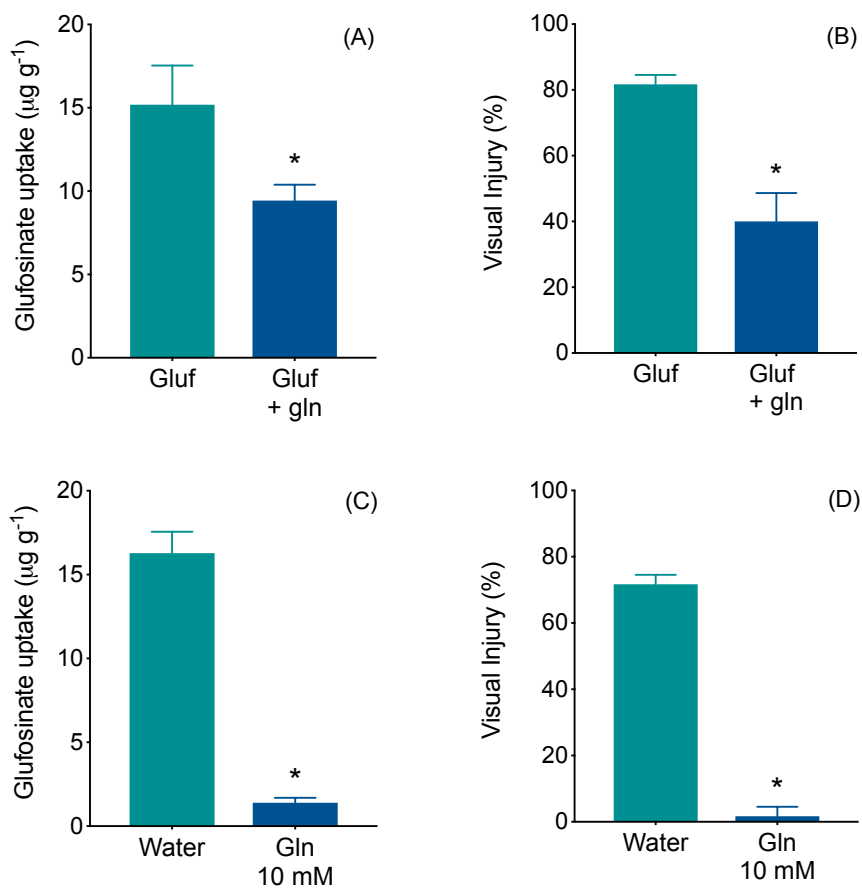
Figure 1.2: Effect of foliar applied glutamine on glufosinate foliar uptake (A) and visual injury (B) in Palmer amaranth. Glufosinate only (560 g ha^{-1} equivalent to 20 mM) or glufosinate + glutamine (584 g ha^{-1} equivalent to 20 mM) were foliar sprayed on 12-cm tall plants. Effect of root applied glutamine on glufosinate foliar uptake (C) and visual injury (D) in Palmer amaranth. Plant roots were incubated for one hour in hydroponic solution of glufosinate only (20 mM) or glufosinate + glutamine (20 mM). Data was pooled from two experiments with three replications each (n = 6). *means are significantly different by t-test ($p<0.05$).
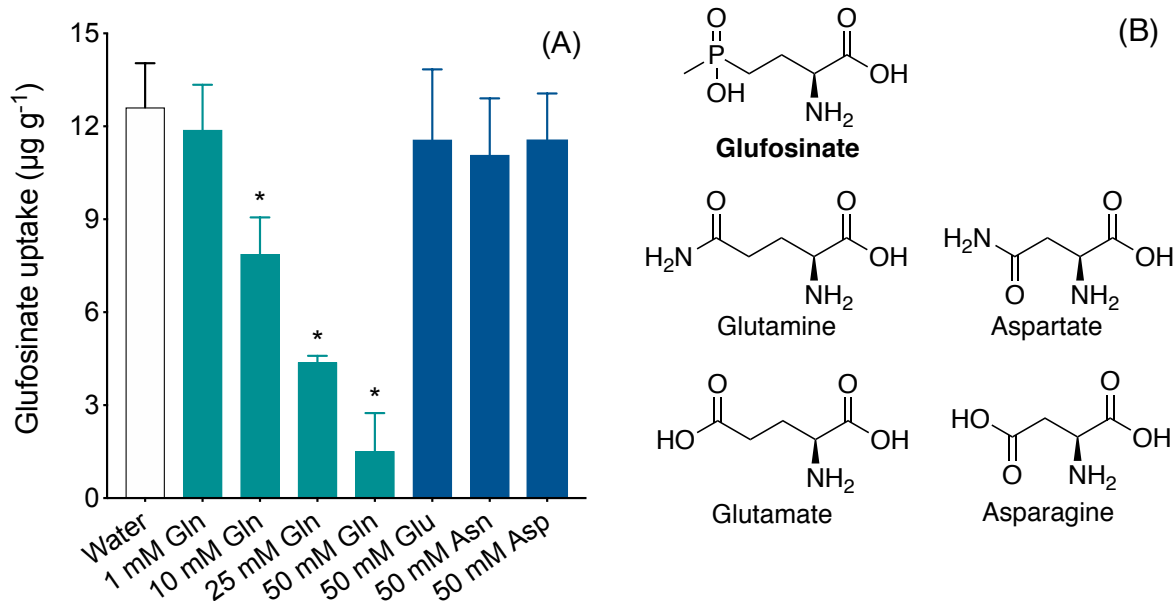
Figure 1.3: Glufosinate foliar uptake in Palmer amaranth plants hydroponically growing in water or 50 mM solutions of glutamine (Gln), glutamate (Glu), asparagine (Asn) or aspartate (Asp) (A). Plants were grown in potting soil, roots were carefully washed and transferred to each aqueous solution. Glufosinate (560 g ha^{-1}) was immediately foliar sprayed following root incubation. Structural similarity between glufosinate and amino acids with acidic side chains and amides (B). Data was pooled from two experiments with three replications (n = 6). *means are significantly different from water (control) by t-test (p<0.05).
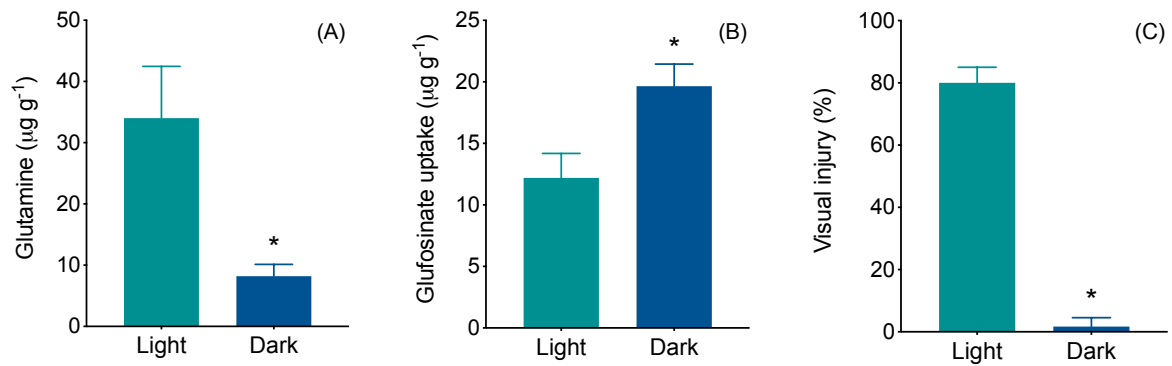
Figure 1.4: Glutamine levels in plants growing under light or dark (A). Glufosinate uptake (B) and visual injury (C) in plants growing under these two conditions. Data was pooled from two experiments with three replications (n = 6). *means are significantly different from water (control) by t-test (p<0.05).
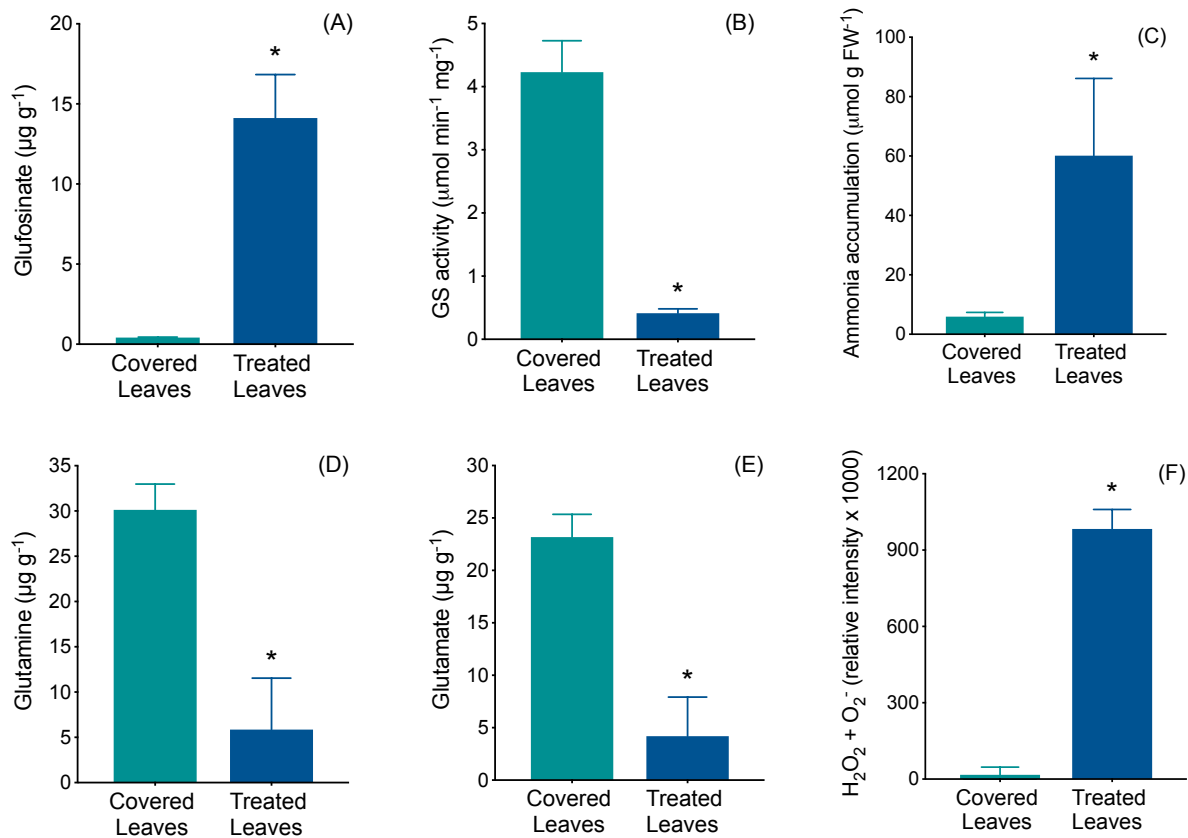
Figure 1.5: Glufosinate concentration (A), glutamine synthetase, GS, activity (B), ammonia accumulation (C), glutamine (D), glutamate (E), and reactive oxygen species (F) levels in covered (green) and treated leaves (blue) of Palmer amaranth. Plants had the two newest fully expanded leaves covered with aluminum foil while the other leaves were treated with 560 g ha^{-1} glufosinate. Covered and treated leaves were collected separately at 24 h after treatment. Data were pooled from two experiments with three replications each (n = 6). *means are significantly different by t-test (p<0.05).
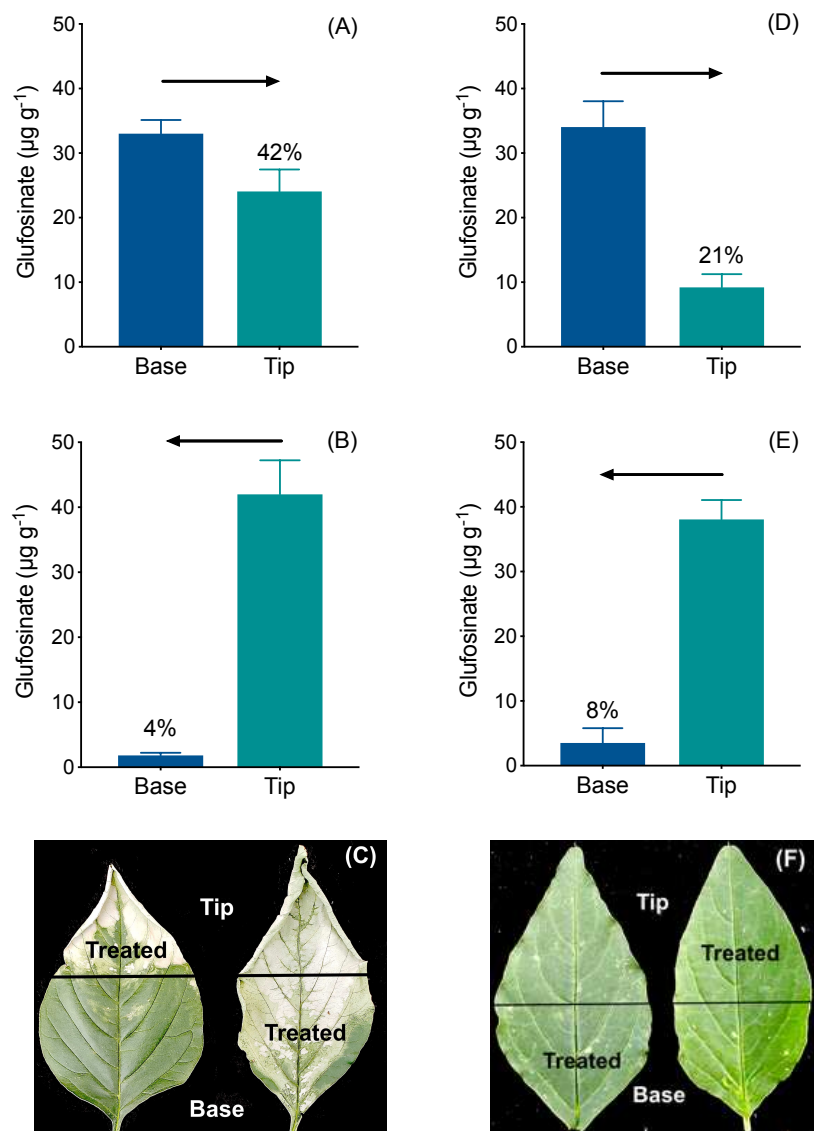
Figure 1.6: Glufosinate movement within a Palmer amaranth leaf under light (A, B and C) and dark (D, E and F) conditions. Glufosinate was applied only on the base side (A and D) or only on the tip side (B and E) of the leaf. Illustration of the acropetal (on the left) and basipetal (on the right) movement (C and F). Data was pooled from two experiments with three replications each (n = 6).
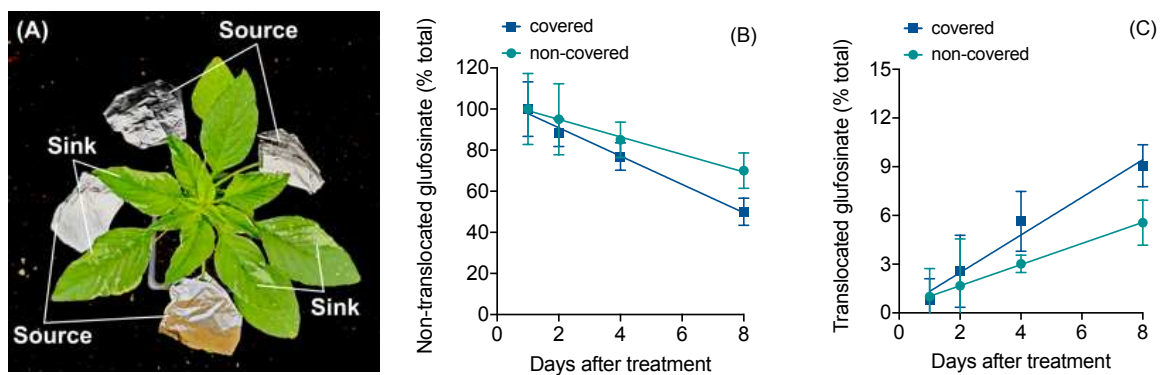
Figure 1.7: Glufosinate movement from source leaves to sink leaves. Four source leaves were treated with glufosinate (140 µg leaf⁻¹, equivalent to 560 g ha⁻¹) and immediately covered with aluminum foil to prevent the light-dependent rapid tissue damage (A). Glufosinate concentration was quantified in applied source leaves (B) and young sink leaves (C).

References

Anderson, D.M.; Swanton, C.J.; Hall, J.C.; Mersey, B.G., 1993. The influence of temperature and relative humidity on the efficacy of glufosinate-ammonium. Weed Research 33: 139-147.

Avila-Garcia, W.V.; Mallory-Smith, C., 2011. Glyphosate-resistant Italian ryegrass (*Lolium perenne*) populations also exhibit resistance to glufosinate. Weed Science 59: 305-309.

Barker, A.L.; Dayan, F.E., 2019. Fate of glyphosate during production and processing of glyphosate-resistant sugar beet (*Beta vulgaris*). Journal of Agricultural and Food Chemistry 67: 2061-2065.

Bayer, E.; Gugel, K.H.; Hägele, K.; Hagenmaier, H.; Jassipow, S.; König, W.A.; Zähner, H., 1972. Stoffwechselprodukte von mikroorganismen. Phosphinothricin und phosphinothricyl-alanyl-alanin. Helvetica Chimica Acta 55: 224-239.

Beriault, J.N.; Horsman, G.P.; Devine, M.D., 1999. Phloem transport of D,L-glufosinate and acetyl-L-glufosinate in glufosinate-resistant and -susceptible *Brassica napus*. Plant Physiology 121: 619-627.

Busi, R.; Goggin, D.E.; Heap, I.M.; Horak, M.J.; Jugulam, M.; Masters, R.A.; Napier, R.M.; Riar, D.S.; Satchivi, N.M.; Torra, J.; Westra, P.; Wright, T.R., 2018. Weed resistance to synthetic auxin herbicides. Pest Management Science 74: 2265-2276.

Carbonari, C.A.; Latorre, D.O.; Gomes, G.L.G.C.; Velini, E.D.; Owens, D.K.; Pan, Z.; Dayan, F.E., 2016. Resistance to glufosinate is proportional to phosphinothricin acetyltransferase expression and activity in LibertyLink® and WideStrike® cotton. Planta 243: 925-933.

Coetzer, E.; Al-Khatib, K.; Loughin, T.M., 2001. Glufosinate efficacy, absorption, and translocation in amaranth as affected by relative humidity and temperature. Weed Science 49: 8-13.

Corrêa, E.A.; Dayan, F.E.; Owens, D.K.; Rimando, A.M.; Duke, S.O., 2016. Glyphosate-resistant and conventional canola (*Brassica napus* L.) responses to glyphosate and aminomethylphosphonic acid (AMPA) treatment. Journal of Agricultural and Food Chemistry 64: 3508-3513.

Dayan, F.E.; Cantrell, C.L.; Duke, S.O., 2009. Natural products in crop protection. Bioorganic and Medicinal Chemistry 17: 4022-4034.

Dayan, F.E.; Owens, D.K.; Corniani, N.; Silva, F.M.L.; Watson, S.B.; Howell, J.L.; Shaner, D.L., 2015. Biochemical markers and enzyme assays for herbicide mode of action and resistance studies. Weed Science 63: 23-63.

Devine, M.D.; Bestman, H.D.; Vanden Born, W.H., 1987. Uptake and accumulation of the herbicides chlorsulfuron and clopyralid in excised pea root tissue. Plant Physiology 85: 82-86.

Forlani, G., 2000. Purification and properties of a cytosolic glutamine synthetase expressed in *Nicotiana plumbaginifolia* cultured cells. Plant Physiology and Biochemistry 38: 201−207.

Hetherington, P.R.; Marshall, G.; Kirkwood, R.C.; Warner, J.M., 1998. Absorption and efflux of glyphosate by cell suspensions. Journal of Experimental Botany 49: 527-533.

Hsu, F.C.; Kleier, D.A., 1996. Phloem mobility of xenobiotics VIII. A short review. Journal of Experimental Botany 47: 1265-1271.

Jalaludin, A.; Yu, Q.; Powles, S.B., 2015. Multiple resistance across glufosinate, glyphosate, paraquat and ACCase-inhibiting herbicides in an *Eleusine indica* population. Weed Research 55: 82-89.

Kondo, Y., 1973. Studies on a new antibiotic SF-1293. I. Isolation and physico-chemical and biological characterization of SF-1293 substance. Scientific Reports of Meijiseika 13: 34-41.

Kumaratilake, A.R.; Lorraine-Colwill, D.F.; Preston, C., 2002. A comparative study of glufosinate efficacy in rigid ryegrass (*Lolium rigidum*) and sterile oat (*Avena sterilis*). Weed Science 50: 560-566.

Kumaratilake, A.R.; Preston, C., 2005. Low temperature reduces glufosinate activity and translocation in wild radish (*Raphanus raphanistrum*). Weed Science 53: 10-16.

Leason, M.; Cunliffe, D.; Parkin, D.; Lea, P.J.; Miflin, B.J., 1982. Inhibition of pea leaf glutamine synthetase by methionine sulphoximine, phosphinothricin and other glutamine analogues. Phytochemistry 21: 855-857.

McNally, S.F.; Hirel, B.; Gadal, P.; Mann, A.F.; Stewart, G.R., 1983. Glutamine synthetases of higher plants: Evidence for a specific isoform content related to their possible physiological role and their compartmentation within the leaf. Plant Physiology 72: 22-25.

Mersey, B.G.; Hall, J.C.; Anderson, D.M.; Swanton, C.J., 1990. Factors affecting the herbicidal activity of glufosinate-ammonium: Absorption, translocation, and metabolism in barley and green foxtail. Pesticide Biochemistry and Physiology 37: 90-98.

Molin, W.T.; Khan, R.A., 1995. Microbioassays to determine the activity of membrane disrupter herbicides. Pesticide Biochemistry and Physiology 53: 172-179.

Oliveira, I.C.; Brears, T.; Knight, T.J.; Clark, A.; Coruzzi, G.M., 2002. Overexpression of cytosolic glutamine synthetase. Relation to nitrogen, light, and photorespiration. Plant Physiology 129: 1170-1180.

Pline, W.A.; Wu, J.; Hatzios, K.K., 1999. Absorption, translocation, and metabolism of glufosinate in five weed species as influenced by ammonium sulfate and pelargonic acid. Weed Science 47: 636-643.

Rubery, P.H., 1977. The specificity of carrier-mediated auxin transport by suspension-cultured crown gall cells. Planta 135: 275-283.

Sellers, B.A.; Smeda, R.J.; Johnson, W.G., 2003. Diurnal fluctuations and leaf angle reduce glufosinate efficacy. Weed Technology 17: 302-306.

Shaner, D.L., 2009. Role of translocation as a mechanism of resistance to glyphosate. Weed Science 57: 118-123.

Shaner, D.L., 2014. Herbicide Handbook. 10th edn. Weed Science Society of America, Lawrence, KS

Sørensen, H.; Cedergreen, N.; Skovgaard, I.M.; Streibig, J.C., 2007. An isobole-based statistical model and test for synergism/antagonism in binary mixture toxicity experiments. Environmental and Ecological Statistics 14: 383-397.

Steckel, G.J.; Hart, S.E.; Wax, L.M., 1997. Absorption and translocation of glufosinate on four weed species. Weed Science 45: 378-381.

Sterling, T.M., 1994. Mechanism of herbicide absorption of plant membranes and accumulation in plant cells. Weed Science 42: 263-276.

Struve, I.; Golle, B.; Lüttge, U., 1987. Sethoxydim-uptake by leaf slices of sethoxydim resistant and sensitive grasses. Zeitschrift für Naturforschung 42C: 279-284.

Takano, H.K.; Beffa, R.; Preston, C.; Westra, P.; Dayan, F.E., 2019a. Reactive oxygen species trigger the fast action of glufosinate. Planta 249: 1837-1849.

Takano, H.K.; Patterson, E.L.; Nissen, S.J.; Dayan, F.E.; Gaines, T.A., 2019b. Predicting herbicide movement across semi-permeable membranes using three phase partitioning. Pesticide Biochemistry and Physiology 159: 22-26.

Thompson, C.J.; Moval, N.R.; Tizard, R.; Crameri, R.; Davies, J.E.; Lauwereys, M.; Botterman, J., 1987. Characterization of the herbicide-resistance gene *bar* from *Streptomyces hygroscopicus*. EMBO Journal 6: 2519-2523.

van Ellis, M.R.; Shaner, D.L., 1988. Mechanism of cellular absorption of imidazolinones in soybean (*Glycine max*) leaf discs. Pesticide Science 23: 25-34.

Womac, A.R.; Melnichenko, G.; Steckel, L.; Montgomery, G.; Hayes, R.M., 2016. Spray tip effect on glufosinate canopy deposits in Palmer amaranth (*Amaranthus palmeri*) for pulse-width modulation versus air-induction technologies. Transactions of the ASABE 59: 1597-1608.

Chapter 2: Why Is Inhibition of Glutamine Synthetase Toxic to Plants?[1]

INTRODUCTION

Glutamine synthetase (GS) is the second most abundant protein in plant leaves, where it plays a vital role in plant nitrogen assimilation by catalyzing the condensation of glutamate and ammonia to yield glutamine (Bernard and Habash, 2009). Plants have two nuclear-encoded GS isoforms; GS_1 localized in the cytosol and GS_2 compartmentalized in the chloroplast, although the proportion of each isoform varies among plant species (McNally et al., 1983; Thomsen et al., 2014). GS_1 is present mainly in vascular bundles (Kamachi et al., 1992) and might be involved in glutamine export to other parts of the plant. GS_2 is mostly present in mesophyll cells, assimilating ammonia from photorespiration into glutamine (Kamachi et al., 1992; Edwards et al., 1990). Even though GS uses glutamate as a substrate to yield glutamine, the formation of glutamate is dependent on the transamination of glutamine to α-ketoglutarate by glutamine-2-oxoglutarate aminotransferase (GOGAT). Both of these enzymes work in concert for the GS/GOGAT cycle (Miflin and Lea, 1976).

Many GS inhibitors have been useful tools to study nitrogen metabolism in plants, but glufosinate ($C_5H_{12}NO_4P$) is the only one that has been developed into a commercial herbicide (Dayan and Duke, 2014). Unlike other inhibitors of amino acid biosynthesis, glufosinate is classified as a contact, broad-spectrum and non-selective herbicide, causing plant tissue death within only a few hours after treatment. It is used in non-crop areas, orchards and vineyards, and for postemergence weed control in transgenic glufosinate-resistant soybean, canola, cotton and corn expressing a phosphinothricin acetyltransferase gene (Liberty Link, BASF).

---

[1] This chapter contains published work from: Takano HK, Beffa R, Preston C, Westra P, Dayan FE (2019) Reactive oxygen species trigger the fast action of glufosinate. Planta 249: 1837–1849.

Commercialized as a synthetic mixture of D- and L-phosphinothricin, only the L-isomer has herbicidal activity, competing with glutamate for the same binding site on GS (Bayer et al., 1972); (Gill and Eisenberg, 2001). This irreversible inhibition stops the conversion of glutamate into glutamine, causing up to 100-fold accumulation of ammonia (Wild et al., 1987). Studies with $[^{15}N]O_3$ suggest that up to 90% of the accumulated ammonia comes from photorespiration (Frantz et al., 1982), possibly by the glycine decarboxylase activity (Douce et al., 2001).

There is a definite association between the mechanism of action of glufosinate and its alteration of the photorespiration pathway (Wendler et al., 1992), with the effect of glufosinate on photosynthesis being higher under photorespiratory conditions (high light intensity and warm temperature), and stronger on C3 species than C4 species (Wendler et al., 1990). However, the cascade of events leading to the extremely rapid glufosinate-induced foliar injury is still unclear. There are two main hypotheses proposed to explain the relationship between inhibition of GS activity and the reduction of photosynthetic carbon assimilation: a) the dramatic accumulation of ammonia inhibits photosynthetic electron flow by binding to the water-splitting complex in photosystem II (Bernard and Habash, 2009; Izawa, 1977), and b) the depletion of glutamate and glutamine affects aminotransferase reactions and results in accumulation of toxic intermediates such as glyoxylate, a known inhibitor of ribulose-1,5-biphosphate carboxylase/oxygenase (Lu et al., 2014; Johansson and Larsson, 1986). Additionally, the lack of amino donors could also restrict the return of glycerate to the Calvin cycle, leading to photosynthesis inhibition (Blackwell et al., 1988).

The effects of GS inhibition on ammonia accumulation and its consequence on carbon assimilation form the basis of our current understanding of the factors leading to plant death. However, our data challenge this paradigm by demonstrating that none of these factors are

directly responsible for the light-dependent generation of reactive oxygen species (ROS) that leads to rapid cell death observed in plants treated with glufosinate. Consequently, the origin of the massive light-dependent production of ROS driving the catastrophic lipid peroxidation of the cell membranes, and rapid cell death, must be reevaluated.

MATERIALS AND METHODS

Chemical Sources

Glufosinate commercial formulation (Liberty 280 g L^{-1}) and analytical D, L-glufosinate were provided by Bayer CropScience, Frankfurt, Germany. Phenol nitroprusside solution, alkaline hypochlorite solution, Tris, ethylenediaminetetraacetic acid (EDTA), dithiothreitol (DTT), MgCl$_2$, polyvinylpyrrolidone (PVP10), and ADP were purchased from Fisher Scientific. Imidazole, MnCl$_2$, L-glutamine, L-glutamate, sodium arsenate, hydroxylamine, anhydrous ferric chloride, nitro blue tetrazolium chloride, potassium phosphate monobasic, sodium azide, 3,3'-diaminobenzidine and hydrochloride acid were purchased from Sigma-Aldrich.

Plant Material Growth

The following weed species were used for experiments: horseweed (*Conyza canadensis*) C3, Palmer amaranth (*Amaranthus palmeri*) C4, johnsongrass (*Sorghum halepense*) C4, kochia (*Kochia scoparia*) C4, and ryegrass (*Lolium rigidum*) C3. Pots with 0.3 L of volume were filled with soil (SunGro Horticulture, Agawam, MA 01001) to grow one plant per pot in the greenhouse until the desired developmental stage. Environmental conditions inside the greenhouse were set up for 25 C, 75% relative humidity, and 12 h light d^{-1} with natural sunlight or 500 μmol m^{-1} s^{-1} PAR for cloudy days. Glufosinate applications were always performed in full sunlight to achieve maximum activity.

Visual Injury

When plants reached 7.5±1.0 cm growth stage, they were sprayed with increasing doses of glufosinate commercial product at 0, 9, 28, 93, 280, 560, 1120 and 2240 g ai ha^{-1}. All doses were sprayed with 2% (w/v) ammonium sulfate (AMS) using a commercial chamber track sprayer equipped with an 8002EVS single even, flat-fan nozzle (TeeJet; Spraying Systems Co., Wheaton, IL, USA) calibrated to deliver 187 L ha^{-1} spray solution at the level of the plant canopy. There were 3 replications for each combination of species and herbicide dose. Visual injury was evaluated at 14 d after treatment using a scale from 0 (no symptoms) to 100 (plant death). Visual injury (visual rating from 0 to 100%) was evaluated over time at 1, 2, 4, 8, 24, 48, 72, 96 and 192 h after treatment (HAT) with 560 g ha^{-1} glufosinate.

Glutamine Synthetase Activity *in Planta*

Glutamine synthetase (GS) activity was quantified by the GS-dependent formation of γ-glutamyl hydroxamate by measuring the transferase activity (Forlani, 2000; Dayan et al., 2015). Similar doses, growth stage, number of replications and spray settings from glufosinate dose response section were used for this assay. Eight HAT, 2 g of leaf material was collected and homogenized in a chilled mortar with 3 mL of extraction buffer. The extraction buffer (pH 8) consisted of 50 mM Tris base, 1 mM EDTA, 2 mM DTT, 10 mM MgCl$_2$, and 50% (w/v) PVP10. The extract was then filtered through miracloth layered on top of cheesecloth after washing the mortar with additional 1 mL extraction buffer. The filtered extract was centrifuged at 12,000 x *g* for 10 min at 4 C. The reaction consisted of 0.9 mL of assay buffer and 0.1 mL of crude enzyme extract, incubated for 30 min at 30 C. The assay buffer consisted of 25 mM imidazole-HCl (pH 7.5), 4 mM MnCl$_2$, 5 mM ADP, 50 mM L-glutamine, 40 mM sodium arsenate, and 25 mM hydroxylamine. To stop the reaction, 0.5 mL ferric chloride reagent was added, and the mixture

was incubated for 10 min at room temperature, followed by centrifugation at 12,000 x g for 10 min. The ferric chloride reagent consisted of 32% (w/v) anhydrous ferric chloride dissolved in 0.5 M HCl. The concentration of γ-glutamyl hydroxamate was determined by measuring absorbance at 540 nm on a spectrophotometer (SynergyTM 2 Multi-Mode Microplate Reader; BioTek, Winooski, VT).

Glutamine Synthetase Activity *in Vitro*

This assay differed from GS activity *in planta* only by the way that GS was exposed to the inhibitor. Crude extract was obtained from untreated plants using the same method from the previous section. An aliquot of 20 μL crude extract was then incubated with 155 μL assay buffer without L-glutamine, and with 5 μL of increasing glufosinate concentrations (0, 0.1, 1, 3, 10, 30, and 100 μM final concentration) for 30 min at 30 C. After the first incubation, 20 μL of 500 mM L-glutamine was added to the solution, followed by a second incubation at 30 C for 30 min. The reaction was stopped and the concentration of γ-glutamyl hydroxamate determined as described above.

Ammonia Accumulation in Leaf Discs

The assay was conducted with leaf discs placed in microtiter plates (Dayan et al., 2015). One 5-mm-diam leaf disc was placed into each well containing 100 μL of eight increasing glufosinate concentrations: 0.0, 1.5, 3.1, 6.2, 12.5, 25.0, 50.0, and 100.0 μM. The plate was then sealed with two layers of micropore tape and placed in a growth chamber at 25 C and 500 μmol $m^{-1} s^{-1}$ PAR of light for 24 h. The assay was stopped by freezing the plate at -80 C, and the cell membranes lysed with two freeze-thaw cycles. An aliquot of 50 μL from each well was transferred to a new plate. Ammonia was measured by adding 150 μL water, 100 μL phenol

nitroprusside solution, and 50 μL alkaline hypochlorite solution (Molin and Khan, 1995). After 30 min incubation at room temperature, absorbance was measured at 540 nm as described above.

Ammonia Accumulation *in Planta*

To quantify ammonia *in planta* the same method used for the assay *in vitro* was employed, except 7.5±1.0 cm-tall plants were treated with glufosinate at the same doses used for visual injury. At 24 h after treatment (HAT), 5-mm-diam leaf discs were collected and placed in each well containing 100 μL water. The plate was immediately frozen at -80 C and ammonia extracted and measured as described above.

Glutamine, Glutamate and Glufosinate Concentrations in Leaf Tissue

Plants 7.5±1.0 cm tall were sprayed with 560 g ha^{-1} glufosinate plus 2% (w/v) AMS as described previously. Control plants were sprayed with AMS only. Leaf tissue (200 mg) was ground with liquid nitrogen with a mortar and pestle. Once ground, 10 mL methanol:water (75:25, v/v) was added, the solution vortexed vigorously for one min, incubated in ultrasonic bath for 30 min and then centrifuged at 4,000 *g* for 10 min. An aliquot of 1.5 mL of the supernatant was filtered through a 0.2 μm nylon filter into an UHPLC vial, and 1 μL of this solution was injected for liquid chromatography - tandem mass spectrometry (LC-MS/MS) analysis.

All samples were analyzed by an LC-MS/MS system (Shimadzu Scientific Instruments, Columbia, MD, USA). The LC–MS/MS system consisted of a Nexera X2 UPLC with 2 LC-30 AD pumps, an SIL-30 AC MP autosampler, a DGU-20A5 Prominence degasser, a CTO-30A column oven, and SPD-M30A diode array detector coupled to an 8040-quadrupole mass-spectrometer. Glutamine, glutamate and glufosinate were separated on an iHilic-Fusion column (100 × 2.1 mm, 3.5 μm; Silica) at a flow rate of 0.2 mL min^{-1} using a linear gradient of

acetonitrile (B) and 25 mM ammonium acetate (A): 2 min, 80% B; 8 min, 30% B; 12 min, 30% B; 12.1 min, 80% B. The MRMs were optimized to 181.95>136.05, 147.95>130.10, 147.10>130.00 for glufosinate, glutamate and glutamine, respectively. Standard curves of serial dilutions of authentic standards were used for quantification. An example of the total ion chromatogram profile is demonstrated as supplemental material (Figure A2.1).

Carbon Assimilation

Control and treated plants (560 g ha^{-1} glufosinate) were sprayed as described above. Carbon assimilation rates were determined by CO_2 exchange measurements using an infrared gas analyzer - IRGA photosynthesis system (LI-COR 6400xt, LI-COR Biosciences). All measurements were performed on the last fully expanded leaf from five replications per species, in treated and untreated plants. As some species show symptoms a few hours after exposure to glufosinate, plants were evaluated at 0.5, 1.5 and 2.5 h after treatment (HAT). CO_2 exchange was assessed at 25 C and 60% relative humidity under 500 μmol m^{-2} s^{-1} irradiation. The air flow rate through the leaf chamber was maintained at 500 μmol s^{-1} and CO_2 concentration of 400 μmol CO_2 mol^{-1}. Following these measurements, leaf area was recorded and used for standardization.

Reactive Oxygen Species

The production of hydrogen peroxide (H_2O_2) and superoxide (O_2^-) was measured by staining leaf discs in solutions containing 3,3'-diaminobendizine (DAB) and nitro blue tetrazolium chloride (NBT), respectively (Fryer et al 2002; Dayan et al 2019). One experiment was conducted with Palmer amaranth (10 cm-tall) only, using stained leaf discs and also whole plants at 1, 2, 4 and 8 HAT with 560 g ha^{-1} glufosinate. After that, all five species were evaluated in another experiment, collecting leaf disc samples at 4 HAT. A third experiment was conducted to compare the amount of ROS produced with glufosinate and other contact herbicides including

atrazine (2000 g ha^{-1}), bentazon (600 g ha^{-1}), saflufenacil (35 g ha^{-1}), lactofen (150 g ha^{-1}) and

paraquat (400 g ha^{-1}). Palmer amaranth was used in this last experiment and measurements were

taken 4 HAT.

The DAB solution contained 0.1 g DAB solubilized in 200 mL water with pH 3.8. The

NBT solution was composed by 0.1 g NBT, 13.6 g potassium phosphate monobasic and 1.3 g

sodium azide in 200 mL water. Sixteen leaf discs (5-mm diam) from control and treated (560 g

ha^{-1} glufosinate) leaves were placed in 20 mL glass tubes containing each staining solution. The

samples were then shaken under 20 Hg vacuum for 1 h. Leaf discs were washed in distilled water

and boiled in 70% (v/v) ethanol solution, having the solution replaced every 20 min for four

cycles. Leaf discs were then stored in 70% (v/v) ethanol solution for 12 h and scanned (Brother

DCP-L2550DW; Bridgewater, NJ, USA). The levels of hydrogen peroxide or superoxide were

quantified using CS3 Photoshop (Adobe Systems, San Jose, CA, USA), measuring the color

intensity in each leaf disc, and removing background levels. Data was represented as relative

intensity of treated samples compared to control samples (treated intensity – control intensity).

Lipid Peroxidation

The levels of malondialdehyde (MDA) were evaluated at 24 HAT in order to quantify

lipid oxidation due to ROS accumulation for all species. The extraction procedure followed the

method described in Hodges *et al*. (1999) with modifications. Shoot tissue samples from control

and glufosinate-treated (560 g ha^{-1}) plants were homogenized with 3 mL of 80:20 (v:v)

ethanol:water. A 2-mL aliquot of the homogenized solution was transferred to a test tube

containing 1 mL of 20% (w/v) trichloroacetic acid and 0.65% (w/v) 2-thiobarbituric acid.

Samples were mixed vigorously for 30 s, heated at 95 C for 30 min, cooled in ice for 5 min, and

centrifuged at 5,000 g for 10 min. Absorbance was measured at 532 and 600 nm and malondialdehyde was calculated as: $MDA\ equivalents\ (nmol\ mL^{-1}) = \frac{[A_{532}-A_{600}]}{155,000}\ 10^6$

Comparison Between Old and New Leaves

A separate experiment was conducted measuring visual injury, glufosinate uptake, *in planta* GS activity and ammonia accumulation, and ROS production (H_2O_2 and O_2^-) in old *vs* new leaves of Palmer amaranth. Plants were grown, sprayed with 560 g ha^{-1} glufosinate and analyzed at 12 HAT as described in the previous sections.

Comparison Between Light and Dark Conditions

Palmer amaranth plants were sprayed with 560 g ha^{-1} glufosinate and placed either under complete dark or light (500 µmol m^2 s^{-1}) conditions. Visual injury and ROS levels ($H_2O_2 + O_2^-$) were evaluated at 12 HAT as described above.

Statistical Analysis

Glufosinate dose response, ammonia leaf disc assay, and GS activity *in planta* and *in vitro* were subjected to non-linear regression using a log-logistic four-parameter model from GraphPad Prism 7 software (GraphPad Software Inc.; La Jolla, CA, USA). Carbon assimilation, glutamate and glutamine levels, ammonia accumulation, visual injury, and malondialdehyde were compared by t-test ($p<0.05$) and standard errors. Glufosinate concentration, and accumulation of reactive oxygen species data were analyzed with ANOVA followed by Tukey's honest significant difference test ($p<0.05$). All graphs were designed using GraphPad Prism 7 software.

RESULTS

Visual Injury

Broadleaf weeds were more sensitive to glufosinate than grasses based on visual injury (Figure 2.1; Table A2.1). Horseweed was the most sensitive species, followed by Palmer amaranth, kochia, johnsongrass and ryegrass. All species, except ryegrass, were 100% controlled by the highest glufosinate dose tested (2,240 g ha^{-1}). The recommended field dose for broadleaves (560 g ha^{-1}) provided 100% phytotoxicity on horseweed, Palmer amaranth and kochia. However, this rate was not effective on the two grasses, causing only 67 and 33% injury to johnsongrass and ryegrass, respectively. By comparing the I_{50} values, ryegrass was 29, 15, 9 and 2-fold more tolerant than horseweed, Palmer amaranth, kochia and johnsongrass, respectively.

The percentage of injury over time also differed among species (Figure 2.1). Palmer amaranth exhibited injury 4 HAT. These symptoms increased until plant death at 96 HAT. Horseweed and kochia responded to glufosinate similarly with symptoms starting at 24 HAT and plants dead at 196 HAT. Symptoms appeared on johnsongrass at 24 HAT, but the plants were not completely killed with 560 g ha^{-1} glufosinate. Glufosinate did not control ryegrass either and symptoms started at low levels at 48 HAT for this species.

Glutamine Synthetase Activity *in Vitro*

When GS was extracted and exposed to the inhibitor *in vitro*, all enzymes responded similarly regardless of the species (Figure 2.2). The I_{50} values ranged from 8.2 μM for horseweed to 17.0 μM for kochia (Table A2.1). Palmer amaranth, ryegrass and johnsongrass had similar I_{50}. Considering all species, the highest glufosinate concentration, 300 μM, provided an average of 91% inhibition of GS activity.

Glutamine Synthetase Activity *in Planta*

In contrast to the *in vitro* enzyme assay, the *in planta* inhibition of GS showed significant differences among species. In general, GS activity in Palmer amaranth was inhibited more than horseweed, kochia, johnsongrass and ryegrass (Figure 2.2). GS activity in all species except ryegrass was almost completely inhibited in plants treated with 2,240 g ha^{-1} glufosinate. For ryegrass plants, this rate only reduced GS activity by 71%. For GS measured *in planta*, ryegrass I$_{50}$ value was 18, 17, 7 and 2 times higher than for Palmer amaranth, horseweed, kochia and johnsongrass, respectively (Table A2.1).

Glufosinate Concentration in Leaves

The highest glufosinate concentrations within leaves were observed for Palmer amaranth, followed by horseweed (Figure 2.3). Kochia and johnsongrass had similar concentrations of glufosinate and ryegrass the least. Palmer amaranth had 4.5-fold more glufosinate in leaf tissues compared to ryegrass. No glufosinate was detected in leaf tissue from untreated plants of any species.

Ammonia Accumulation in Leaf Discs

Ammonia accumulation in leaf discs increased with glufosinate concentrations in all species (Figure 2.4) and correlated with injury. Considering I$_{50}$ values, ryegrass was the least sensitive species to glufosinate for ammonia accumulation and horseweed slightly more sensitive than johnsongrass and the other broadleaf species (Table A2.1).

Ammonia Accumulation *in Planta*

The accumulation of ammonia *in planta* in response to glufosinate application was different for each species (Figure 2.4). Horseweed accumulated high levels of ammonia with low doses of glufosinate. This species was the most sensitive to glufosinate for accumulation of ammonia, followed by Palmer amaranth, kochia, johnsongrass and ryegrass. Comparing the I$_{50}$

values for glufosinate for accumulation of ammonia *in planta*, ryegrass was 33, 15, 9 and 4-fold more tolerant than horseweed, Palmer amaranth, kochia and johnsongrass, respectively. The accumulation of ammonia over time also showed differences among species (Figure A2.2). Horseweed accumulated high levels of ammonia faster than other species. When exposed to glufosinate, horseweed reached the highest levels of ammonia at 2.5 HAT. Palmer amaranth and kochia had an intermediate accumulation of ammonia in response to glufosinate exposure. At 2.5 HAT, kochia and Palmer amaranth had accumulated 58 and 65% of total ammonia, respectively. On the other hand, ryegrass and johnsongrass accumulated very low levels of ammonia at 2.5 HAT.

Glutamate and Glutamine Concentration in Leaves

The amount of glutamate within leaves varied among plant species for untreated plants (Figure 2.5). The highest glutamate level was observed in untreated Palmer amaranth, while it was lowest in the grasses. Glufosinate treatment reduced glutamate concentrations in all species (Table A2.2); however, the amount of depletion varied. Glufosinate reduced glutamate most for kochia (97%), followed by Palmer amaranth (82%), horseweed (86%), ryegrass (49%) and then johnsongrass (24%). Glutamine concentrations were also variable among species (Figure 2.5). As with glutamate, glufosinate treatment resulted in a high depletion of glutamine of 99% in horseweed, 98% in kochia, 97% in Palmer amaranth, 94% in johnsongrass, but only 79% in ryegrass.

Carbon Assimilation

At 0.5 h after treatment (HAT) with glufosinate, Palmer amaranth, johnsongrass and kochia did not exhibit a significant change in carbon assimilation; however, carbon assimilation in horseweed and ryegrass was inhibited (Figure 2.6). At 1.5 HAT, glufosinate inhibited carbon

assimilation in all species, except johnsongrass. Carbon assimilation was inhibited by 25, 38, 61 and 83% for kochia, Palmer amaranth, ryegrass and horseweed, respectively. Carbon assimilation was further inhibited in horseweed and kochia at 2.5 HAT, but not for ryegrass or Palmer amaranth. Carbon assimilation in johnsongrass was not affected by glufosinate treatment.

Reactive Oxygen Species

Glufosinate treatment resulted in the production of reactive oxygen species, which increased over time in Palmer amaranth up to 8 HAT for superoxide and 4 HAT for hydrogen peroxide (Figure 2.7). In general, broadleaf plants produced more reactive oxygen species than grasses in response to 560 g ha^{-1} glufosinate treatment (Table 2.1). Among the broadleaf plants, Palmer amaranth showed the highest production of both hydrogen peroxide and superoxide. Kochia and horseweed produced similar levels of hydrogen peroxide, but higher superoxide levels were observed in kochia. Both grasses produced low levels of the two reactive oxygen species, especially ryegrass.

Lipid Peroxidation

The MDA levels observed in glufosinate-treated plants were greater than those in control samples for all species at 24 HAT (Table 2.1). However, higher MDA accumulation was observed for Palmer amaranth and horseweed than other species. Kochia also showed high accumulation of MDA but lower than the other broadleaves. Johnsongrass and ryegrass had low MDA values.

Comparison Between Old and New Leaves

Visual injury in Palmer amaranth old leaves reached 91±3.7%, whereas new leaves showed little injury (5±1.5%) (Figure 2.8). Uptake of glufosinate was eight times higher in old leaves than in new leaves, but both tissues had similar reduction in GS activity. Both leaf types

also accumulated ammonia proportionally to enzyme inhibition, but old leaves had a much stronger increase in ROS levels than the new leaves (Figure 2.8).

Comparison Between Light and Dark Conditions

Palmer amaranth plants showed 82±1.5% of visual injury under light condition, but only 4±1.2% under dark condition. The production of ROS was also evident only when plants were kept under light. No ROS accumulation was detected in plants placed under complete dark.

DISCUSSION

Even though glufosinate is classified as a non-selective herbicide (Shaner 2014), there was a 29-fold difference in visual injury between ryegrass and horseweed, the most tolerant and most sensitive species in our study, respectively (Figure 2.1 and Table A2.1). Differences of up to 70-fold in sensitivity levels have also been reported for seven other plant species (Ridley and McNally, 1985). Consistent with previous research reporting that glufosinate is generally more toxic to dicot species than to annual monocots (Culpepper et al., 2000), Palmer amaranth and horseweed were sensitive to glufosinate, whereas johnsongrass and ryegrass were more tolerant. The differential response to glufosinate observed for these species was used as a platform to study the physiological basis for the toxic effect of this herbicide on plants. The hypotheses leading to the main findings of this study are discussed below.

Visual Injury Is Proportional to Glufosinate Concentration in Leaves

The five different plant species in our study varied greatly in their sensitivity to glufosinate. However, there was no difference in sensitivity of their respective GS response to the herbicide when tested *in vitro* with I_{50} ranging from 11.2 and 14.1 μM (Figure 2.2). Glufosinate is a transition-state analogue that binds irreversibly to GS (Manderscheid and Wild,

1986). The catalytic domain of GS is highly conserved across species, which may account for the similar sensitivity displayed by various GS from the plants tested in this study. However, when GS activity was measured *in planta*, significant differences in enzyme inhibition by glufosinate occurred among species, correlating with visual injury (Figure 2.1; Figure 2.2). Sensitivity to glufosinate appears to be dependent on the amount of herbicide reaching GS due to differences in uptake, translocation and/or metabolism of glufosinate between species.

Glufosinate concentration in leaves of the grasses (ryegrass and johnsongrass) was lower than in the broadleaf plants (kochia, Palmer amaranth and horseweed) (Figure 2.3), which correlated with their respective *in planta* GS inhibition and ultimately to visual injury. This is consistent with previous reports showing that sensitivity to glufosinate between species correlates with the amount of glufosinate absorbed and translocated. Sensitive species such as sterile oat (*Avena sterilis*) translocate more herbicide than tolerant species like ryegrass (Kumaratilake et al., 2002).

Amino Acid Depletion, Ammonia Accumulation and Carbon Assimilation Inhibition Do Not Explain Differences in Whole Plant Sensitivity Among Species

Inhibition of GS by glufosinate depleted the pool of free glutamine in leaves of all species (Figure 2.5), though less dramatically in ryegrass than the other species. Variation in the amount of glutamine depletion is probably the result of differential inhibition of GS *in planta* among species as discussed above. Similarly, the free pool of glutamate decreased in all species, but less so for ryegrass (Figure 2.5). Although glutamate is a substrate of the reaction catalyzed by GS, the formation of this amino acid depends on the activity of GOGAT, an enzyme that uses glutamine and oxoglutarate to form glutamate (Forde and Lea, 2007). Therefore, the formation of glutamate depends on glutamine and, once glutamine is depleted, glutamate concentration also

decreases. The depletion of glutamine and glutamate can be toxic to plants by restricting the availability of amino group donors (Blackwell et al., 1987). However, if amino acid depletion was the main cause of glufosinate-induced rapid injury, plants would be expected to show symptoms very slowly as seen with other amino acid biosynthesis inhibitors such as glyphosate (Duke and Powles, 2008) and ALS inhibitors (Whitcomb 1999).

It has been argued that high ammonia levels inside the cell could inhibit photosynthetic carbon assimilation (Coetzer and Al-Khatib, 2001). However, we did not find a consistent correlation between ammonia accumulation and carbon assimilation inhibition (Figure A2.2; Figure 2.6). In Palmer amaranth, for example, there was high accumulation of ammonia but only a 30% reduction in carbon assimilation at 2.5 HAT. On the other hand, ryegrass had low accumulation of ammonia, but 81% inhibition of carbon assimilation. These findings suggest that the accumulation of ammonia by itself is insufficient to explain plant injury through inhibition of carbon assimilation. These findings are supported by the fact that ammonia accumulation (up to 40 μmol g^{-1}) did not affect carbon assimilation in mustard leaves under non-photorespiratory conditions (Sauer et al., 1987).

Although a number of studies have demonstrated inhibition of photosynthesis by glufosinate and its relationship with photorespiration (Frantz et al., 1982); (Wendler et al., 1990; Wallsgrove et al., 1987), they have not shown that inhibition of photosynthesis is directly associated with visual injury. In general, inhibition of carbon assimilation was stronger for C3 species than C4 species (Figure 2.6), as reported in other studies (Wendler et al., 1990). For horseweed, strong inhibition of carbon assimilation correlated with high visual injury; however, Palmer amaranth is also sensitive to glufosinate, but its carbon assimilation was only inhibited by 38% at 2.5 HAT. Inhibition of photosynthesis by glufosinate in Palmer amaranth occured over a

56

longer time period. (Coetzer and Al-Khatib, 2001). Likewise, a disconnect between inhibition of carbon assimilation and visual injury was observed for the other species. Ryegrass was highly tolerant to glufosinate in terms of visual injury, but inhibition of photosynthesis was 76% in this species at 2.5 HAT. In contrast, kochia showed high sensitivity to glufosinate but photosynthesis was inhibited less. Thus, the inhibition of carbon assimilation is probably a secondary effect of glufosinate treatment, but not the main driver for the rapid phytotoxicity.

Leaf discs exposed to increasing concentrations of glufosinate accumulated similar levels of ammonia in all species (Figure 2.4). This is probably because floating leaf discs on a solution of the herbicide overcomes differences in glufosinate uptake and the response is commensurate with that of the *in vitro* GS inhibition shown above. However, the various species responded differently when plants were sprayed with glufosinate and ammonia was measured *in planta* (Figure 2.4). While the differences in ammonia accumulation were similar to those observed for visual injury, the ammonia concentrations measured are unlikely to cause rapid plant injury. Krieg et al. (1990) reported a 27-fold ammonia increase in alfalfa exposed to glufosinate compared with untreated plants. However, when untreated plants were then exposed to 100 mM ammonia, exceeding the levels observed in glufosinate-treated plants, no phytotoxicity was observed. The lack of relationship between ammonia accumulation and toxicity was particularly evident in the experiment contrasting the response of young and old leaves of Palmer amaranth (Figure 2.8). GS was inhibited in both leaf-types and was accompanied with dramatic accumulation of ammonia (Figure 2.8). However, old leaves developed severe visual injury whereas young leaves displayed no symptomology (Figure 2.8). Additionally, we have also been able to dramatically increase ammonia levels in leaves by exposing plants to 10 mM glutamine through the roots without causing foliar injury (Figure A2.3). This demonstrates that inhibition

of GS and subsequent accumulation of ammonia are not sufficient to cause injury to plant tissues. The discrepancy between the response in young and old tissue needs to be further investigated as it may provide insight on the inconsistent efficacy of glufosinate in the field.

Reactive Oxygen Species Drive the Fast Action of Glufosinate

Reactive oxygen species (ROS) are extremely phytotoxic and cause loss of membrane integrity via lipid peroxidation (Gill and Tuteja, 2010). This cellular damage can be quantified by measuring malondialdehyde (MDA) content in the leaf tissue, which is a product of this process. Using Palmer amaranth as a model sensitive species, we show that inhibition of GS by glufosinate results in rapid accumulation of ROS, which is consistent with the rapid visual injury observed for this species (Figure 2.7; Table 2.1). Symptoms develop between 4 and 8 HAT (Figure 2.1), matching the time when the ROS levels are increased. Across plant types from our study, broadleaf species had higher concentration of free radicals than grasses, consistent with plant injury (Table 2.1). Palmer amaranth developed injury faster than all other species, which matches with the higher production of both hydrogen peroxide and superoxide in this species. Moreover, the accumulation of ROS was followed by a rapid increase in MDA content, a biomarker of lipid peroxidation and membrane degradation. The accumulation of MDA supports the hypothesis that ROS is the main cause of phytotoxicity, rather than a simple stress in response to GS inhibition.

The contrast between the response of young and old leaves to glufosinate is particularly revealing once again (Figure 2.8). The activity of GS was inhibited in both leaf types, which was accompanied by increase in ammonia levels. However, ROS was induced only in old leaves which developed typical glufosinate injury symptoms whereas the young leaves had no induction of ROS and displayed no injury. In Figure 2.9, we also show that the toxic accumulation of ROS

is light dependent, with the accumulation of these free radicals happening only under light conditions. In this respect, glufosinate's injury by ROS is similar to the mechanism of action of other contact herbicides (Figure 2.10). All these observations support the hypothesis that the rapid injury induced by glufosinate is primarily associated with the production of ROS rather than ammonia accumulation and inhibition of carbon assimilation (Figure 2.11).

In the presence of light, chloroplasts and peroxisomes are the major sources of ROS production in plant cells (Gill and Tuteja 2010). The light-dependent nature of ROS accumulation following glufosinate treatment suggests that the free radicals are generated in these two organelles. In the photorespiration pathway, the conversion of glycolate to glyoxylate by glycolate oxidase generates hydrogen peroxide in the peroxisome (Lu et al. 2014). The inhibition of GS and subsequent photorespiratory ammonia accumulation by glufosinate could enhance the generation of hydrogen peroxide in the peroxisome. Photorespiration and Calvin Cycle constitute major sinks for the excess of electrons generated from the light reactions of photosynthesis (Apel and Hirt, 2004). Inhibition of GS by glufosinate treatment also affected these two pathways, raising the hypothesis that ROS could be generated by the excess of electrons from the light reactions. This could form the basis for why glufosinate has much greater activity under high light intensity. Additional studies are planned to identify the source of the light-dependent ROS accumulating after glufosinate treatment.

In conclusion, our data challenge the long-accepted paradigm that the dramatic accumulation of ammonia and inhibition of carbon assimilation are the main drivers for the rapid phytotoxicity by glufosinate. While ammonia accumulation is a physiological consequence of GS inhibition, it is not the cause of phytotoxicity, and we have now established reactive oxygen species as the main driver for rapid cell death induced by glufosinate. Consequently, the origin

59

of the massive light-dependent production of reactive oxygen species driving the catastrophic

lipid peroxidation of the cell membranes, and rapid cell death, must be evaluated in future

research.

Table 2.1: Levels of hydrogen peroxide (H_2O_2), superoxide (O_2^-) at 4 h after treatment (HAT) and malondialdehyde (MDA) at 12 HAT in horseweed, Palmer amaranth, kochia, ryegrass and johnsongrass treated with 560 g ha^{-1} glufosinate + 2% (w/v) ammonium sulfate. Control plants were sprayed with ammonium sulfate only. Relative intensity (RI) was calculated by the difference between color intensity in leaf discs from treated and control plants. Results are means of 16 replications each (n=16). Different letters indicate significant differences with ANOVA followed by Tukey's test ($p < 0.05$).

	H_2O_2 (RI)[a]		O_2^- (RI)[a]		MDA (nmol mL^{-1})	
Horseweed	853±58	b	482±71	b	1.84±0.06	a
Palmer amaranth	1,552±121	a	625±93	a	1.77±0.05	a
Kochia	963±116	b	375±79	c	1.17±0.03	b
Ryegrass	114±37	d	15±11	e	0.42±0.05	d
Johnsongrass	219±75	c	131±58	d	0.88±0.03	c

[a]RI: Relative Intensity (x1,000) of the dye reaction as percentage of control
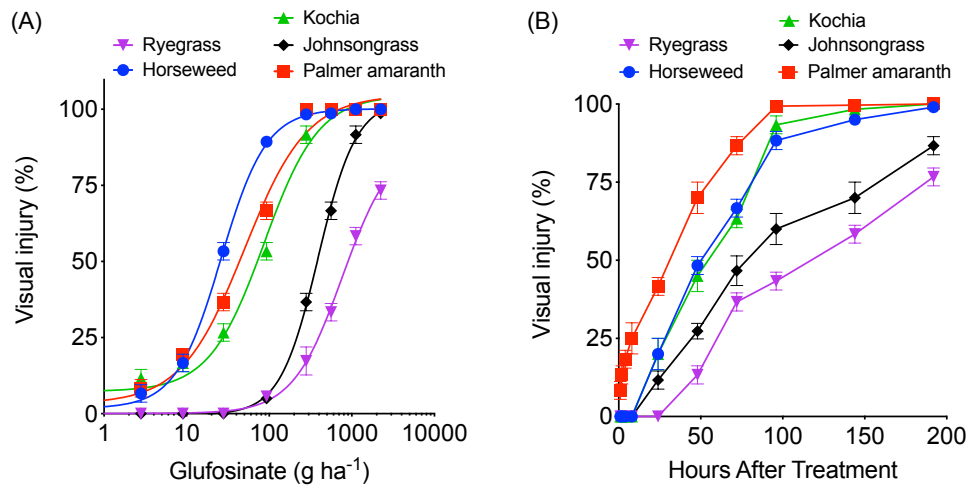
Figure 2.1: Visual injury over increasing doses of glufosinate (A) at 14 DAT and the development of phytotoxicity following 560 g ha^{-1} glufosinate (B) in horseweed, Palmer amaranth, kochia, ryegrass and johnsongrass. All data are presented as percentage of injury compared to the untreated control. Results are pooled means of two experiments with three replications each (n=6). Error bars represent standard errors of the mean.
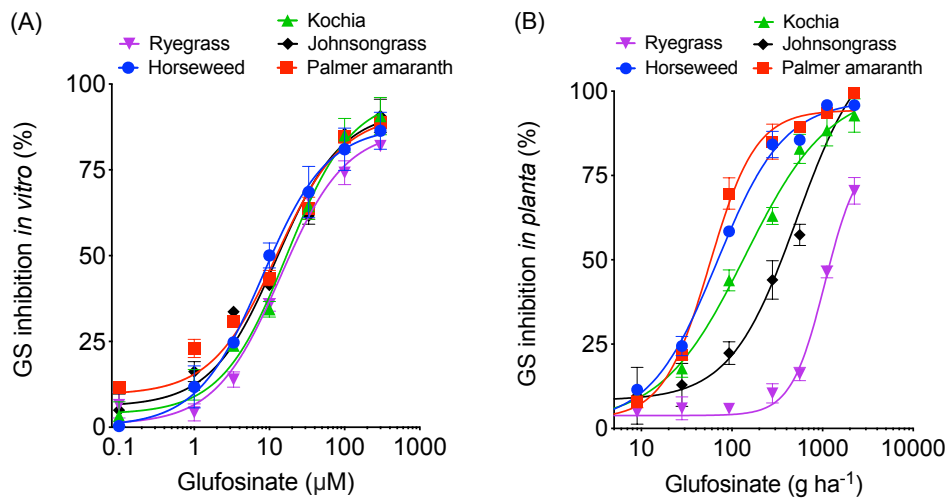
Figure 2.2: Glutamine synthetase (GS) inhibition *in vitro* (A) and glutamine synthetase inhibition *in planta* (B) for horseweed, Palmer amaranth, kochia, ryegrass and johnsongrass. All data are presented as percentage of the untreated control GS activity, which corresponded to 1.64, 2.66, 3.09, 2.75, and 2.97 µmol min^{-1} mg protein^{-1} for ryegrass, johnsongrass, kochia, horseweed, Palmer amaranth, respectively. Results are means of two experiments with three replications each (n=6). Error bars represent standard errors of the mean.
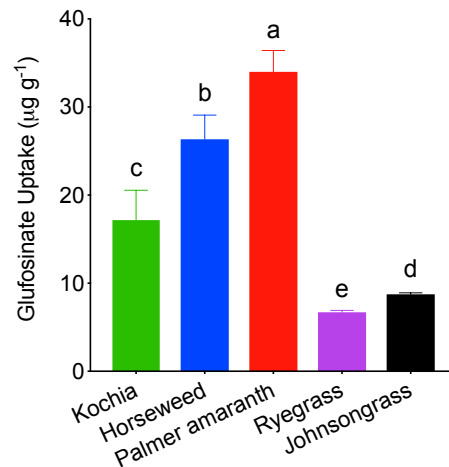
Figure 2.3: Glufosinate uptake in leaves of horseweed, Palmer amaranth, kochia, ryegrass and johnsongrass in response to glufosinate treatment with 560 g ha^{-1} glufosinate + 2% (w/v) ammonium sulfate. Control plants were treated with ammonium sulfate only. Results are means of two experiments with three replications each (n=6). Error bars represent standard errors. Different letters indicate significant differences with ANOVA followed by Tukey's test (p<0.05).
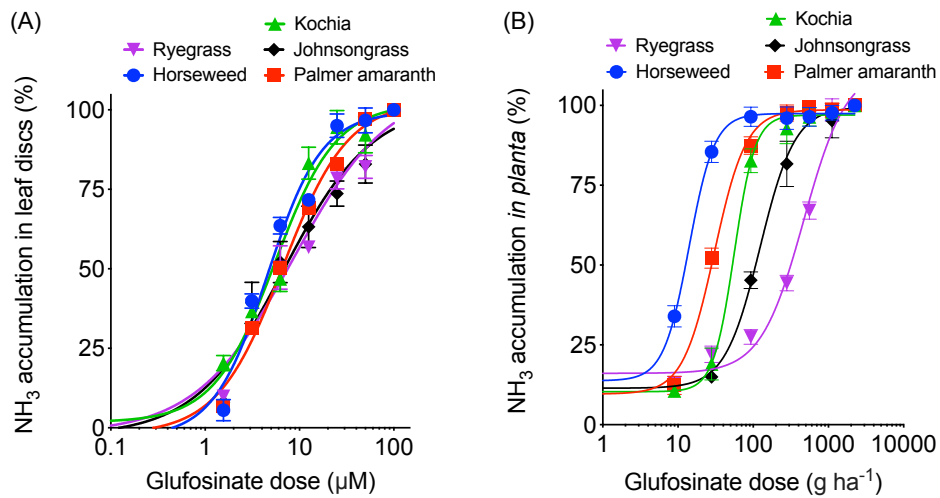
Figure 2.4: Ammonia accumulation in leaf discs (A) and ammonia accumulation *in planta* (B) with increasing glufosinate doses, for horseweed, Palmer amaranth, kochia, ryegrass and johnsongrass. Units were converted to percent of the maximum accumulation of ammonia in each species, which were 26, 33, 44, 52, and 57 µmol g fw^{-1} for ryegrass, johnsongrass, kochia, horseweed, Palmer amaranth, respectively.
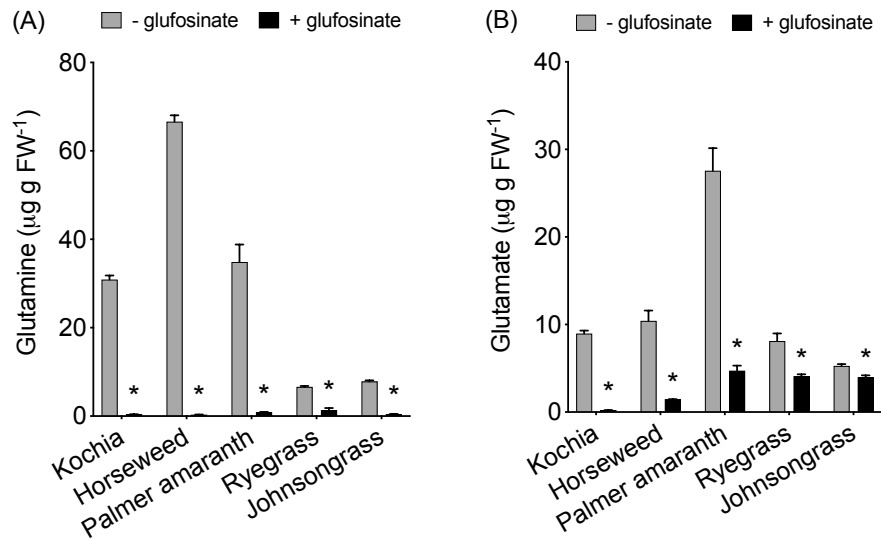
Figure 2.5: Concentrations of glutamine (A) and glutamate (B) in leaves of horseweed, Palmer amaranth, kochia, ryegrass and johnsongrass following treatment with 560 g ha^{-1} glufosinate + 2% (w/v) ammonium sulfate. Untreated plants were treated with ammonium sulfate only. Results are means of two experiments with three replications each (n=6). Error bars represent standard errors of the mean. *, significant by t-test (p<0.05).
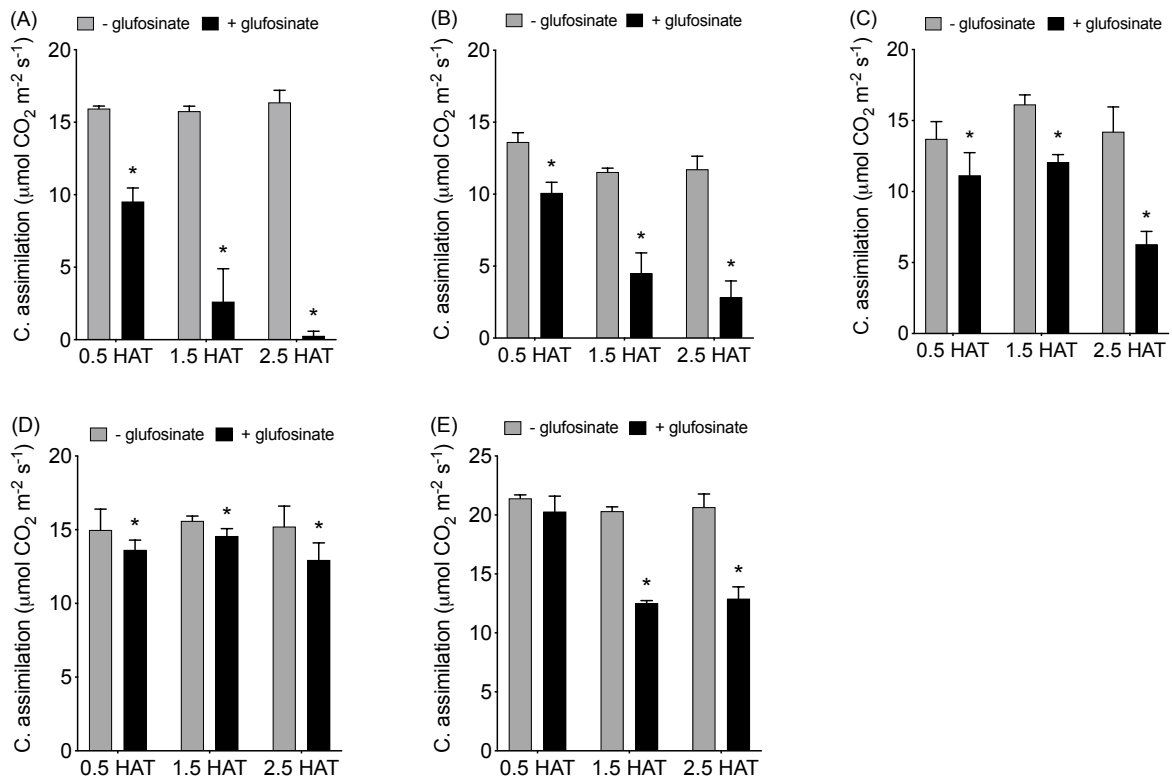
Figure 2.6: Carbon assimilation in horseweed (A), ryegrass (B), kochia (C), johnsongrass (D), and Palmer amaranth (E) at 0.5, 1.5 and 2.5 HAT with 560 g ha^{-1} glufosinate + 2% ammonium sulfate (w/v). Control plants were treated with ammonium sulfate only. Results are means of two experiments with five replications each (n=10). Error bars represent standard errors of the mean. *, significant by t-test (p<0.05).
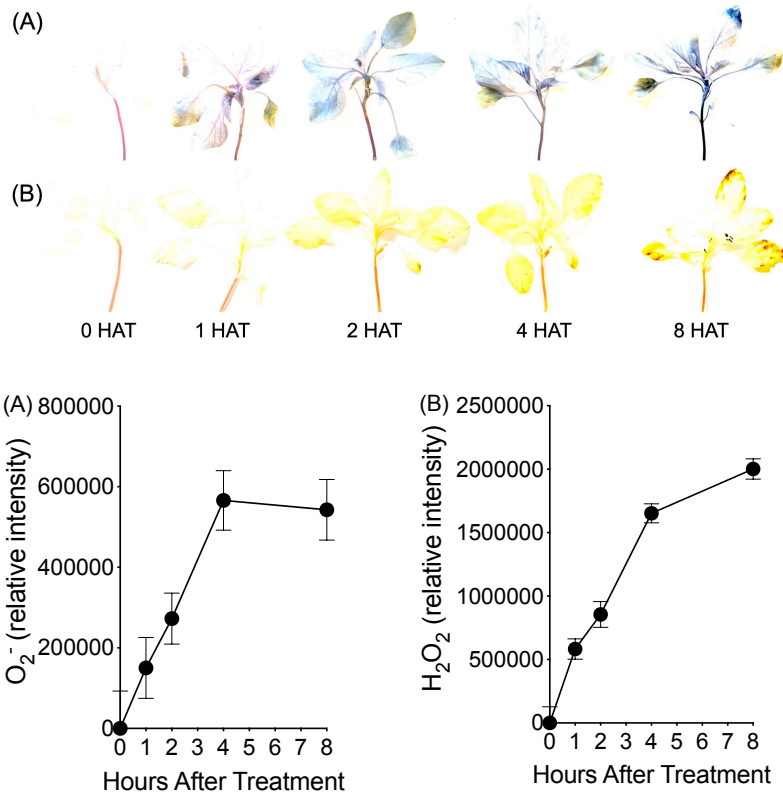
Figure 2.7: Superoxide (A) and hydrogen peroxide (B) levels in Palmer amaranth over time after treatment with 560 g ha^{-1} glufosinate + 2% ammonium sulfate (w/v). Relative intensity was calculated by the difference between color intensity in leaf discs from treated and control plants. Control plants were treated with ammonium sulfate only. Results are means of sixteen replications each (n=16). Error bars represent standard errors of the mean.
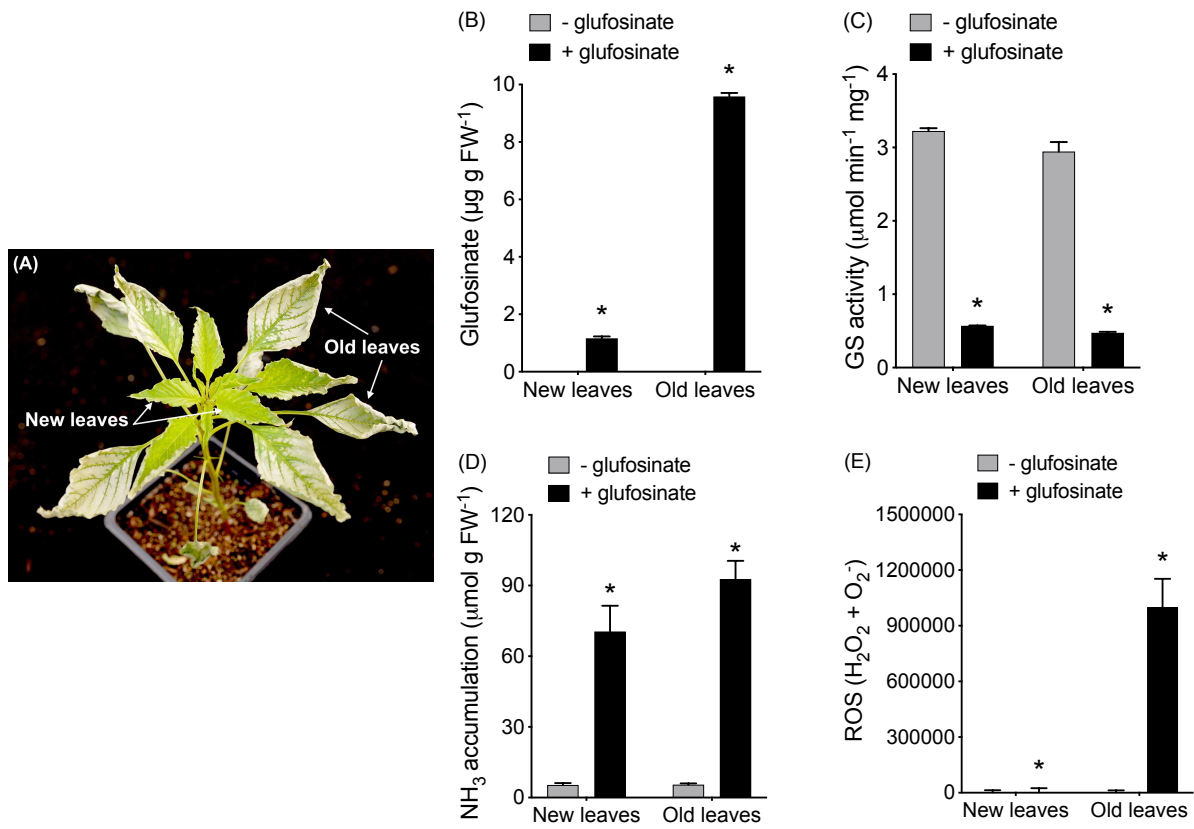
Figure 2.8: Comparison between new *vs* old leaves for visual injury (A), glufosinate levels (B), glutamine synthetase activity (C), ammonia accumulation (D), and reactive oxygen species (E) in Palmer amaranth treated with 560 g ha^{-1} glufosinate + 2% (w/v) ammonium sulfate. Control plants were treated with ammonium sulfate only. Results are means of six replications each (n=6). Error bars represent standard errors of the mean. *, comparison between glufosinate-treated *vs* control plants is significant by t-test (p<0.05).
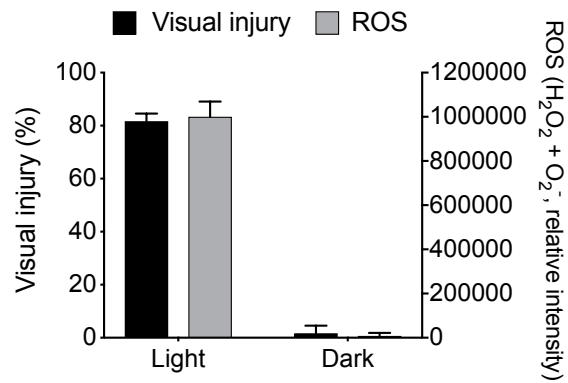
Figure 2.9: Relationship between visual injury and reactive oxygen species in glufosinate-treated Palmer amaranth plants under light *vs* dark conditions. The data indicate light-dependent reactive oxygen species (ROS) production in glufosinate-treated plants. Results are means of three replications each and error bars represent standard errors of the mean.
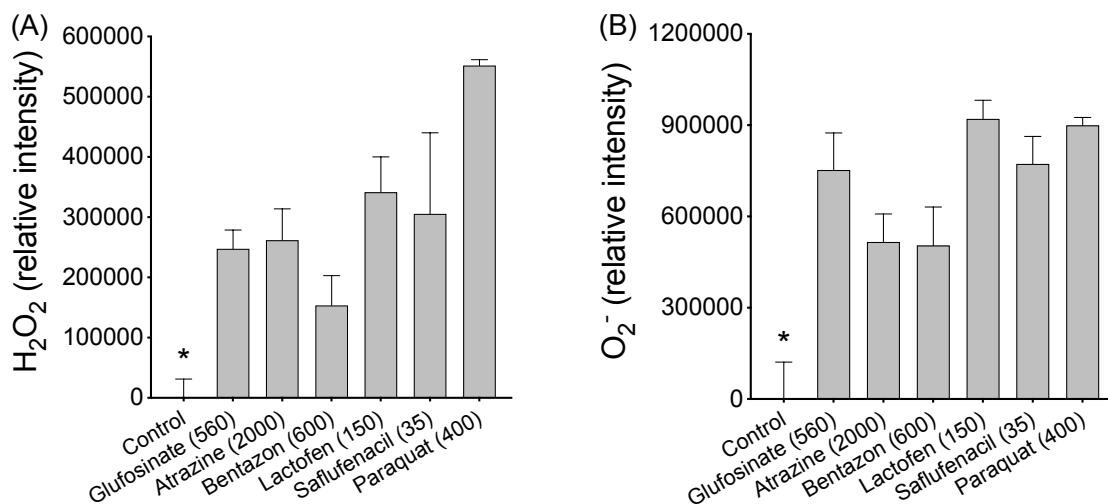
Figure 2.10: Hydrogen peroxide (A) and superoxide (B) levels in Palmer amaranth plants treated with different contact herbicides. Doses are within parenthesis and represented as g of active ingredient ha^{-1}. Results are means of three replications each and error bars represent standard errors of the mean. *, comparison between control plants *vs* other treatments is significant by t-test ($p < 0.05$).
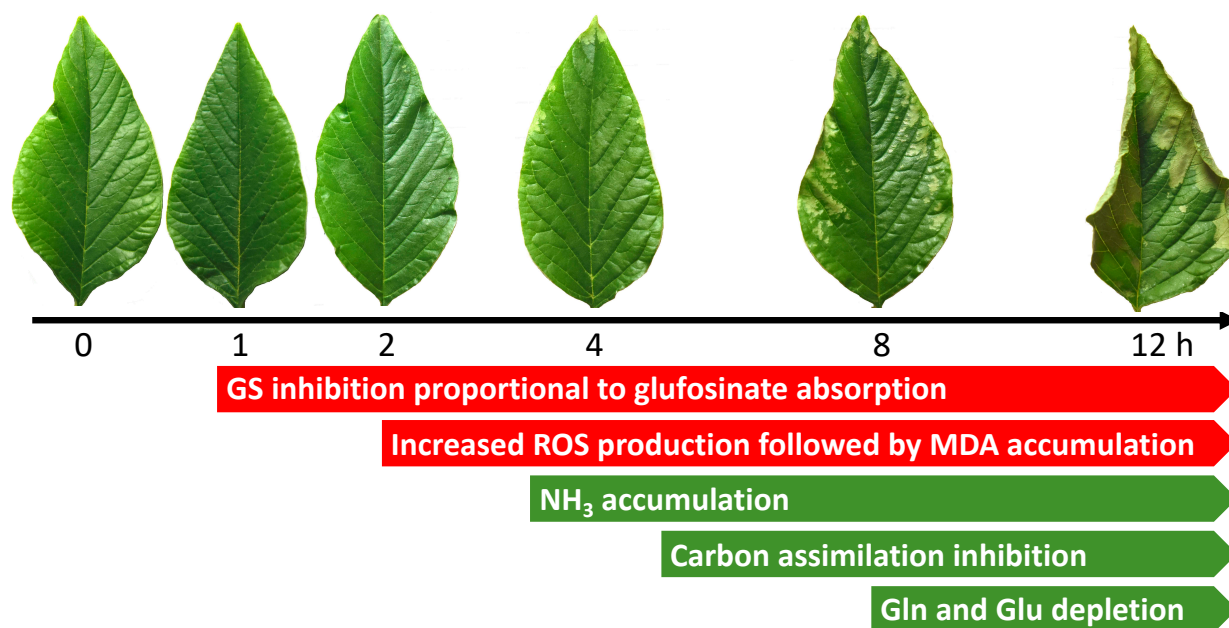
Figure 2.11: The cascade of events leading to glufosinate-induced rapid injury in Palmer amaranth over time. The rapid phytotoxicity results from inhibition of glutamine synthetase, which is proportional to glufosinate absorption, causing increased production of reactive oxygen species (ROS) and malondialdehyde (MDA) (red). Ammonia accumulation, carbon assimilation inhibition and changes in amino acid levels seem to be a secondary effect of glutamine synthetase inhibition. These changes might be toxic to plants only at long term but do not contribute to the contact activity of glufosinate.

References

Apel, K.; Hirt, H., 2004. Reactive oxygen species: metabolism, oxidative stress, and signal transduction. Annual Review of Plant Biology 55: 373-399.

Bayer, E.; Gugel, K.H.; Hägele, K.; Hagenmaier, H.; Jassipow, S.; König, W.A.; Zähner, H., 1972. Stoffwechselprodukte von mikroorganismen. Phosphinothricin und phosphinothricyl-alanyl-alanin. Helvetica Chimica Acta 55: 224-239.

Bernard, S.M.; Habash, D.Z., 2009. The importance of cytosolic glutamine synthetase in nitrogen assimilation and recycling. New Phytologist 182: 608-620.

Blackwell, R.D.; Murray, A.J.S.; Lea, P.J., 1987. Inhibition of photosynthesis in barley with decreased levels of chloroplastic glutamine synthetase activity. Journal of Experimental Botany 38: 1799-1809.

Blackwell, R.D.; Murray, A.J.S.; Lea, P.J.; Kendall, A.C.; Hall, N.P.; Turner, J.C.; Wallsgrove, R.M., 1988. The value of mutants unable to carry out photorespiration. Photosynthesis Research 16: 155-176.

Coetzer, E.; Al-Khatib, K., 2001. Photosynthetic inhibition and ammonium accumulation in Palmer amaranth after glufosinate application. Weed Science 49: 454-459.

Culpepper, A.S.; York, A.C.; Batts, R.B.; Jennings, K.M., 2000. Weed management in glufosinate- and glyphosate-resistant soybean (*Glycine max*). Weed Technology 14: 77-88.

Dayan, F.E.; Duke, S.O., 2014. Natural compounds as next generation herbicides. Plant Physiology 166: 1090-1105.

Dayan, F.E.; Owens, D.K.; Corniani, N.; Silva, F.M.L.; Watson, S.B.; Howell, J.L.; Shaner, D.L., 2015. Biochemical markers and enzyme assays for herbicide mode of action and resistance studies. Weed Science 63: 23-63.

Douce, R.; Bourguignon, J.; Neuburger, M.; Rébeillé, F., 2001. The glycine decarboxylase system: a fascinating complex. Trends in Plant Science 6: 167-176.

Edwards, J.W.; Walker, E.L.; Coruzzi, G.M., 1990. Cell-specific expression in transgenic plants reveals nonoverlapping roles for chloroplast and cytosolic glutamine synthetase. Proceedings of the National Academy of Sciences, USA 87: 3459-3463.

Forde, B.G.; Lea, P.J., 2007. Glutamate in plants: metabolism, regulation, and signalling. Journal of Experimental Botany 58: 2339-2358.

Forlani, G., 2000. Purification and properties of a cytosolic glutamine synthetase expressed in *Nicotiana plumbaginifolia* cultured cells. Plant Physiology and Biochemistry 38: 201−207.

Frantz, T.A.; Peterson, D.M.; Durbin, R.D., 1982. Sources of ammonium in oat leaves treated with tabtoxin or methionine sulfoximine. Plant Physiology 69: 345-348.

Gill, H.S.; Eisenberg, D., 2001. The crystal structure of phosphinothricin in the active site of glutamine synthetase illuminates the mechanism of enzymatic inhibition. Biochemistry 40: 1903-1912.

Gill, S.S.; Tuteja, N., 2010. Reactive oxygen species and antioxidant machinery in abiotic stress tolerance in crop plants. Plant Physiology and Biochemistry 48: 909-930.

Izawa, S. (1977) Inhibition of electron transport. In: Trebst A., Avron M. (eds) Encyclopedia of plant physiology. Springer Verlag, Berlin, pp 266-279

Johansson, L.; Larsson, C.-M., 1986. Relationship between inhibition of CO_2 fixation and glutamine synthetase inactivation in *Lemna gibba* L. treated with L-methionine-D, L-sulphoximine (MSO). Journal of Experimental Botany 37: 221-229.

Kamachi, K.; Yamaya, T.; Hayakawa, T.; Mae, T.; Ojima, K., 1992. Vascular bundle-specific localization of cytosolic glutamine synthetase in rice leaves. Plant Physiology 99: 1481-1486.

Krieg, L.C.; Walker, M.A.; Senaratna, T.; McKersie, B.D., 1990. Growth, ammonia accumulation and glutamine synthetase activity in alfalfa (*Medicago sativa* L.) shoots and cell cultures treated with phosphinothricin. Plant Cell Reports 9: 80-83.

Kumaratilake, A.R.; Lorraine-Colwill, D.F.; Preston, C., 2002. A comparative study of glufosinate efficacy in rigid ryegrass (*Lolium rigidum*) and sterile oat (*Avena sterilis*). Weed Science 50: 560-566.

Lu, Y.; Li, Y.; Yang, Q.; Zhang, Z.; Chen, Y.; Zhang, S.; Peng, X.-X., 2014. Suppression of glycolate oxidase causes glyoxylate accumulation that inhibits photosynthesis through deactivating Rubisco in rice. Physiologia Plantarum 150: 463-476.

Manderscheid, R.; Wild, A., 1986. Studies on the mechanism of inhibition by phosphinothricin of glutamine synthetase isolated from *Triticum aestivum* L. Journal of Plant Physiology 123: 135-142.

McNally, S.F.; Hirel, B.; Stewart, G.R., 1983. Nitrogen metabolism in halophytes 5. The occurence of multiple forms of glutamine synthetase in leaf tissue. New Phytologist 94: 47-56.

Miflin, B.J.; Lea, P.J., 1976. The pathway of nitrogen assimilation in plants. Phytochemistry 15: 873-885.

Molin, W.T.; Khan, R.A., 1995. Microbioassays to determine the activity of membrane disrupter herbicides. Pesticide Biochemistry and Physiology 53: 172-179.

Ridley, S.M.; McNally, S.F., 1985. Effects of phosphinothricin on the isoenzymes of glutamine synthetase isolated from plant species which exhibit varying degrees of susceptibility to the herbicide. Plant Science 39: 31-36.

Sauer, H.; Wild, A.; Rühle, W., 1987. The effect of phosphinothricin (glufosinate) on photosynthesis II. The causes of inhibition of photosynthesis. Zeitschrift für Naturforschung 42C: 270-278.

Sørensen, H.; Cedergreen, N.; Skovgaard, I.M.; Streibig, J.C., 2007. An isobole-based statistical model and test for synergism/antagonism in binary mixture toxicity experiments. Environmental and Ecological Statistics 14: 383-397.

Thomsen, H.C.; Eriksson, D.; Møller, I.S.; Schjoerring, J.K., 2014. Cytosolic glutamine synthetase: a target for improvement of crop nitrogen use efficiency? Trends in Plant Science 19: 656-663.

Wallsgrove, R.M.; Turner, J.C.; Hall, N.P.; Kendall, A.C.; Bright, S.W., 1987. Barley mutants lacking chloroplast glutamine synthetase-biochemical and genetic analysis. Plant Physiology 83: 155-158.

Wendler, C.; Barniske, M.; Wild, A., 1990. Effect of phosphinothricin (glufosinate) on photosynthesis and photorespiration of C_3 and C_4 plants. Photosynthesis Research 24: 55-61.

Wendler, C.; Putzer, A.; Wild, A., 1992. Effect of glufosinate (phosphinothricin) and inhibitors of photorespiration on photosynthesis and ribulose-1,5-bisphosphate carboxylase activity. Journal of Plant Physiology 139: 666-671.

Wild, A.; Sauer, H.; Ruhle, W., 1987. The effect of phosphinothricin (glufosinate) on photosynthesis. I. Inhibition of photosynthesis and accumulation of ammonia. Zeitschrift für Naturforschung 42C: 263-269.

Chapter 3: A New Understanding on the Mechanism of Action of Glufosinate

INTRODUCTION

Glufosinate is commercialized as a racemic mixture of D- and L-phosphinothricin, which was first discovered as a natural tripeptide produced by bacteria of the genus *Streptomyces* (Bayer et al., 1972; Seto et al., 1983). Glufosinate-resistant crops (Liberty Link, BASF) express the *phosphinothricin acetyl-transferase* (*pat*) gene and metabolize L-phosphinothricin into N-acetyl-L-phosphinothricin (Strauch et al., 1988). It is a non-selective herbicide with a broad spectrum of weed control, used mainly in non-crop areas or in glufosinate-resistant crops in post emergence or pre-plant burndown. Glufosinate has been in the market for more than 25 years, but its use has increased in the past few years due to the evolution of glyphosate resistant weeds (Duke, 2011). The total treated area with glufosinate around the world is estimated at 12 million ha, including corn, soybean, cotton, canola, trees, vineyards and orchards (Busi et al., 2018).

L-phosphinothricin irreversibly inhibits glutamine synthetase (GS), a key enzyme responsible for incorporating ammonia from photorespiration into glutamate to yield glutamine (Leason et al., 1982; Edwards and Coruzzi, 1989). Unlike other amino acid biosynthesis inhibitors, glufosinate-treated plants are injured within a few hours after treatment (Dayan and Duke, 2014). When plants are treated with glufosinate, ammonia accumulates at high levels, which has been attributed as the causal agent for rapid response (Tachibana et al., 1986). Another hypothesis that has been associated to phytotoxicity is the inhibition on carbon assimilation (Wild et al., 1987). Recent research has shown that neither ammonia accumulation nor carbon assimilation inhibition is consistent with the development of symptoms in glufosinate-treated plants. The reason for the rapid phytotoxicity is the massive accumulation of

76

reactive oxygen species (ROS) (Takano et al., 2019). The formation of these free radicals causes lipid membrane peroxidation and, therefore, rapid plant cell death (Halliwell, 1987); however, the mechanism for ROS generation in glufosinate-treated plants has not been reported.

In order to generate ROS, ground state oxygen becomes reactive by either energy transfer or electron transport reactions, leading to singlet oxygen or superoxide formation, respectively (Apel and Hirt, 2004). Singlet oxygen is the first excited electronic state of molecular oxygen with all electrons in parallel spin (Triantaphylidès and Havaux, 2009). Once a singlet oxygen is formed, it can also be reduced to superoxide, hydrogen peroxide, and hydroxyl radical (Cadenas, 1989). Chloroplasts, mitochondria and peroxisomes are the main organelles where ROS are generated in plants (Gill and Tuteja, 2010). Aerobic metabolic processes in plants such as photosynthesis and respiration naturally form ROS, but plants have scavenging mechanisms to protect themselves against the damage caused by these molecules (Apel and Hirt, 2004). ROS accumulation by glufosinate treatment demonstrates that the equilibrium between the production and scavenging of these free radicals is disturbed when GS is inhibited.

In this manuscript, we describe how the inhibition of GS by glufosinate leads to the massive light-dependent ROS accumulation in plants. Photorespiration is one of the major sinks for the excess of electrons generated in the light reactions (Kozaki and Takeba, 1996), in which GS plays a key role assimilating ammonia into amino acids. Under high light intensity, the inhibition of GS and subsequent accumulation of ammonia stops photorespiration, and consequently, the electron flow from light reactions. The excess of electrons is then accepted by oxygen atoms, leading to the generation of ROS. These findings form a new paradigm for the mechanism of action of glufosinate.

MATERIAL AND METHODS

Chemical Sources

Glufosinate commercial formulation (Liberty 280 g L^{-1}), analytical D, L-glufosinate and atrazine were provided by Bayer CropScience (Monheim am Rhein, Germany 40789). Phenol nitroprusside solution, alkaline hypochlorite solution, Tris, ethylenediaminetetraacetic acid (EDTA), dithiothreitol (DTT), $MgCl_2$, polyvinylpyrrolidone (PVP10), dinoseb, sorbitol, and ADP were purchased from Fisher Scientific (Waltham, WI 02451). Imidazole, $MnCl_2$, L-glutamine, L-glutamate, sodium arsenate, hydroxylamine, anhydrous ferric chloride, nitro blue tetrazolium chloride, potassium phosphate monobasic, sodium azide, 3,3'-diaminobenzidine, malondialdehyde, L-methionine, Triton-X100, H_2O_2, cysteine, DTNB, glutathione, NADPH, *N,N*-dimethiylformamide in the presence of ribitol and hydrochloride acid were purchased from Sigma-Aldrich (St. Louis, MO 63103).

Plant Material and Growth

Palmer amaranth (*Amaranthus palmeri*) was used as a model species to investigate the sources of reactive oxygen species (ROS) when glutamine synthetase is inhibited by glufosinate. Plants were grown until the 6-leaf-stage in 0.3 cm^3 pots filled with soil (SunGro Horticulture, Agawam, MA 01001). Greenhouse conditions were 25/21 C day/night, 16 h photoperiod with natural sunlight or 500 μmol m^{-2} s^{-1}, and 70% relative humidity.

Effect of Light on Glufosinate Activity

Plants were sprayed with 560 g ha^{-1} glufosinate + 3% ammonium sulfate (AMS) using a commercial chamber track sprayer (DeVries Manufacturing, Inc., Hollandale, MN 56045) equipped with an 8002EVS single even, flat-fan nozzle (TeeJet; Spraying Systems Co., Denver, CO 80207) calibrated to deliver 187 L ha^{-1} spray solution at the level of the plant canopy.

Sprayed plants were immediately placed under complete dark or light (500 µmol m^{-2} s^{-1}) conditions. At 8 h after treatment (HAT), three replications for each condition were evaluated for visual injury (0-100% scale), glutamine synthetase activity, and levels of hydrogen peroxide, superoxide, and malondialdehyde. The experiment was repeated and data were pooled (n = 6).

Glutamine synthetase (GS) activity was quantified by the GS-dependent formation of γ-glutamyl hydroxamate by measuring the transferase activity (Forlani, 2000; Dayan et al., 2015). Two g of leaf material was collected and homogenized in a chilled mortar with 3 mL of extraction buffer. The extraction buffer (pH 8) consisted of 50 mM Tris base, 1 mM EDTA, 2 mM DTT, 10 mM MgCl$_2$, and 50% (w/v) PVP10. The extract was then filtered through miracloth layered on top of cheesecloth after washing the mortar with additional 1 mL extraction buffer. The filtered extract was centrifuged at 12,000 × g for 10 min at 4 C. The reaction consisted of 0.9 mL of assay buffer and 0.1 mL of crude enzyme extract, incubated for 30 min at 30 C. The assay buffer consisted of 25 mM imidazole-HCl (pH 7.5), 4 mM MnCl$_2$, 5 mM ADP, 50 mM L-glutamine, 40 mM sodium arsenate, and 25 mM hydroxylamine. To stop the reaction, 0.5 mL ferric chloride reagent was added, and the mixture was incubated for 10 min at room temperature, followed by centrifugation at 12,000 × g for 10 min. The ferric chloride reagent consisted of 32% (w/v) anhydrous ferric chloride dissolved in 0.5 M HCl. The concentration of γ-glutamyl hydroxamate was determined by measuring absorbance at 540 nm on a spectrophotometer (Synergy^{TM} 2 Multi-Mode Microplate Reader; BioTek, Winooski, VT).

Ammonia was quantified using leaf discs collected from the sprayed plants (Dayan et al., 2015). One 5-mm-diam leaf disc was placed into each well containing 100 µL of water. The plate was then sealed with two layers of micropore tape and placed in the growth chamber at 25 C and 500 µmol m^{-1} s^{-1} PAR of light for 24 h. The assay was stopped by freezing the plate at -80

C, and the cell membranes lysed with two freeze-thaw cycles. An aliquot of 50 µL from each well was transferred to a new plate. Ammonia was measured by adding 150 µL water, 100 µL phenol nitroprusside solution, and 50 µL alkaline hypochlorite solution (Molin and Khan, 1995). After 30 min incubation at room temperature, absorbance was measured at 540 nm.

Hydrogen peroxide (H_2O_2) and superoxide (O_2^-) were measured by staining leaf discs in solutions containing 3,3'-diaminobendizine (DAB) and nitro blue tetrazolium chloride (NBT), respectively (Fryer et al., 2002; Dayan et al., 2019). The DAB solution contained 0.1 g DAB solubilized in 200 mL water with pH 3.8. The NBT solution was composed by 0.1 g NBT, 13.6 g potassium phosphate monobasic and 1.3 g sodium azide in 200 mL water. Sixteen leaf discs (5-mm diam) from control and treated (560 g ha^{-1} glufosinate) leaves were placed in 20 mL glass tubes containing each staining solution. The samples were then shaken under 20 Hg vacuum for 1 h. Leaf discs were washed in distilled water and boiled in 70% (v/v) ethanol solution, having the solution replaced every 20 min for four cycles. Leaf discs were then stored in 70% (v/v) ethanol solution for 12 h and scanned (Brother DCP-L2550DW; Bridgewater, NJ, USA). The levels of hydrogen peroxide or superoxide were quantified using CS3 Photoshop (Adobe Systems, San Jose, CA, USA), measuring the color intensity in each leaf disc, removing background levels. Data was represented as relative intensity of treated samples compared to control samples (treated intensity – control intensity).

Levels of malondialdehyde (MDA) were quantified to estimate ROS-based lipid oxidation. The protocol followed the method described elsewhere (Hodges et al., 1999; Morales and Munné-Bosch, 2019). Shoot tissue samples were homogenized with 3 mL of 80:20 (v:v) ethanol:water. A 2-mL aliquot of the homogenized solution was transferred to a test tube containing 1 mL of 20% (w/v) trichloroacetic acid and 0.65% (w/v) 2-thiobarbituric acid.

Samples were mixed vigorously for 30 s, heated at 95 C for 30 min, cooled in ice for 5 min, and centrifuged at $5,000 \times g$ for 10 min. Absorbance was measured at 532 and 600 nm to estimate MDA levels (nmol mL^{-1}).

Quantification of Photorespiration Metabolites

Plants were sprayed with glufosinate as described above and leaf tissue was collected and frozen at 8 HAT. Samples were analyzed with gas chromatography coupled to a time-of-flight mass spectrometry (GC-MS, Thermo Scientific TOF-MS) as described elsewhere (Lisec et al., 2006; Kerchev et al., 2016) with modifications. An aliquot of 0.1 g was ground with liquid nitrogen and homogenized with 600 μL ice-cold *N,N*-dimethilformamide in the presence of 6 μg ribitol as internal standard. Water (400 μL) was added to each sample before shaking for 10 min at 4 C and centrifuging for 10 min at $16,000 \times g$. The supernatant was transferred to a new tube, mixed with 600 μL xylene for 10 min and centrifuged at $16,000 \times g$ for 5 min. The lower aqueous phase was dried under vacuum before derivatizing with 40 μL of 20 mg mL^{-1} methoxyamine hydrochloride in pyridine for 120 min at 37 C, followed by 30-min incubation with 70 μL of *N*-methyl-*N*-(trimethylsilyl)trifluoroacetamide. Helium was the carrier gas at 2 mL s^{-1}, and the stationary phase was performed by a TG-5MS column. The injection temperature was 230°C, and the transfer line and ion source were set to 250°C. The initial temperature of the oven was 85°C and increased at a rate of 15°C/min up to a final temperature of 360°C. After a solvent delay of 3 min, mass spectra were recorded at 20 scans s^{-1} with m/z 70 to 600 scanning range and peaks were detected based on the molecular features of each analytical standard.

Effect of External Glycolate Supply on Glufosinate Activity

Plants were grown in soil until they reached the 6-leaf growth stage. Roots were washed with tap water and plants were transferred into 50 mL glass flasks containing distilled water or

10 mM glycolate solution. Glufosinate was immediately sprayed on these plants as described above. Control plants were not treated and included for comparisons. Visual injury, ammonia accumulation, and hydrogen peroxide and superoxide levels were evaluated at 8 HAT. Three replications per treatment were used and the experiment was repeated.

Activity of Antioxidant Enzymes

Superoxide dismutase (SOD), catalase (CAT), ascorbate peroxidase (APX) and glutathione reductase (GR) activity were measured in glufosinate-treated and -untreated plants. Three plants per treatment were used and the experiment was repeated. Enzyme extraction and activity followed protocol described elsewhere (Asada, 1999). Approximately 200 mg of leaf tissue was weighed and ground to a fine powder in liquid nitrogen using a precooled mortar and pestle. The exact weight of each powdered sample was determined before it was thoroughly homogenized in 1.2 mL of 0.2 M potassium phosphate buffer (pH 7.8 with 0.1 mM EDTA). Samples were centrifuged at $15,000 \times g$ for 20 min at 4 C, and the supernatant was used for enzyme activities.

Total SOD activity was assayed using a modified NBT method (Beyer and Fridovich, 1987). The assay was conducted in 2 mL tubes and the reaction mixture consisted of 50 mM KH_2PO_4 (pH 7.8), 2 mM EDTA, 4 mM L-methionine, 0.1 mM NBT, and 0.1% (v/v) Triton-X100. Crude extract (20 μL) and same volume of 0.2 mM riboflavin were added to the reaction, which was initiated by illuminating the samples under a 15 W fluorescent tube at a distance of 12 cm from the light source. Duplicate tubes with the same reaction mixture were kept in the dark and used as blanks. Absorbance was measured immediately at 560 nm. Enzyme activity (U mg FW^{-1}) was determined from a standard curve obtained with pure SOD.

CAT activity was determined through the decomposition of H_2O_2 based on the decrease in absorbance at 240 nm (Aebi, 1984). The 3 mL assay mixture contained 2 mL leaf extract (diluted 200X in 50 mM potassium phosphate + 2 mM EDTA, pH 7.0) and 1 mL of 10 mM H_2O_2. The extinction coefficient (40 mM^{-1} cm^{-1}) was used to calculate the enzyme activity (mmol min^{-1} g FW^{-1}).

APX activity was determined from the decrease in absorbance at 290 nm due to oxidation of ascorbate in the reaction (Nakano and Asada, 1981). The 1 mL assay mixture (pH 7) contained 50 mM potassium phosphate, 2 mM EDTA, 0.5 mM ascorbate, 0.5 mM H_2O_2, and 10 μL of crude leaf extract. H_2O_2 was added last to initiate the reaction, and absorbance was monitored for 3 min. The extinction coefficient of 2.8 mM^{-1} cm^{-1} for reduced ascorbate was used to calculate enzyme activity (mmol min^{-1} g FW^{-1}).

GR activity was assayed using 5,5-dithiobis-2-nitrobenzoic acid (DTNB) (Smith et al., 1988). The increase in absorbance at 412 nm was measured when DTNB was reduced to TNB by reduced glutathione in the reaction. Leaf extract (10 μL) was used in the assay along with 0.75 mM DTNB, 0.1 mM NADPH, and 1 mM oxidized glutathione in a total of 1 mL assay volume. Oxidized glutathione was added last to initiate the reaction and the increase in absorbance was recorded for 3 min. The extinction coefficient of TNB (14.15 M^{-1} cm^{-1}) was used to calculate GR activity (mmol min^{-1} g FW^{-1}).

Sites of ROS Formation in the Light Reactions

Low doses of atrazine and dinoseb were used to investigate the sources of ROS in the light reactions of photosynthesis when GS is inhibited by glufosinate. Plants were grown until the desired growth stage. The following treatments were foliar sprayed as previously described: glufosinate (280 g ha^{-1}), atrazine (40 g ha^{-1}), dinoseb (64 g ha^{-1}), glufosinate + atrazine, and

glufosinate + dinoseb. Visual injury, linear electron flow (LEF), ROS and oxygen evolution were evaluated at 8 HAT. A fluorescence-based portable device (MultispeQ 2.0, PhotosynQ LLC, East Lansing, MI 48823) was used to measure LEF in leaves.

Oxygen evolution was quantified according to the method described elsewhere (Dayan et al., 2015). Chloroplasts were isolated by homogenizing 5 g of fresh leaf tissue with 25 mL extraction buffer consisting of 1,650 mM sorbitol, 50 mM HEPES, 25 mM cysteine, 5 mM $MgCl_2$ and 5 mM EDTA. The homogenate was filtered with miracloth and centrifuged at 80,000 × g at 4 C for 60 min. The lower layer was resuspended with resuspension buffer (1,650 mM sorbitol, 50 mM HEPES, 5 mM dithiothreitol, 5 mM $MgCl_2$ and 5 mM EDTA) and centrifuged for 15 min at 6,000 x g. A soft pellet was resuspended with 0.5 mL resuspension buffer. The assay was conducted under saturating light conditions (2400 µmol m^{-2} sec^{-1} PAR), and oxygen was measured using a computer-controlled oxygen probe (Oxytherm, Hansatech, King's Lynn, UK). The reaction assay buffer consisted of 800 mM sucrose, 50 mM MES-NaOH (pH 6.2), 15 mM $CaCl_2$, and 1 mM $K_3[FeCN_6]$. All assays were performed in 1 mL assay buffer at 30 C and 900 rpm gentle agitation. Test compounds were diluted in ethanol, and control treatments received the same concentration of ethanol (less than 1% v/v). Crude extracts were incubated with test compounds (100 µM for glufosinate and 10 µM for atrazine and dinoseb) on ice for 20 min prior to the assay. The assay was initiated by adding the crude extract to the reaction assay buffer, and the rate of oxygen evolution was measured for 100 s over the linear portion of the curve.

RESULTS

ROS Formation Is Light-Dependent

Phytotoxicity was observed only in plants that were kept under light conditions (Figure 3.1A). Glufosinate caused more than 80% injury to plants under light conditions, whereas less than 5% injury was observed under dark conditions (Figure 3.1B). Interestingly, glutamine synthetase activity was inhibited by glufosinate under both dark and light conditions (Figure 3.1C). Ammonia accumulated at higher levels under light (5.7-fold) compared to dark (1.9-fold) conditions following glufosinate treatment (Figure 3.1D). Only those plants under light conditions showed increased levels of ROS and subsequent accumulation of MDA, indicating lipid peroxidation (Figure 3.1E and Figure 3.1F).

Glufosinate Blocks the Photorespiration Pathway

The levels of metabolites involved in photorespiration were affected by GS inhibition, except for P-glycolate, the first product of the oxidenase activity of Rubisco (Figure 3.2). While both glycolate and glyoxylate accumulated after glufosinate treatment in 9-fold and 7-fold, respectively, the levels of glycine, serine, hydroxypyruvate and glycerate were reduced.

Glycolate Enhances ROS Formation in Glufosinate-Treated Plants

Glycolate supplied to the roots of *Amaranthus palmeri* increased visual injury levels up to 79% compared to glufosinate only (39%) (Figure 3.3A). Glycolate-supplied plants showed only 10% injury compared to those growing in water (control). Compared to untreated plants, ammonia accumulated following glufosinate (58 µmol g FW^{-1}), glycolate (51 µmol g FW^{-1}), and glufosinate + glycolate (77 µmol g FW^{-1}) treatment (Figure 3.3B). While both superoxide and hydrogen peroxide accumulated at high levels in glufosinate-treated plants, glycolate enhanced hydrogen peroxide formation with a 1.8-fold increase compared to glufosinate only (Figure 3.3C and Figure 3.3D).

Glufosinate Treatment Induces Plant Antioxidant Enzymes

Antioxidant enzymes showed increased activity after glufosinate treatment (2 HAT) in *Amaranthus palmeri* (Figure 3.4). Compared to the untreated control, glufosinate treated plants showed 1.8-, 1.9-, 1.4- and 1.3-fold increase in the activity of superoxide dismutase, catalase, ascorbate peroxidase and glutathione reductase, respectively.

Sources of ROS Formation in Glufosinate-Treated Plants

When herbicides were sprayed individually, glufosinate (280 g ha^{-1}) provided 37% injury while low doses of atrazine (40 g ha^{-1}) and dinoseb (64 g ha^{-1}) caused less than 10% injury (Figure 3.5A). The addition of a low dose of atrazine (40 g ha^{-1}) to glufosinate decreased injury levels to 8%. On the other hand, glufosinate + dinoseb provided more than 75% injury to *A. palmeri*. Consistent with visual injury, ROS accumulation decreased with glufosinate + atrazine and increased with glufosinate + dinoseb, compared to glufosinate only (Figure 3.5B). All treatments reduced linear electron flow (Figure 3.5C). Compared to the untreated control, electron flow inhibition levels were 76, 30, 97, 93 and 99% for glufosinate, atrazine, dinoseb, glufosinate + atrazine, and glufosinate + dinoseb, respectively. Finally, oxygen evolution was dramatically inhibited by atrazine and glufosinate + atrazine (Figure 3.5D). Glufosinate and dinoseb had lower effect on oxygen evolution compared to atrazine (Figure A3.2).

DISCUSSION

The mechanism responsible for the fast action of glufosinate has been controversial for many years. Ammonia accumulation and carbon assimilation inhibition used to be accepted as main factors contributing to the rapid phytotoxicity driven by GS inhibition (Platt and Anthon, 1981). However, recent research has shown that the fast action of glufosinate is triggered by reactive oxygen species (ROS) (Takano et al., 2019). Glufosinate is a light-dependent herbicide

with symptoms developing only under light conditions (Figure 3.1B). Interestingly, GS inhibition was observed under both situations (Figure 3.1C; Fig S1), indicating that ROS accumulation requires the presence of light in addition to enzyme inhibition. Higher ammonia levels were observed in the light, consistent with previous work which has demonstrated that more than 60% of total accumulated ammonia comes from the photorespiration pathway (Wild et al., 1987).

The major plant cellular compartments for ROS generation are the chloroplast, mitochondria, peroxisome and cytoplasm (Apel and Hirt, 2004; Gill and Tuteja, 2010). Typically, any electron transport chain is subjected to electron leakage, which can react and activate molecular oxygen generating superoxide and other free radicals (Møller, 2001). Because the glufosinate-driven oxidative stress is light-dependent, ROS are probably formed in the chloroplasts where light reactions of photosynthesis take place. The reaction centers of PSI and PSII in chloroplast thylakoids are the major sites for ROS formation (Pospíšil, 2009; Takahashi and Badger, 2011). The oxidized form of the P680 radical in PSII is the strongest oxidant found in nature with a midpoint redox potential estimated to be 1.17 V (Barber and Archer, 2001), more than enough to form free radicals under full sunlight. In the light reactions of photosynthesis, the rate of ROS photoproduction depends on the balance between the levels of carbon assimilation and photon intensity (Asada, 2006). When photon energy exceeds the carbon assimilation capacity, plants have mechanisms to suppress the production of ROS, such as the photorespiration pathway and the water-water cycle involving the antioxidant enzyme machinery (Asada, 1999; Gill and Tuteja, 2010).

In addition to ammonia, glutamine synthetase inhibition led to the accumulation of P-glycolate, glycolate and glyoxylate in the photorespiration pathway (Figure 3.1 and Figure 3.2).

In contrast, glycine, serine, hydroxypyruvate and glycerate levels are decreased, indicating that glyoxylate is not converted into glycine by glutamate glyoxylate aminotransferase, which is probably because glutamate levels are depleted when GS is inhibited (Takano et al., 2019). Carbon assimilation is also inhibited following glufosinate treatment (Wild et al., 1987; Coetzer and Al-Khatib, 2001). These results emphasize that glufosinate blocks the photorespiration pathway, a major sink for excess of energy (Kozaki and Takeba, 1996). P-glycolate, glycolate and glyoxylate have been reported as inhibitors of Rubisco (Campbell and Ogren, 1990; González-Moro et al., 1997). When glufosinate was sprayed on glycolate-supplied plants, more injury and more ROS were observed (Figure 3.3; Figure A3.4). Glycolate supply led to accumulation of ammonia, supporting the hypothesis that ammonia comes from photorespiration (Kumar et al., 1984; Wild et al., 1987). This increase in ammonia content, however, did not result in enhanced injury, consistent with previous literature (Sauer et al., 1987; Takano et al., 2019). The conversion of glycolate into glyoxylate is catalyzed by glycolate oxidase, and this reaction produces hydrogen peroxide, which is then neutralized by the catalase activity (Figure 3.6) (Zelitch et al., 2009). This is consistent with our results and may suggest that glycolate oxidase activity could partially contribute to ROS generation in glufosinate-treated plants.

ROS can function either as useful (e.g. plant signaling) or phytotoxic molecules, and this is controlled by a tight regulation system including reducing agents and antioxidant enzymes (Apel and Hirt, 2004; Gill and Tuteja, 2010). Superoxide dismutase converts O_2^- to H_2O_2 and O_2, ascorbate peroxidase and catalase reduce H_2O_2 into H_2O and O_2, and glutathione reductase keeps glutathione in the reduced state to work as an electron donor (Asada, 2006; Gill and Tuteja, 2010). Here we show that all of these enzymes increase activity in response to the massive accumulation of ROS (Figure 3.4). In contrast, glutathione levels also go down after glufosinate

treatment (Figure A3.6). Ultimately, the plant is unable to maintain its oxidative stress balance and prevent cells from lipid peroxidation. Antioxidant enzymes are typically located in the plastids, but catalase is a peroxisomal enzyme (Corpas et al., 2001), supporting the hypothesis that these organelles are involved in ROS generation by glufosinate.

Because PSII and PSI are sites of ROS generation in the light reactions (Pospíšil, 2009), we used low doses of atrazine (PSII inhibitor) and dinoseb (uncoupler) to investigate where these free radicals are being formed. Based on our data, ROS formation depends on inhibition of linear electron flow, but also on the evolution of oxygen in PSII water splitting complex (Figure 3.7). When atrazine was added to glufosinate, both electron flow and oxygen evolution were blocked, ROS accumulation was insignificant and glufosinate efficacy was drastically decreased. Ammonia accumulated in similar levels by glufosinate treatment regardless the presence of atrazine (Figure A3.2), supporting the fact that ROS is not driven by ammonia. On the other hand, oxygen evolution was not completely blocked with dinoseb and linear electron flow was closely lowered to zero, enhancing glufosinate activity. Therefore, the light reactions of photosynthesis are probably the main generation site of ROS following GS inhibition by glufosinate.

We propose a model to demonstrate the relationship between glutamine synthetase inhibition and ROS accumulation (Figure 3.7). Glufosinate inhibits glutamine synthetase leading to glutamine and glutamate depletion and photorespiratory ammonia accumulation. Consequently, glyoxylate is not converted into glycine by glutamate glyoxylate aminotransferase, and P-glycolate, glycolate, and glyoxylate accumulate. This leads to a feedback inhibition of the photorespiration pathway and subsequent inactivation of rubisco activase (Lu et al., 2014). With these two pathways shuttled down, the equilibrium between

photon/electrons income and consumption is broken. Consequently, the excess of electrons activates molecular oxygen, which comes from the breakdown of water molecules in PSII water splitting complex. The massive buildup of ROS in chloroplast thylakoids lead to the catastrophic consequences of cell membrane peroxidation (Demidchik, 2015; Takano et al., 2019).

In conclusion, glufosinate breaks the balance between generation and scavenging of ROS. Hydrogen peroxide is produced partially by glycolate oxidase activity in the peroxisome. Inhibition of glutamine synthetase leads to a feedback blockage of the photorespiration pathway and linear electron flow in the light reactions. The excess of electrons is then accepted by molecular oxygen coming from the breakdown of water in PSII. The subsequent ROS accumulation leads to lipid peroxidation and forms the basis for the fast action of glufosinate.
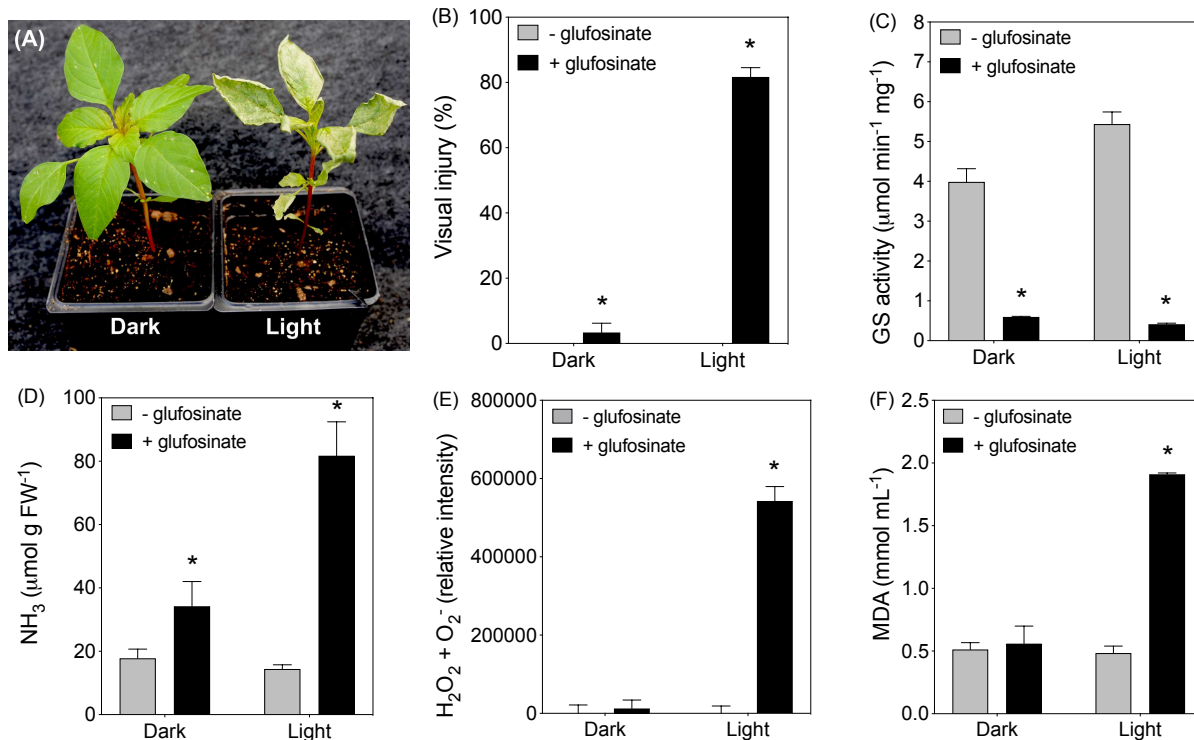
Figure 3.1: Glufosinate herbicidal activity is light-dependent (A). Visual injury (B), glutamine synthetase activity (C), ammonia accumulation (D), reactive oxygen species (E), and malondialdehyde levels (F). *Means are significantly different by t-test ($p<0.05$) between untreated (-) and treated (+) plants.
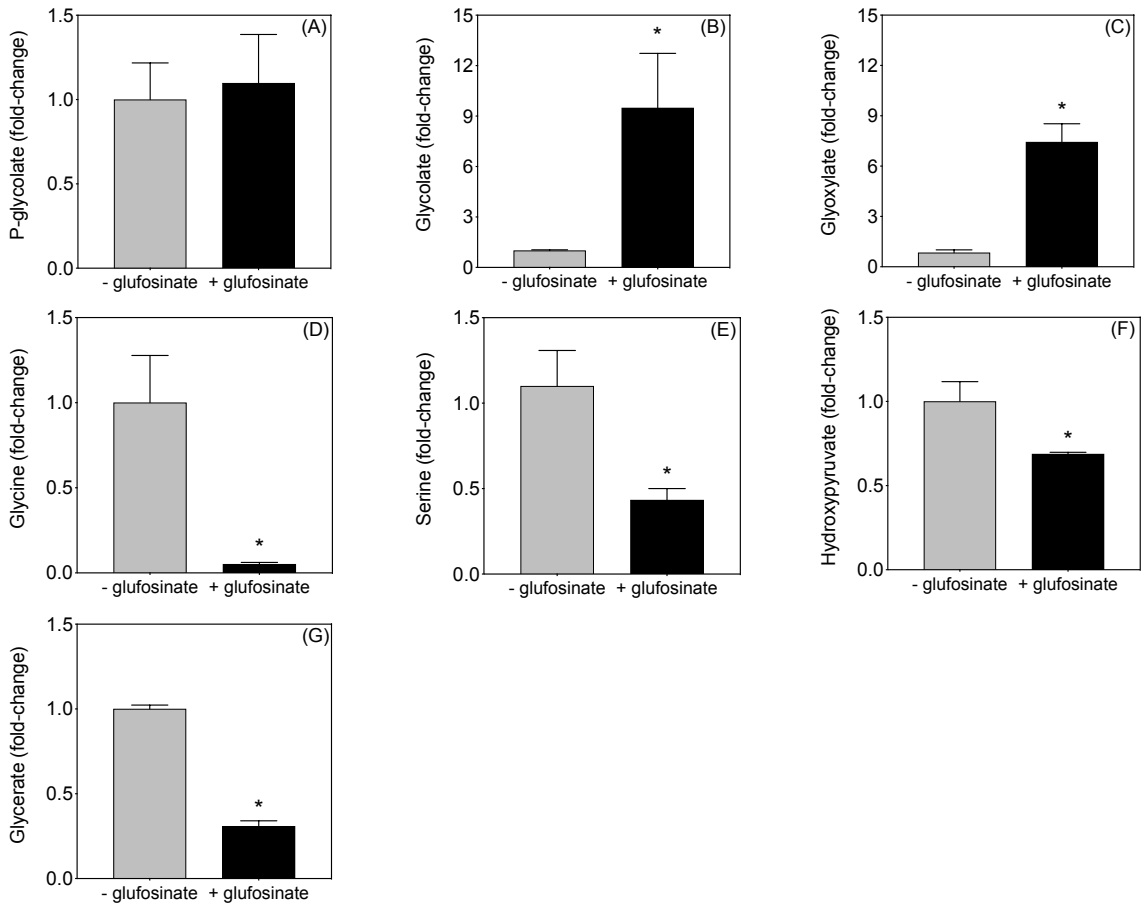
Figure 3.2: Glycolate and glyoxylate accumulate in response to glufosinate treatment. Levels of phosphoglycolate (A), glycolate (B), glyoxylate (C), glycine (D), serine (E), hydroxypyruvate (F), and glycerate (G) in *Amaranthus palmeri* leaves from untreated (-) and treated (+) plants. *Means are significantly different by t-test ($p < 0.05$).
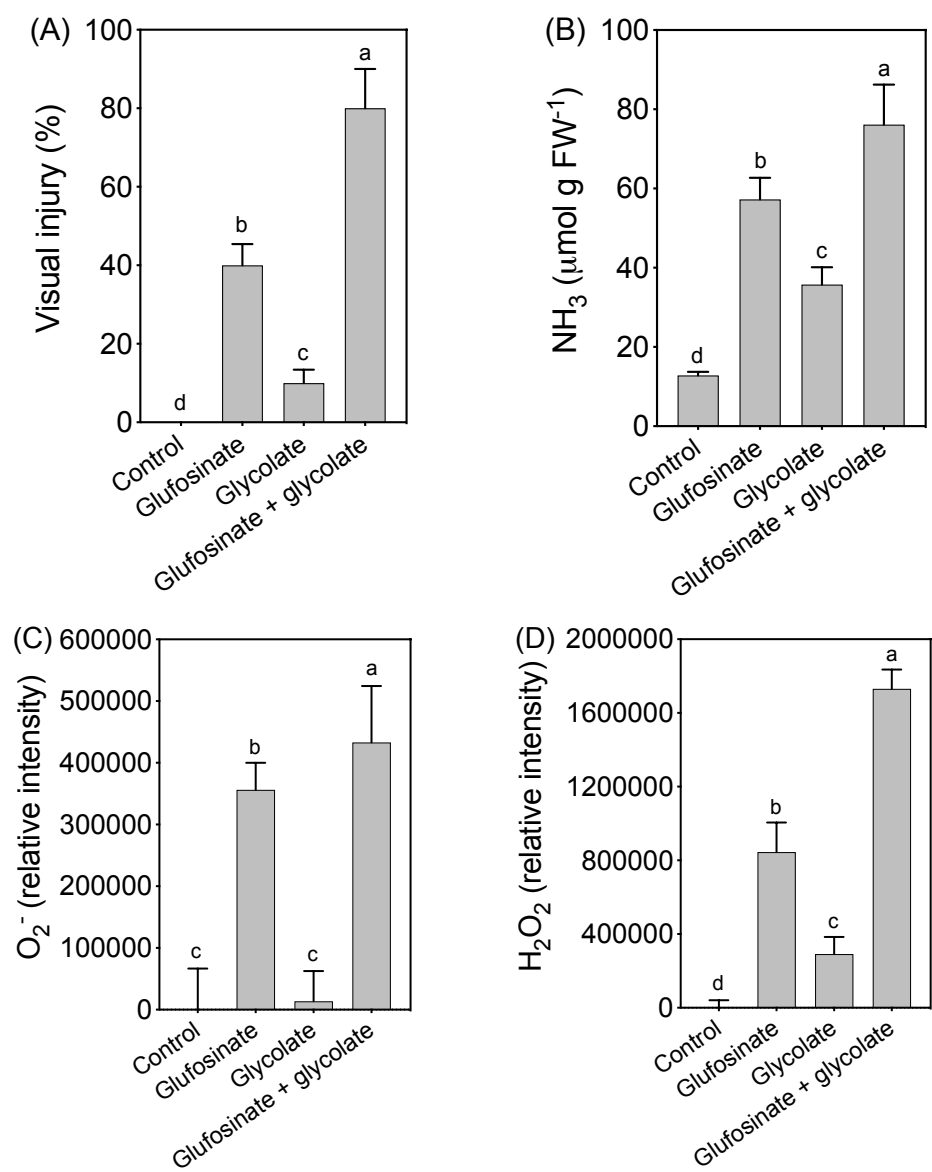
Figure 3.3: Glycolate enhances the accumulation of reactive oxygen species in glufosinate-treated plants. Visual injury (A), ammonia accumulation (B), superoxide (C) and hydrogen peroxide (D) in response to glufosinate, glycolate, and glufosinate + glycolate treatment. Glycolate was applied through the roots while glufosinate was sprayed on leaves. Means followed by the same letter do not differ by Tukey test ($p < 0.05$).
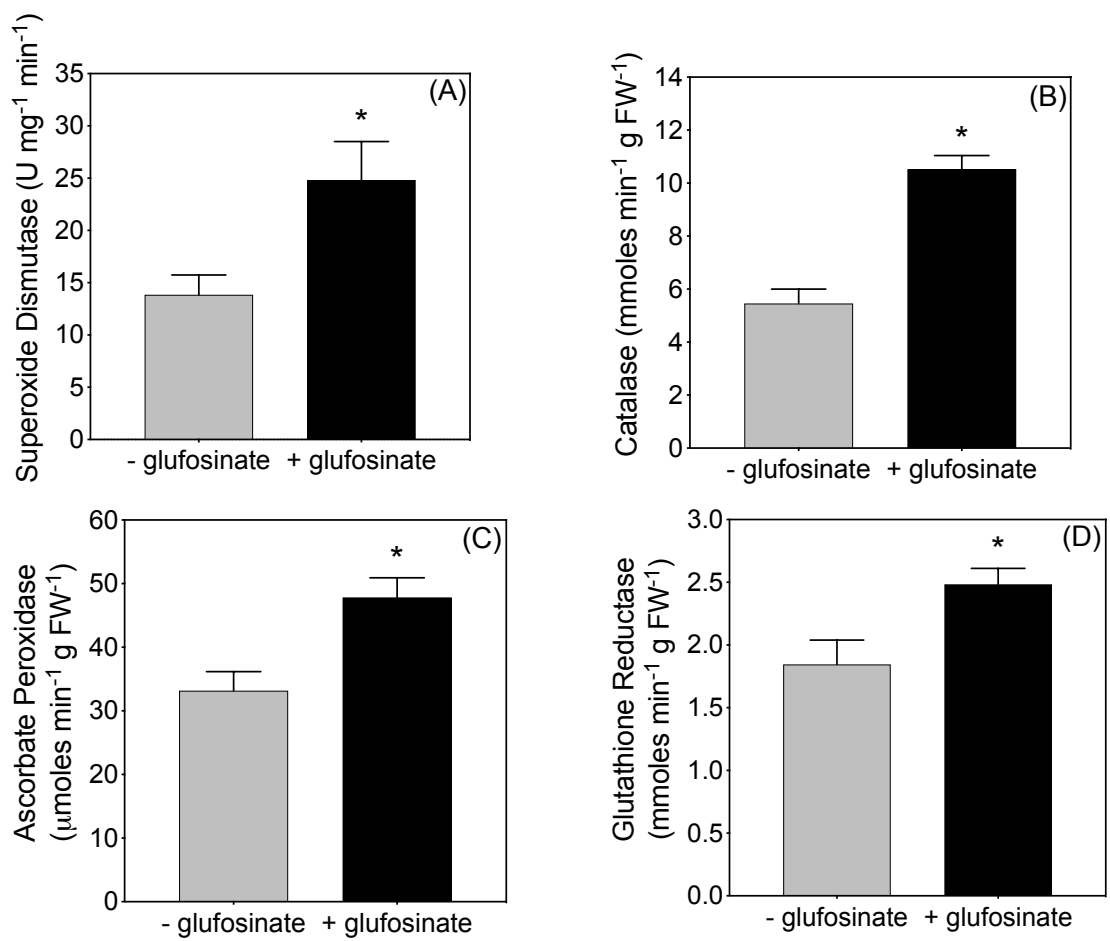
Figure 3.4: Glufosinate induces the activity of antioxidant enzymes in *Amaranthus palmeri*. Effect of glufosinate treatment on superoxide dismutase (A), catalase (B), ascorbate peroxidase (C), and glutathione reductase (D). *Means are significantly different by t-test ($p<0.05$).
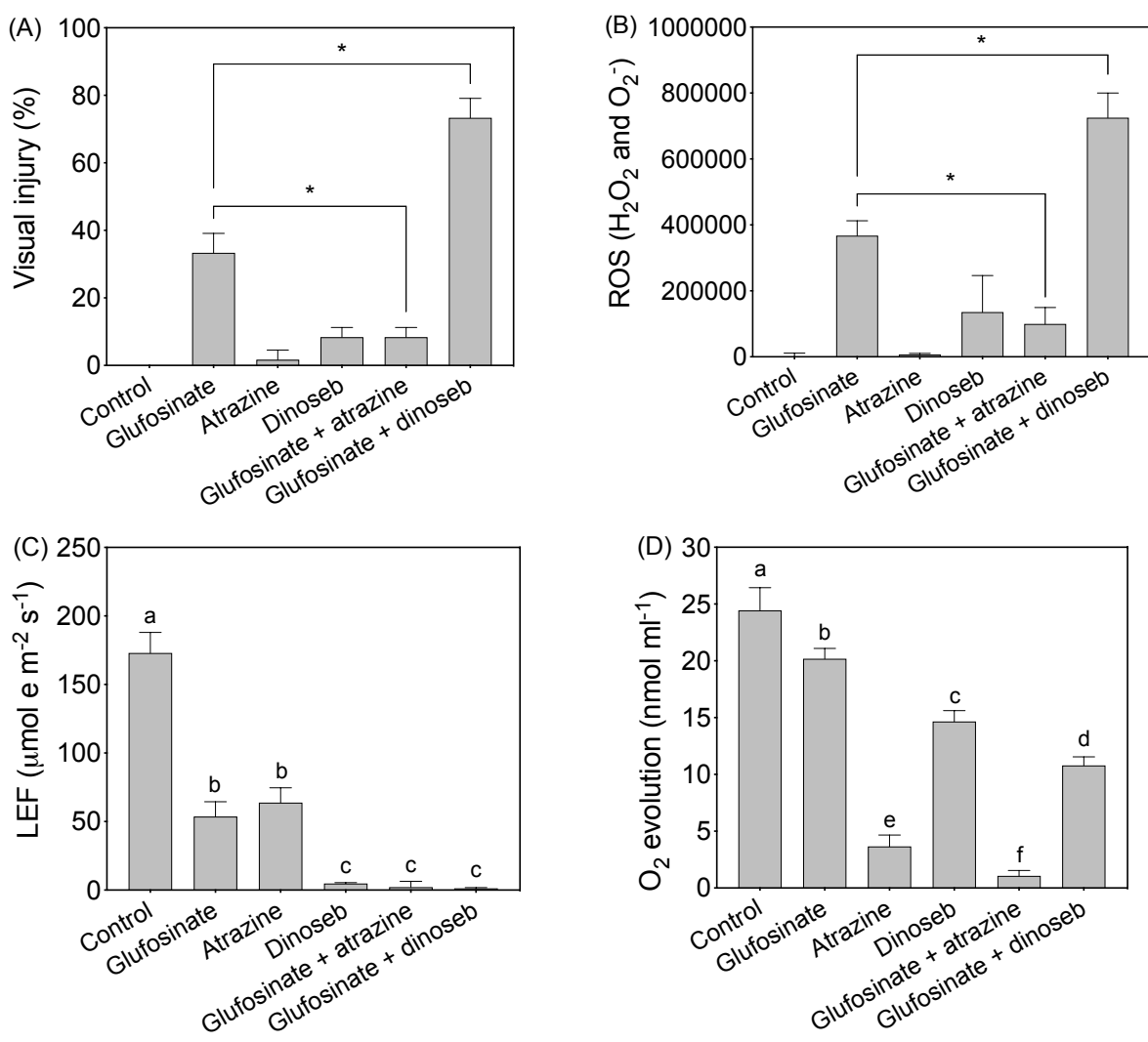
Figure 3.5: Investigating the sources of ROS formation by glufosinate using PSII-inhibitor atrazine and the uncoupler dinoseb. Visual injury (A), linear electron flow (B), reactive oxygen species (C) and oxygen evolution (D) in response to glufosinate, atrazine, dinoseb, glufosinate + atrazine, and glufosinate + dinoseb. *Means are significantly different by t-test ($p < 0.05$). Means followed by the same letter do not differ by Tukey test ($p < 0.05$).
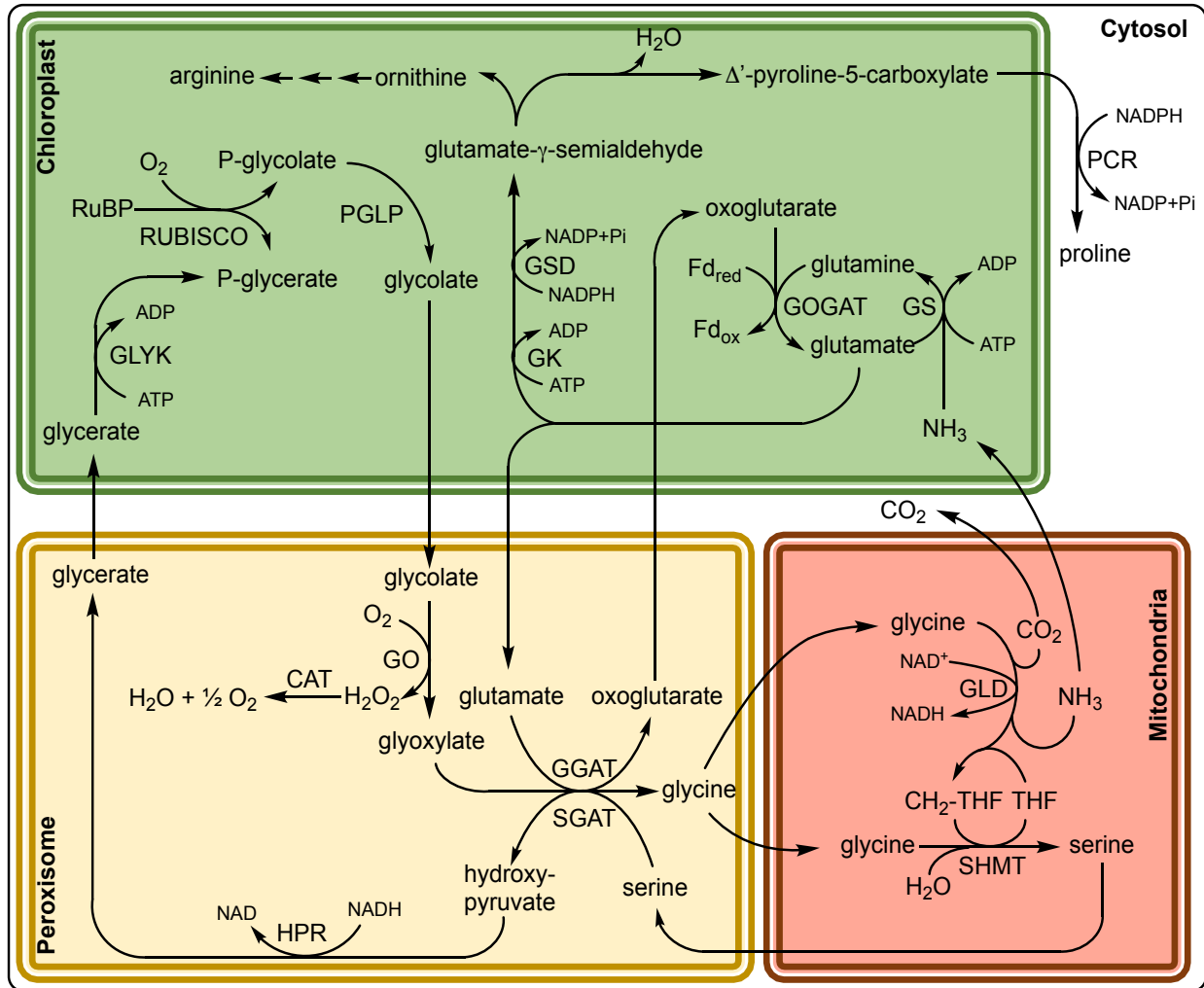
Figure 3.6: The central role of glutamine synthetase (GS) in recycling ammonia generated by the photorespiration pathway. Inhibition of GS (red x) by glufosinate causes accumulation of phosphoglycolate, glycolate and glyoxylate (within rex boxes) and depletion of glycine, serine, hydroxypyruvate and glycerate. RUBISCO: ribulose-1,5-biphosphate carboxylase/ oxygenase, PGLP: 2-phosphoglycolate phosphatase, GO: glycolate oxidase, CAT: catalase, GGAT: glutamate:glyoxylate aminotransferase, SGAT: serine:glyoxylate amino transferase, GLD: glycine decarboxylase, SHMT: serine hydroxymethyltransferase, THF: tetrahydrofolate, GOGAT: glutamate:oxoglutarate aminotransferase, HPR: hydroxypyruvate reductase, and GLYK: glycerate kinase.
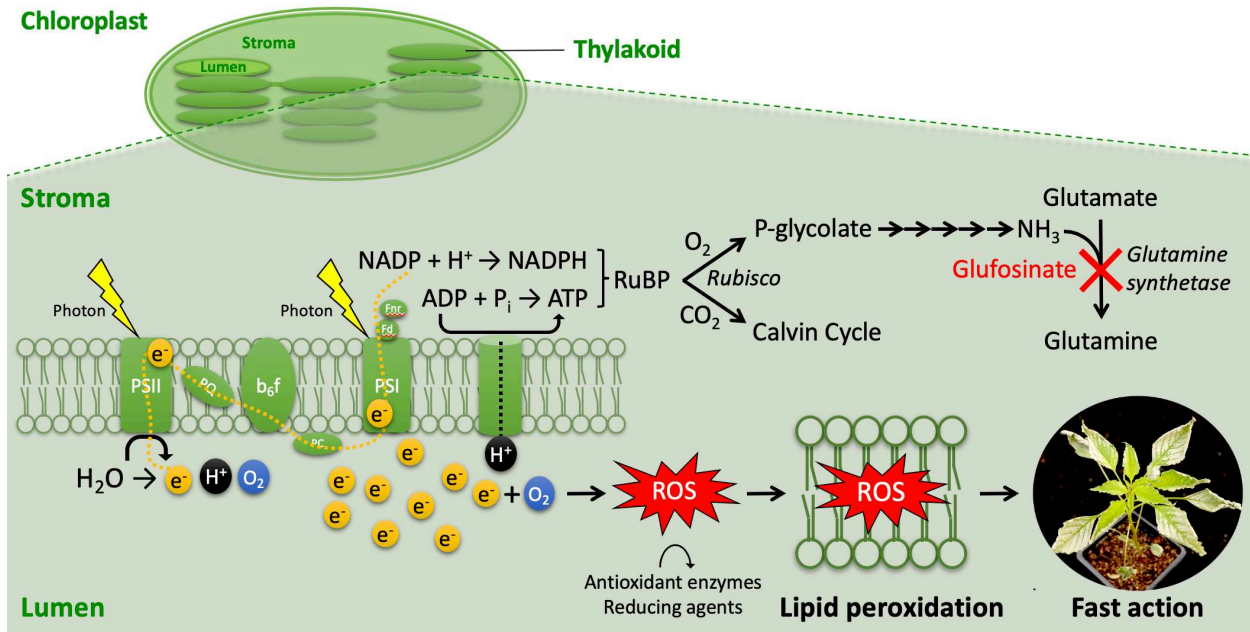
Figure 3.7: Relationship between glutamine synthetase (GS) and the light reactions of photosynthesis. Inhibition of GS feedback inhibits Rubisco's carboxylase and oxygenase activity, a major sink for chemical energy produced by the electron flow in the light reactions. The excess of electrons is accepted by molecular oxygen leading to reactive oxygen species (ROS) formation, lipid peroxidation and rapid cell death. PS: photosystem, PQ: plastoquinone, b_6f: cytochrome b_6f, PC: plastocyanine, Fd: ferredoxin, Fnr: ferredoxin NADP reductase, and Rubisco: ribulose-1,5-biphosphate carboxylase/oxygenase.

References

Aebi, H., 1984. Catalase in vitro. Methods in Enzymology 105: 121-126.

Apel, K.; Hirt, H., 2004. Reactive oxygen species: metabolism, oxidative stress, and signal transduction. Annual Review of Plant Biology 55: 373-399.

Asada, K., 1999. The water-water cycle in chloroplasts: Scavenging of active oxygens and dissipation of excess photons. Annual Review of Plant Physiology and Plant Molecular Biology 50: 601-639.

Asada, K., 2006. Production and scavenging of reactive oxygen species in chloroplasts and their functions. Plant Physiology 141: 391-396.

Barber, J.; Archer, M.D., 2001. P680, the primary electron donor of photosystem II. Journal of Photochemistry and Photobiology A: Chemistry 142: 97-106.

Bayer, E.; Gugel, K.H.; Hägele, K.; Hagenmaier, H.; Jessipow, S.; König, W.A.; Zähner, H., 1972. Stoffwechselprodukte von Mikroorganismen. 98. Mitteilung. Phosphinothricin und Phosphinothricyl-Alanyl-Alanin. Helvetica Chimica Acta 55: 224-239.

Beyer, W.F.; Fridovich, I., 1987. Assaying for superoxide dismutase activity: Some large consequences of minor changes in conditions. Analytical Biochemistry 161: 559-566.

Busi, R.; Goggin, D.E.; Heap, I.M.; Horak, M.J.; Jugulam, M.; Masters, R.A.; Napier, R.M.; Riar, D.S.; Satchivi, N.M.; Torra, J., 2018. Weed resistance to synthetic auxin herbicides. Pest Management Science 74: 2265-2276.

Cadenas, E., 1989. Biochemistry of oxygen toxicity. Annual Review of Biochemistry 58: 79-110.

Campbell, W.J.; Ogren, W.L., 1990. Glyoxylate inhibition of ribulosebisphosphate carboxylase/oxygenase activation in intact, lysed, and reconstituted chloroplasts. Photosynthesis Research 23: 257-268.

Coetzer, E.; Al-Khatib, K., 2001. Photosynthetic inhibition and ammonium accumulation in Palmer amaranth after glufosinate application. Weed Science 49: 454-459.

Corpas, F.J.; Barroso, J.B.; del Río, L.A., 2001. Peroxisomes as a source of reactive oxygen species and nitric oxide signal molecules in plant cells. Trends in Plant Science 6: 145-150.

Dayan, F.E.; Barker, A.; Dayan, L.; Ravet, K., 2019. The role of antioxidants in the protection of plants against inhibitors of protoporphyrinogen oxidase. Reactive Oxygen Species 7: 55-63.

Dayan, F.E.; Duke, S.O., 2014. Natural compounds as next-generation herbicides. Plant Physiology 166: 1090-1105.

Dayan, F.E.; Owens, D.K.; Corniani, N.; Silva, F.M.L.; Watson, S.B.; Howell, J.L.; Shaner, D.L., 2015. Biochemical markers and enzyme assays for herbicide mode of action and resistance studies. Weed Science 63: 23-63.

Demidchik, V., 2015. Mechanisms of oxidative stress in plants: From classical chemistry to cell biology. Environmental and Experimental Botany 109: 212-228.

Duke, S.O., 2011. Comparing conventional and biotechnology-based pest management. Journal of Agricultural and Food Chemistry 59: 5793-5798.

Edwards, J.W.; Coruzzi, G.M., 1989. Photorespiration and light act in concert to regulate the expression of the nuclear gene for chloroplast glutamine synthetase. The Plant Cell 1: 241-248.

Forlani, G., 2000. Purification and properties of a cytosolic glutamine synthetase expressed in *Nicotiana plumbaginifolia* cultured cells. Plant Physiology and Biochemistry 38: 201−207.

Fryer, M.J.; Oxborough, K.; Mullineaux, P.M.; Baker, N.R., 2002. Imaging of photo-oxidative stress responses in leaves. Journal of Experimental Botany 53: 1249-1254.

Gill, S.S.; Tuteja, N., 2010. Reactive oxygen species and antioxidant machinery in abiotic stress tolerance in crop plants. Plant Physiology and Biochemistry 48: 909-930.

González-Moro, B.; Lacuesta, M.; Becerril, J.M.; Gonzalez-Murua, C.; Muñoz-Rueda, A., 1997. Glycolate accumulation causes a decrease of photosynthesis by inhibiting RUBISCO activity in maize. Journal of Plant Physiology 150: 388-394.

Halliwell, B., 1987. Oxidative damage, lipid peroxidation and antioxidant protection in chloroplasts. Chemistry and Physics of Lipids 44: 327-340.

Hodges, D.M.; DeLong, J.M.; Forney, C.F.; Prange, R.K., 1999. Improving the thiobarbituric acid-reactive-substances assay for estimating lipid peroxidation in plant tissues containing anthocyanin and other interfering compounds. Planta 207: 604-611.

Kerchev, P.; Waszczak, C.; Lewandowska, A.; Willems, P.; Shapiguzov, A.; Li, Z.; Alseekh, S.; Mühlenbock, P.; Hoeberichts, F.A.; Huang, J.; Van Der Kelen, K., 2016. Lack of GLYCOLATE OXIDASE1, but not GLYCOLATE OXIDASE2, attenuates the photorespiratory phenotype of CATALASE2-deficient *Arabidopsis*. Plant Physiology 171:1704-1719.

Kozaki, A.; Takeba, G., 1996. Photorespiration protects C3 plants from photooxidation. Nature 384: 557-560.

Kumar, P.A.; Nair, T.V.R.; Abrol, Y.P., 1984. Effect of photorespiratory metabolites, inhibitors and methionine sulphoximine on the accumulation of ammonia in the leaves of mung bean and *Amaranthus*. Plant Science Letters 33: 303-307.

Leason, M.; Cunliffe, D.; Parkin, D.; Lea, P.J.; Miflin, B.J., 1982. Inhibition of pea leaf glutamine synthetase by methionine sulphoximine, phosphinothricin and other glutamate analogues. Phytochemistry 21: 855-857.

Lisec, J.; Schauer, N.; Kopka, J.; Willmitzer, L.; Fernie, A.R., 2006. Gas chromatography mass spectrometry–based metabolite profiling in plants. Nature Protocols 1: 387-396.

Lu, Y.; Li, Y.; Yang, Q.; Zhang, Z.; Chen, Y.; Zhang, S.; Peng, X.-X., 2014. Suppression of glycolate oxidase causes glyoxylate accumulation that inhibits photosynthesis through deactivating Rubisco in rice. Physiologia Plantarum 150: 463-476.

Molin, W.T.; Khan, R.A., 1995. Microbioassays to determine the activity of membrane disrupter herbicides. Pesticide Biochemistry and Physiology 53: 172-179.

Møller, I.M., 2001. Plant mitochondria and oxidative stress: Electron transport, NADPH turnover, and metabolism of reactive oxygen species. Annual Review of Plant Physiology and Plant Molecular Biology 52: 561-591.

Morales, M.; Munné-Bosch, S., 2019. Malondialdehyde: facts and artifacts. Plant Physiology 180: 1246-1250.

Nakano, Y.; Asada, K., 1981. Hydrogen peroxide is scavenged by ascorbate-specific peroxidase in spinach chloroplasts. Plant and Cell Physiology 22: 867-880.

Platt, S.G.; Anthon, G.E., 1981. Ammonia accumulation and inhibition of photosynthesis in methionine sulfoximine treated spinach. Plant Physiology 67: 509-513.

Pospíšil, P., 2009. Production of reactive oxygen species by photosystem II. Biochimica et Biophysica Acta 1787: 1151-1160.

Sauer, H.; Wild, A.; Rühle, W., 1987. The effect of phosphinothricin (glufosinate) on photosynthesis II. The causes of inhibition of photosynthesis. Zeitschrift für Naturforschung C 42: 270-278.

Seto, H.; Sasaki, T.; Imai, S.; Tsuruoka, T.; Ogawa, H.; Satoh, A.; Inouye, S.; Niida, T.; Otake, N., 1983. Studies on the biosynthesis of bialaphos (SF-1293). The Journal of antibiotics 36: 96-98.

Smith, I.K.; Vierheller, T.L.; Thorne, C.A., 1988. Assay of glutathione reductase in crude tissue homogenates using 5,5′-dithiobis(2-nitrobenzoic acid). Analytical Biochemistry 175: 408-413.

Strauch, E.; Wohlleben, W.; Pühler, A., 1988. Cloning of a phosphinothricin N-acetyltransferase gene from *Streptomyces viridochromogenes* Tü494 and its expression in *Streptomyces lividans* and *Escherichia coli*. Gene 63: 65-74.

Tachibana, K.; Watanabe, T.; Sekizawa, Y.; Takematsu, T., 1986. Accumulation of ammonia in plants treated with bialaphos. Journal of Pesticide Science 11: 33-37.

Takahashi, S.; Badger, M.R., 2011. Photoprotection in plants: a new light on photosystem II damage. Trends in Plant Science 16: 53-60.

Takano, H.K.; Beffa, R.; Preston, C.; Westra, P.; Dayan, F.E., 2019. Reactive oxygen species trigger the fast action of glufosinate. Planta 249: 1837–1849.

Triantaphylidès, C.; Havaux, M., 2009. Singlet oxygen in plants: production, detoxification and signaling. Trends in Plant Science 14: 219-228.

Wild, A.; Sauer, H.; Rühle, W., 1987. The effect of phosphinothricin (glufosinate) on photosynthesis I. Inhibition of photosynthesis and accumulation of ammonia. Zeitschrift für Naturforschung C 42: 263-269.

Zelitch, I.; Schultes, N.P.; Peterson, R.B.; Brown, P.; Brutnell, T.P., 2009. High glycolate oxidase activity is required for survival of maize in normal air. Plant Physiology 149: 195-204.

Chapter 4: Exploring Changes in Fluxomics to Enhance Glufosinate Activity

INTRODUCTION

Glufosinate is commercialized as a racemic mixture of D-phosphinothricin and L-phosphinothricin but only the L-isomer binds to GS (Beriault et al., 1999). Glufosinate resistant crops (Liberty Link®) are genetically engineered for phosphinothricin acetyltransferase (*pat*) expression to metabolize L-phosphinothricin into *N*-acetyl-L-phosphinothricin, a non-phytotoxic compound (Dröge et al., 1992). To date, only two weed species have evolved glufosinate resistance in the world (Jalaludin et al., 2010; Brunharo et al., 2019). While it is a good option for weed control, glufosinate efficacy is greatly affected by environmental conditions and plant size (Steckel et al., 1997; Coetzer et al., 2001; Sellers et al., 2003). Glufosinate is a fast-acting and broad-spectrum herbicide targeting glutamine synthetase (GS), a key enzyme for nitrogen metabolism and photorespiration in plants (Bayer et al., 1972; Oliveira et al., 2002). GS catalyzes the incorporation of ammonia into glutamate to form glutamine (Bernard and Habash, 2009). Glufosinate inhibits GS competing with glutamate for the active site. This leads to ammonia accumulation, a massive light-dependent generation of reactive oxygen species (ROS), and changes in amino acid levels (Takano et al., 2019).

Fluxomics refers to small molecule fluxes and networks across different metabolic pathways in systems biology of living cells (Winter and Krömer, 2013). Glutamate is an interesting example to study fluxomics because it occupies a central position in amino acid metabolism. In addition to the role as a substrate for GS, glutamate is also a precursor for proline, arginine, and chlorophyll biosynthesis (Forde and Lea, 2007). Protoporphyrinogen oxidase (PPO) is a key enzyme for the chlorophyll biosynthesis pathway, catalyzing the

conversion of protoporphyrinogen (protogen) into protoporphyrin (proto) (Lermontova et al., 1997). Inhibition of PPO leads to accumulation of the product of the reaction, by compartmentalization of proto intermediates (Matringe et al., 1989; Lee et al., 1993). Herbicides targeting PPO are also fast-acting because proto reacts with light and generates ROS, causing lipid peroxidation (Dayan and Duke, 2010). Resistance to PPO inhibitors has been reported for 13 species around the world (Heap, 2019). In a PPO resistant waterhemp (*Amaranthus tuberculatus*) population, a codon deletion (ΔG210) affects herbicide binding to the active site and provides 53-fold resistance to lactofen (Dayan et al., 2010; Patzoldt et al., 2006).

Herbicide mixtures are commonly used in agriculture to improve efficacy, increase the spectrum of weed control, and manage herbicide resistance (Zhang et al., 1995; Busi et al., 2019). The combination of two herbicides is synergistic when the combined effect is larger than predicted (Sørensen et al., 2007). The fact that glutamate levels are depleted following GS inhibition is particularly intriguing because a substrate is expected to accumulate when the enzyme is inhibited. We used a fluxomics approach to investigate the fate of glutamate following glufosinate treatment. Our hypothesis was that glutamate is diverted to other pathways including chlorophyll biosynthesis when GS is inhibited, therefore, glufosinate could enhance the activity of PPO inhibitors by increasing the carbon flow towards chlorophyll biosynthesis and proto accumulation. We studied the interaction between glufosinate and PPO inhibitors, and demonstrate the physiological and biochemical basis for the enhanced activity with their combination.

MATERIAL AND METHODS

Chemical Sources

Glufosinate commercial formulation (Liberty 280 g L^{-1}) and analytical D, L-glufosinate were provided by Bayer CropScience (Monheim am Rhein, Germany 40789). Other PPO inhibitors were purchased from their respective manufacturers: saflufenacil (Sharpen, BASF), flumioxazin (Valor, Valent), lactofen (Cobra, Valent), fomesafen (Reflex, Syngenta), pyraflufen (Venue, Nichino). Analytical L-glutamate, proto IX, nitro blue tetrazolium chloride, potassium phosphate monobasic, sodium azide, 3,3'-diaminobenzidine were purchased from Sigma-Aldrich (St. Louis, MO 63103) or Fisher Scientific (Waltham, WI 02451).

Plant Growth and Spraying Conditions

Plants were grown until the 6-leaf-stage in 0.3 cm^3 pots filled with soil (SunGro Horticulture, Agawam, MA 01001). Greenhouse conditions were 25/21 C day/night, 16 h photoperiod with natural sunlight or 500 μmol m^{-2} s^{-1}, and 70% relative humidity. For all herbicide applications, a commercial chamber track sprayer (DeVries Manufacturing, Inc., Hollandale, MN 56045) equipped with an 8002EVS single even, flat-fan nozzle (TeeJet; Spraying Systems Co., Denver, CO 80207) calibrated to deliver 187 L ha^{-1} spray solution at the level of the plant canopy was used.

Amino Acid Levels

Palmer amaranth (*Amaranthus palmeri*) plants were sprayed with 560 g ha^{-1} glufosinate plus 2% (w/v) AMS as described previously. Control plants were sprayed with AMS only. Leaf tissue (200 mg) was ground with liquid nitrogen with a mortar and pestle. Once ground, 10 mL methanol:water (75:25, v/v) was added, the solution vortexed vigorously for one min, incubated in ultrasonic bath for 30 min and then centrifuged at 4,000 *g* for 10 min. An aliquot of 1.5 mL of the supernatant was filtered through a 0.2 μm nylon filter into an UHPLC vial, and 1 μL of this

solution was injected for liquid chromatography - tandem mass spectrometry (LC-MS/MS) analysis.

All samples were analyzed by an LC-MS/MS system (Shimadzu Scientific Instruments, Columbia, MD, USA). The LC–MS/MS system consisted of a Nexera X2 UPLC with 2 LC-30 AD pumps, an SIL-30 AC MP autosampler, a DGU-20A5 Prominence degasser, a CTO-30A column oven, and SPD-M30A diode array detector coupled to an 8040-quadrupole mass-spectrometer. Glutamine, glutamate and glufosinate were separated on an iHilic-Fusion column (100 × 2.1 mm, 3.5 μm; Silica) at a flow rate of 0.2 mL min^{-1} using a linear gradient of acetonitrile (B) and 25 mM ammonium acetate (A): 2 min, 80% B; 8 min, 30% B; 12 min, 30% B; 12.1 min, 80% B. The MRMs were optimized to 147.95>130.10, 147.10>130.00, 106.10>60.10, 116.15>70.15, and 175.00>70.10 for glutamate, glutamine, serine, proline, and arginine, respectively. Standard curves of serial dilutions of authentic standards were used for quantification.

Isobole Analysis

A dose response experiment was conducted for both herbicides glufosinate and saflufenacil. The evaluated doses were 0, 9, 17, 35, 70, 140, 280 and 560 g ha^{-1} for glufosinate and 0, 0.5, 1, 2, 4, 8, 16, 32 g ha^{-1} for saflufenacil. Each dose was tested in three replications and the experiment was repeated. The variable response was shoot dry mass (percent of control) and a four-parameter logistic regression was used. The ratios of mixtures were chosen based on the LD$_{50}$ values obtained with inhibitors tested individually (Table 4.1). An extension of the additive model was used to study the interaction between the two herbicides and predict the shape of the isobole (Sørensen et al., 2007). If the shape is linear, the mixture effect is additive. If the curve is convex, the two herbicides have antagonism. Finally, a concave shape indicates that the

compounds increase each other's activity and the mixture has synergism (Streibig et al., 1998). Statistical analysis was performed with R software.

Response of PPO-Resistant *A. tuberculatus* and Glufosinate-Resistant Soybean

In order to understand whether glufosinate enhances PPO-inhibitors or PPO-inhibitors enhance glufosinate, we used PPO-resistant waterhemp (*A. tuberculatus*) and glufosinate resistant soybean (Liberty Link, BASF). Susceptible plants for both herbicides were included for comparison. Plants were grown until the six-leaf stage and sprayed with glufosinate (280 g ha^{-1}), PPO-inhibitor (lactofen at 5 g ha^{-1} for *A. tuberculatus*, and saflufenacil at 1 g ha^{-1} for soybean), or the mixture of the two herbicides. Three replicates were evaluated and the experiments were repeated. Response variables were visual injury, ROS accumulation, and proto for *A. tuberculatus*, and visual injury, proto, glufosinate and glutamate levels in soybean. While glufosinate and glutamate were quantified over time up to 48 HAT, other variables were evaluated at 8 HAT only.

Hydrogen peroxide (H2O2) and superoxide (O2-) were measured by staining leaf discs in solutions containing 3,3'-diaminobendizine (DAB) and nitro blue tetrazolium chloride (NBT), respectively 21-22. The DAB solution contained 0.1 g DAB solubilized in 200 mL water with pH 3.8. The NBT solution was composed by 0.1 g NBT, 13.6 g potassium phosphate monobasic and 1.3 g sodium azide in 200 mL water. Sixteen leaf discs (5-mm diam) from control and treated (560 g ha-1 glufosinate) leaves were placed in 20 mL glass tubes containing each staining solution. The samples were then shaken under 20 Hg vacuum for 1 h. Leaf discs were washed in distilled water and boiled in 70% (v/v) ethanol solution, having the solution replaced every 20 min for four cycles. Leaf discs were then stored in 70% (v/v) ethanol solution for 12 h and scanned (Brother DCP-L2550DW; Bridgewater, NJ, USA). The levels of hydrogen peroxide or

superoxide were quantified using CS3 Photoshop (Adobe Systems, San Jose, CA, USA), measuring the color intensity in each leaf disc, removing background levels. Data was represented as relative intensity of treated samples compared to control samples (treated intensity – control intensity).

Proto extraction and analysis followed protocol described elsewhere (Dayan 2015). Leaf tissue (0.2 g) was ground to a powder in liquid nitrogen and homogenized in 2 mL methanol: 0.1M NH_4OH (9:1) and centrifuged at $10,000 \times g$ for 15 min. The supernatant was saved and the pellet re-homogenized in 1 mL methanol: 0.1M NH_4OH (9:1) then centrifuged again at $10,000 \times g$ for 15 min. Supernatants were pooled and then filtered through a 0.25 μm nylon syringe membrane filter prior to quantification with the LC-MS/MS system described above. Metabolites were separated in a biphenyl column (100×4.6 mm, 2.6 μm, 40 C) at a flow rate of 0.4 mL min^{-1} using a linear gradient of methanol (B) and 10 mM ammonium acetate (A): 0 min, 50% B; 8 min, 70% B; 11 min, 90% B; 13 min, 90% B; 13.5 min, 50% B; 17 min, 50% B. The MRM was optimized to 340.10>227.95 (Moulin et al., 2008). Standard curves of serial dilutions of authentic standards were used for quantification.

Field Performance of Glufosinate + PPO Inhibitors on *Kochia scoparia*

Two separate experiments were conducted in a field located in Fort Collins, Colorado (40°38'49'' N; 104°59'50'' W) between May 10th and June 20th of 2018 and 2019. Plants were 15-cm tall, and weed densities were 11 and 8 plants m^{-1} in 2019 and 2020, respectively. Plots were 3 m wide and 7 m long with the central 18 m^2 being used for evaluations. Glufosinate (420 g ha^{-1}) was tested alone or in tank mix with different PPO inhibitors (g ha^{-1}): flumioxazin (2.5), saflufenacil (1), pyraflufen-ethyl (0.2), lactofen (5), and fomesafen (7). Methylated soybean oil (0.5%, v/v) was added to all treatments, which were sprayed using a CO_2-pressured backpack

106

sprayer attached to a boom equipped with six flat spray nozzles (Teejet Louisville, KY 40245) spaced 0.5 m from each other. Pressure was maintained at 25 kPa and speed at 0.9 m s^{-1}, which provided 160 L ha^{-1} spray volume. Weed control was visually evaluated at 21 d after treatment using a scale where 0 means no control and 100 means death of all plants. Data were subjected to ANOVA and means compared by Tukey test (p<0.05).

Efficacy of Glufosinate + PPO Inhibitors Under Low Temperature and Humidity

A. palmeri plants were grown until the six-leaf stage and incubated under either 25 C and 70% relative humidity (RH) or 13 C and 30% RH for 24 h. Plants were sprayed with glufosinate (280 g ha^{-1}), saflufenacil (1 g ha^{-1}), and glufosinate + saflufenacil (280 + 1 g ha^{-1}) and returned to their respective environmental conditions. Visual injury was evaluated at 14 DAT.

RESULTS

Amino Acid Levels

Inhibition of GS by glufosinate disturbed the levels of glutamine, glutamate, serine, proline and arginine at 24 h after treatment (HAT) (Figure 4.1). While glutamine levels are expected to decrease, glutamate should accumulate. Instead, both glutamate and glutamine are depleted with glufosinate treatment. On the other hand, serine, proline and arginine accumulate after GS inhibition (Figure 4.1).

Isobole Analysis

The LD$_{50}$ values for glufosinate and saflufenacil in *A. palmeri* were 50 and 2.5 g ha^{-1} respectively (Figure 4.2A and Figure 4.2B). These doses were used to evaluate the interaction between these two herbicides with the isobole analysis (Figure 4.3C). Lower LD$_{50}$ values were obtained with the mixture compared to the herbicides used individually and the isobole indicated

strong synergism between the two chemistries. In addition to *A. palmeri*, we also tested the effect of glufosinate and PPO inhibitors individually or in association to control *A. tuberculatus*, *Bassia scoparia*, *Lolium rigidum*, *Sorghum halepense* and *Echinochloa colona* (Figure A4.1). The enhanced activity with the mixture was more evident for broadleaf than grass species.

Effect of Glufosinate + PPO Inhibitor on PPO-Resistant *Amaranthus tuberculatus*

Glufosinate (280 g ha^{-1}) provided 20% control on both PPO-susceptible and resistant *A. tuberculatus* (Figure 4.3C). Lactofen (5 g ha^{-1}) caused less than 5% injury on both biotypes. The herbicide mixture controlled the susceptible biotype by 94%, whereas only 20% injury was observed for the resistant. A similar response was found for ROS accumulation (Figure 4.3D). Hydrogen peroxide and superoxide accumulated to high levels in the susceptible biotype treated with glufosinate + lactofen. Low levels of these free radicals were observed with glufosinate treated on both biotypes, similar to the effect of the herbicide mixture on the PPO-resistant biotype. Proto levels increased up to 19 nmol g^{-1} in the susceptible biotype treated with glufosinate + lactofen. Small quantities (<1 nmol g^{-1}) were detected in the PPO-susceptible biotype treated with lactofen alone and in the PPO-resistant treated with the herbicide mixture. Proto did not accumulate with glufosinate in neither biotype. These results suggest that glufosinate enhances lactofen activity by protoporphyrin accumulation.

Effect of Glufosinate + PPO Inhibitor on Glufosinate-Resistant Soybean

Glufosinate (280 g ha^{-1}) caused more injury to glufosinate-susceptible (40%) than glufosinate-resistant (5%) soybean (Figure 4.4A). Low dose of saflufenacil (1 g ha^{-1}) provided less than 3% injury to both soybean varieties. The association between these two herbicides, however, caused high levels of injury to both glufosinate-resistant (68%) and glufosinate-susceptible (80%). These levels of injury provided by saflufenacil isolated or in association with

glufosinate are consistent with proto accumulation (Figure 4.4B). Proto levels were very low (<1 nmol g^{-1}) in plants treated with saflufenacil only. The addition of glufosinate to saflufenacil enhanced proto accumulation in both soybean types, especially glufosinate-susceptible.

For glufosinate-susceptible soybean, glufosinate levels increased over time due to the absence of herbicide metabolism (Figure 4.4C). In glufosinate-resistant soybean, glufosinate levels increased up to 4 HAT and decreased after that, probably due to their conversion into *N*-acetyl-L-phosphinothricin by herbicide metabolism. This peak of glufosinate levels at 4 HAT is enough to cause GS inhibition and a transient glutamate accumulation even for glufosinate-resistant soybeans (Figure 4.4D). These results support the hypothesis that glufosinate synergizes PPO-inhibitors by increasing glutamate levels and diversion into the chlorophyll biosynthesis pathway.

Field performance of Glufosinate + PPO Inhibitors on *Bassia scoparia*

Glufosinate (420 g ha^{-1}) provided 25% control on *B. scoparia* (Figure 4.5). Similar levels of control were observed for all PPO inhibitors with no statistical differences ($p<0.05$) among them, except for flumioxazin. The addition of PPO inhibitors to glufosinate significantly increased control levels compared to glufosinate only. These results support our findings obtained in the greenhouse and laboratory, demonstrating enhancement of activity with glufosinate + PPO inhibitors compared to the two herbicides applied individually.

PPO Inhibitors Can Overcome Lack of Control with Glufosinate Under Low Temperature and Low Humidity

Glufosinate does not provide good weed control in low temperature and humidity. Both glufosinate (280 g ha^{-1}) and glufosinate + saflufenacil (280 + 1 g ha^{-1}) provided 100% control of *A. palmeri* under 25 C and 70% humidity (Figure 4.6A). Less than 10% control was obtained

with saflufenacil under both conditions. Glufosinate efficacy decreased to 60% under 13 C and 30% humidity. The association between glufosinate and saflufenacil, however, still provided 100% control even under low temperature and relative humidity. These results suggest that low dose of saflufenacil may help glufosinate overcome the effect of low temperature and humidity.

DISCUSSION

Both glufosinate and PPO-inhibitors are fast-acting herbicides due to the accumulation of reactive oxygen species (ROS), and therefore, could sum each other's activity. The isobole analysis confirmed our hypothesis of synergism between glufosinate and saflufenacil (Figure 4.2C). However, our results show that the synergism is actually one sided. PPO inhibitors target the chlorophyll biosynthesis by inhibiting PPO, a key enzyme in the pathway (Figure 4.7). Inhibition of PPO leads to proto accumulation, the product of the reaction catalyzed by the enzyme (Duke et al., 1991). Cellular localization studies demonstrated that protoporphyrinogen, the substrate for PPO, leaks out of the chloroplast and is then converted to proto in the cytoplasm (Lee et al., 1993). The accumulation of proto is toxic because this molecule can absorb light energy and transfer to molecular oxygen, which generates ROS causing lipid peroxidation and cell death (Dayan and Duke, 2010).

The biochemical basis for the synergism observed with glufosinate + saflufenacil relies on enhanced accumulation of proto with the mixture (Figure 4.3). Therefore, glufosinate enhances the mechanism of action of PPO inhibitors but not the opposite. This is supported by the fact that PPO-resistant *A. tuberculatus* plants were not controlled by the herbicide mixture and showed similar injury levels to glufosinate sprayed alone (Figure 4.3). Glutamate, the substrate for glutamine synthetase (GS), does not seem to accumulate in response to glufosinate

110

treatment. Instead, the amino acid is used by other metabolic pathways including proline, arginine and chlorophyll biosynthesis (Figure 4.7). We also show that proline and arginine also accumulate after GS inhibition (Figure 4.1).

Glufosinate-resistant soybeans express the *pat* gene and metabolize glufosinate by adding an acetyl group to the herbicide molecule (Dröge et al., 1992; Strauch et al., 1988). Even though these plants are resistant to the herbicide, glufosinate uptake was greater than metabolism levels until 4 HAT. Thus, glufosinate concentration in the leaf tissue increases over the first four hours and causes some GS inhibition (Figure 4.4A). Consequently, glutamate levels also increase in the first four hours, which is probably enough to increase chlorophyll biosynthesis and proto accumulation in the presence of saflufenacil (Figure 4.4B). An unknown compound with the same mass as glutamate-1-semialdehyde and glutamate-4-semialdehyde accumulates at high levels in glufosinate-treated plants (Figure A4.3). These two metabolites are the products of the first step of the chlorophyll and proline/arginine biosynthesis, respectively, consistent with our hypothesis that glufosinate synergizes PPO inhibitor activity by a transient glutamate accumulation. Increased levels of proto accumulation lead to higher production of ROS and the catastrophic consequences of lipid peroxidation (Dayan and Duke, 2010).

In order to test the applicability of the herbicide mixture, we tested glufosinate in combination with different PPO inhibitors in the field. Tank mix with all PPO inhibitors provided increased levels of control compared to glufosinate alone (Figure 4.5). Higher efficacy on kochia was obtained with glufosinate + saflufenacil or glufosinate + pyraflufen-ethyl compared to other PPO inhibitors. Glufosinate efficacy is strongly affected by low temperature and low humidity (Coetzer et al., 2001; Kumaratilake and Preston, 2005). Here we show that the

lack of glufosinate efficacy under these conditions may be overcome with the addition of low dose of saflufenacil to the tank (Figure 4.6).

In conclusion, the association between glufosinate and PPO-inhibitors provides enhanced activity compared to the products applied individually. The increased herbicidal activity with the mixture is the result of proto accumulation in higher levels. Inhibition of glutamine synthetase by glufosinate leads to a transient accumulation of glutamate, the precursor for chlorophyll biosynthesis in plants. Inhibition of chlorophyll biosynthesis by PPO inhibitors leads to accumulation of proto, which is enhanced in the presence of glufosinate. The combination also works in the field and may help to overcome the lack of efficacy of glufosinate under low temperature and low humidity.

Table 4.1: Proportion of glufosinate and saflufenacil used for the isobole analysis. Five different dose response curves were obtained with different herbicide mixture proportions.

	0% A	25% A	50% A	75% A	100% A
			g ai ha^{-1}		
Glufosinate (A)	0	100	200	300	400
Saflufenacil (B)	20	14.4	9.6	4.8	0
8X	20	114.4	209.6	304.8	400
4X	10	57.2	104.8	152.4	200
2X	5	28.6	52.4	76.2	100
1X (ED$_{50}$)	2.5	14.3	26.2	38.1	50
1/2X	1.25	7.15	13.1	19.05	25
1/4X	0.625	3.575	6.55	9.525	12.5
1/8X	0.3125	1.7875	3.275	4.7625	6.25

1X: estimated dose for 50% reduction in dry weight (ED$_{50}$).
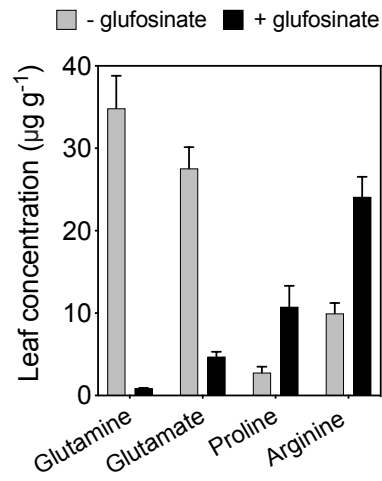
Figure 4.1: Levels of glutamine, glutamate, proline, and arginine in glufosinate-treated and - untreated Palmer amaranth plants.
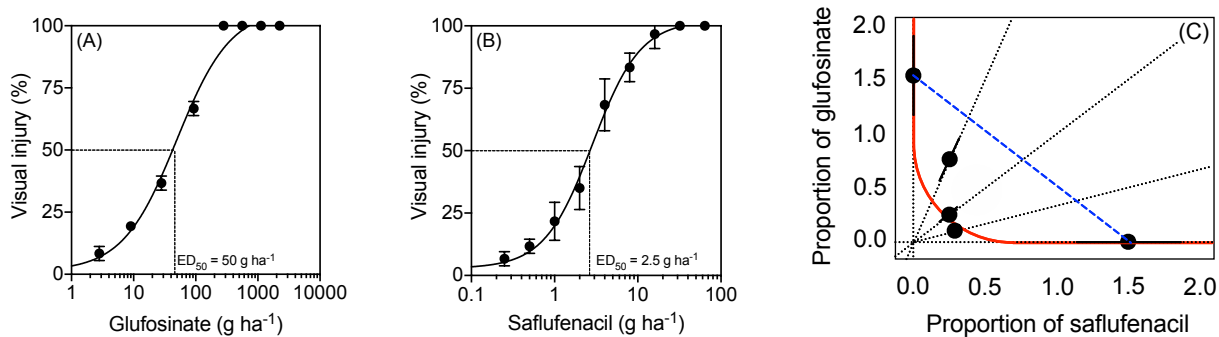
Figure 4.2: Enhanced herbicidal activity with glufosinate and saflufenacil. Dose response for glufosinate (A) and saflufenacil (B) in *Amaranthus palmeri*. Isobole analysis for the combination between the two herbicides in different proportions (C). If no synergism had been observed for the two compounds, data points were expected to fall into the blue dashed line (additive effect). The isobole curve in red indicates high levels of synergism between the two herbicides.
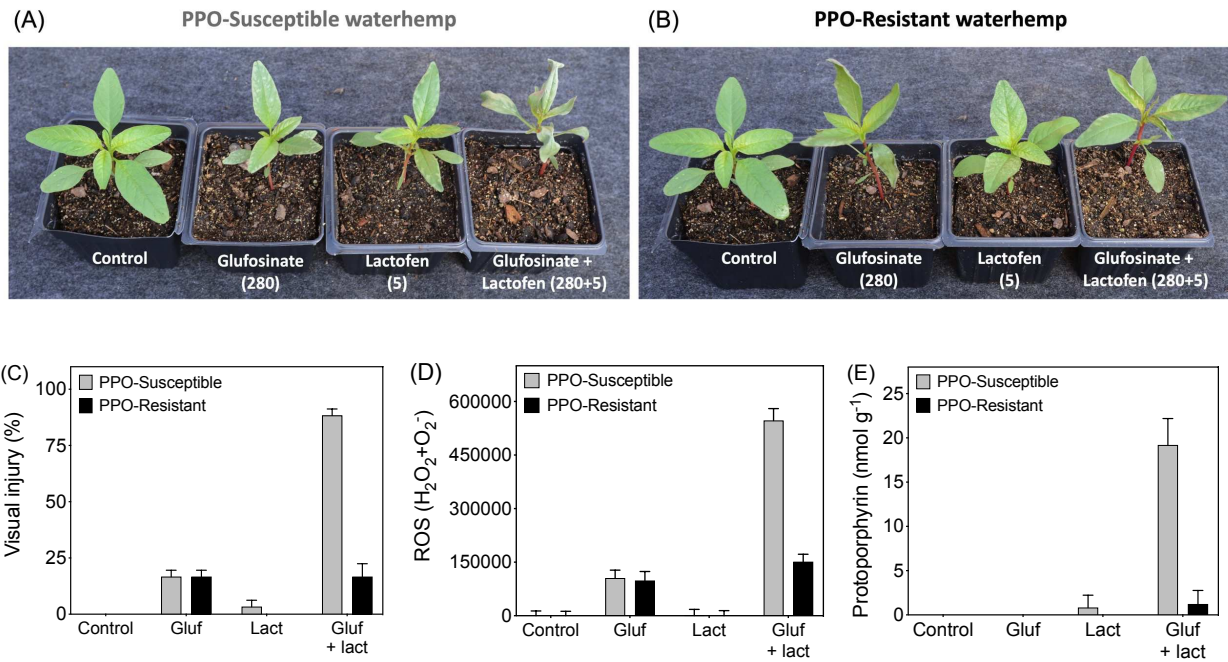
Figure 4.3: Response of waterhemp (*Amaranthus tuberculatus*) susceptible (A) and resistant (B) to protoporphyrinogen oxidase (PPO) inhibitors. Visual injury (C), reactive oxygen species - ROS (D) and protoporphyrin IX (E) in PPO-resistant and -susceptible waterhemp.
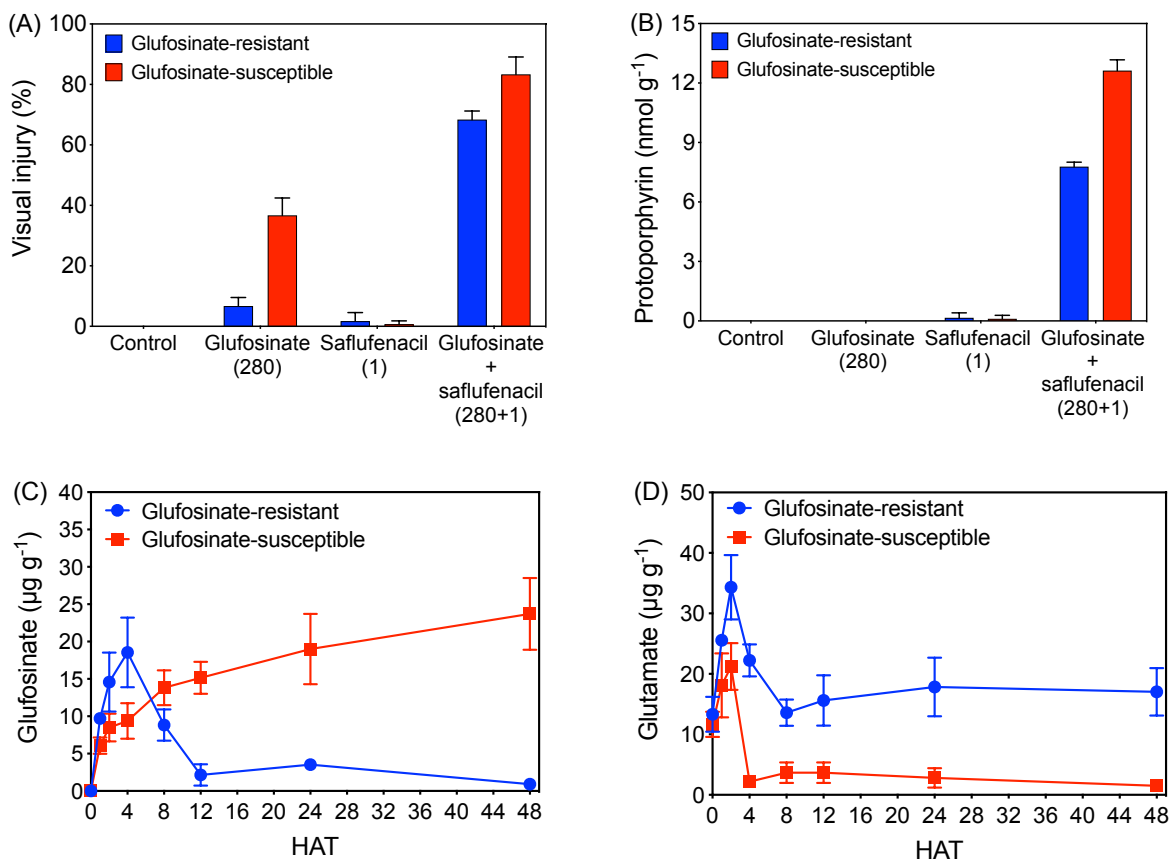
Figure 4.4: Visual injury (A), protoporphyrin IX accumulation (B), and glufosinate (C) and glutamate (D) levels in glufosinate-susceptible (red) and -resistant (blue) soybean.
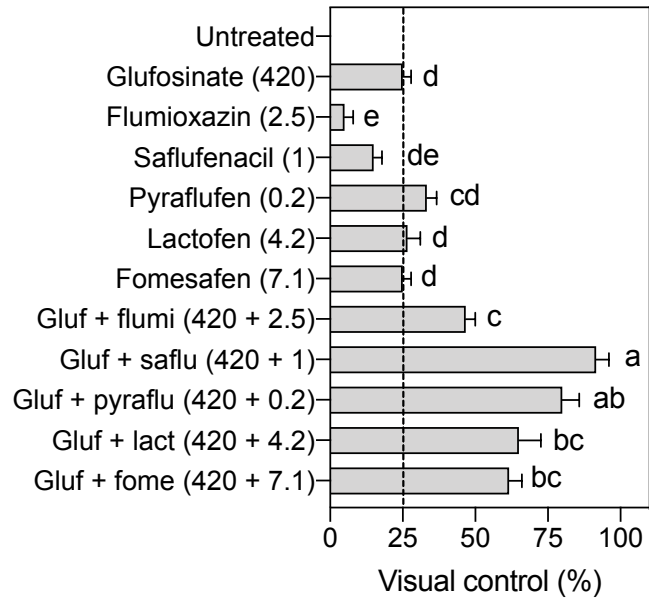
Figure 4.5: Field performance of glufosinate and PPO-inhibiting herbicides applied individually or in tank mix on kochia (*Bassia scoparia*). Means followed by the same letter do not differ by Tukey test ($p<0.05$).
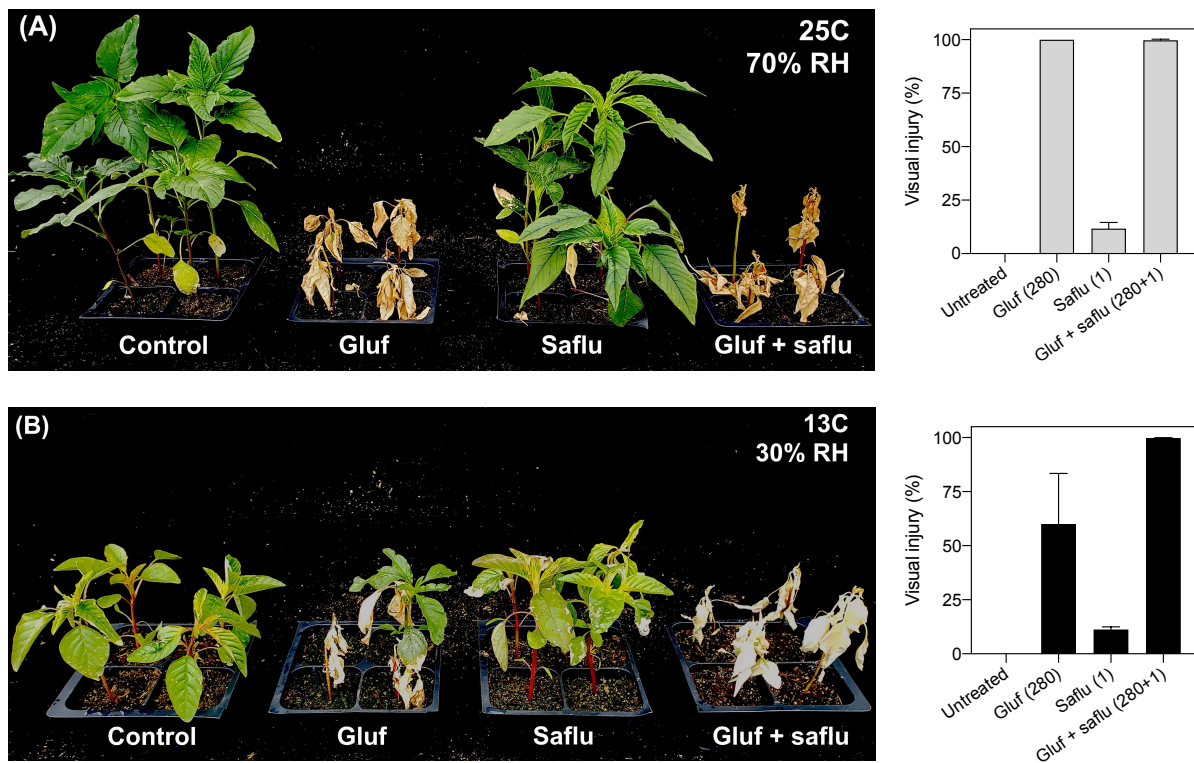
Figure 4.6: Saflufenacil (1 g ha^{-1}) can overcome the lack of efficacy by glufosinate (280 g ha^{-1}) under low temperature and humidity. Visual injury provided with glufosinate + saflufenacil compared to the two herbicides applied individually under high (A) and low (B) temperature and humidity.
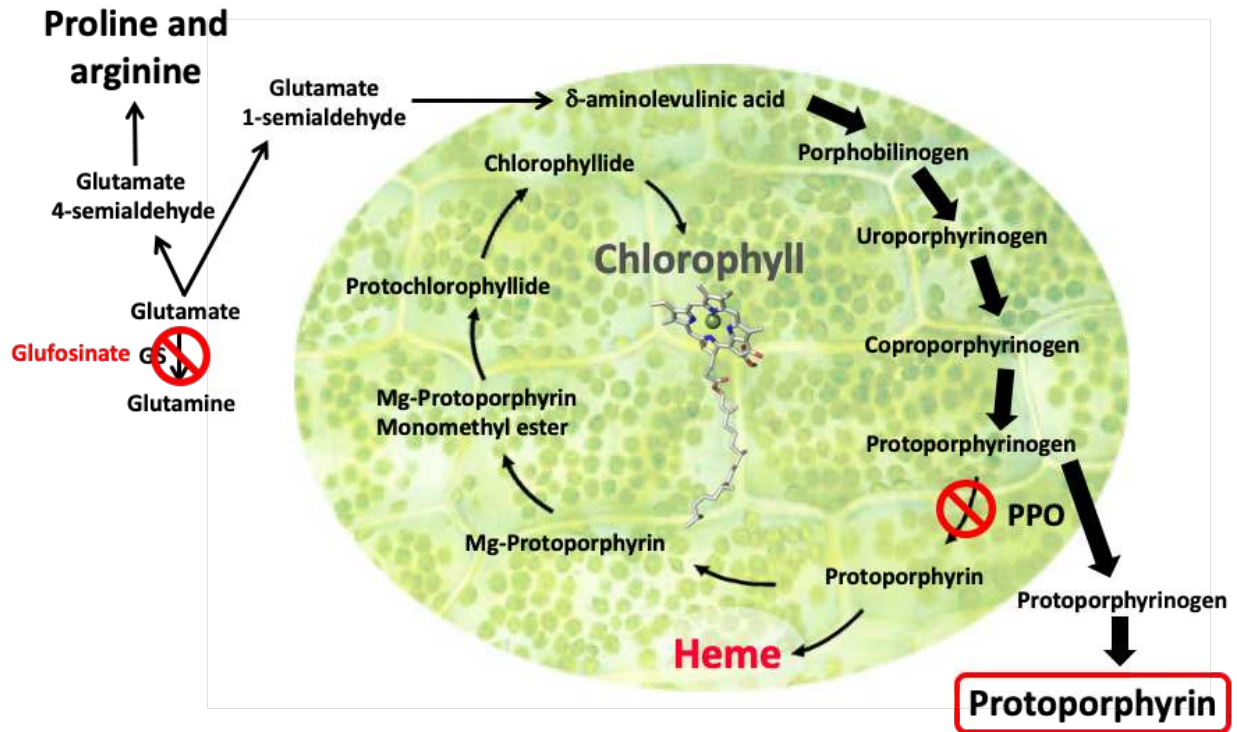
Figure 4.7: The fate of glutamate to the biosynthesis of glutamine, arginine, proline, and chlorophyll. Inhibition of glutamine synthetase (GS) diverge glutamate fate into arginine/proline and chlorophyll biosynthetic pathways. Protoporphyrinogen oxidase (PPO) is the target site for PPO-inhibiting herbicides.

References

Bayer, E.; Gugel, K.H.; Hägele, K.; Hagenmaier, H.; Jessipow, S.; König, W.A.; Zähner, H., 1972. Stoffwechselprodukte von mikroorganismen. 98. Mitteilung. Phosphinothricin und phosphinothricyl-alanyl-alanin. Helvetica Chimica Acta 55: 224-239.

Beriault, J.N.; Horsman, G.P.; Devine, M.D., 1999. Phloem transport of D,L-glufosinate and acetyl-L-glufosinate in glufosinate-resistant and -susceptible *Brassica napus*. Plant Physiology 121: 619-627.

Bernard, S.M.; Habash, D.Z., 2009. The importance of cytosolic glutamine synthetase in nitrogen assimilation and recycling. New Phytologist 182: 608-620.

Brunharo, C.A.C.G.; Takano, H.K.; Mallory-Smith, C.A.; Dayan, F.E.; Hanson, B.D., 2019. Role of glutamine synthetase isogenes and herbicide metabolism in the mechanism of resistance to glufosinate in *Lolium perenne* L. spp. *multiflorum* biotypes from Oregon. Journal of Agricultural and Food Chemistry 67: 8431-8440.

Busi, R.; Powles, S.B.; Beckie, H.J.; Renton, M., 2019. Rotations and mixtures of soil-applied herbicides delay resistance. Pest Management Science *in press*.

Coetzer, E.; Al-Khatib, K.; Loughin, T.M., 2001. Glufosinate efficacy, absorption, and translocation in amaranth as affected by relative humidity and temperature. Weed Science 49: 8-13.

Dayan, F.E.; Daga, P.R.; Duke, S.O.; Lee, R.M.; Tranel, P.J.; Doerksen, R.J., 2010. Biochemical and structural consequences of a glycine deletion in the α-8 helix of protoporphyrinogen oxidase. Biochimica et Biophysica Acta (BBA) - Proteins and Proteomics 1804: 1548-1556.

Dayan, F.E.; Duke, S.O. (2010) Protoporphyrinogen oxidase-inhibiting herbicides. In: Krieger R. (ed) Hayes' Handbook of Pesticide Toxicology (Third Edition), vol 1. 1 edn. Academic Press, New York, pp 1733-1751.

Dröge, W.; Broer, I.; Pühler, A., 1992. Transgenic plants containing the phosphinothricin-*N*-acetyltransferase gene metabolize the herbicide L-phosphinothricin (glufosinate) differently from untransformed plants. Planta 187: 142-151.

Duke, S.O.; Lydon, J.; Becerril, J.M.; Sherman, T.D.; Lehnen, L.P.; Matsumoto, H., 1991. Protoporphyrinogen oxidase-inhibiting herbicides. Weed Science 39: 465-473.

Forde, B.G.; Lea, P.J., 2007. Glutamate in plants: metabolism, regulation, and signalling. Journal of Experimental Botany 58: 2339-2358.

Heap, I.M. (2019) International survey of herbicide resistant weeds. <http://weedscience.org>. Accessed April 1st 2019

Jalaludin, A.; Ngim, J.; Bakar, B.H.; Alias, Z., 2010. Preliminary findings of potentially resistant goosegrass (*Eleusine indica*) to glufosinate-ammonium in Malaysia. Weed Biology and Management 10: 256-260.

Kumaratilake, A.R.; Preston, C., 2005. Low temperature reduces glufosinate activity and translocation in wild radish (*Raphanus raphanistrum*). Weed Science 53: 10-16.

Lee, H.J.; Duke, M.V.; Duke, S.O., 1993. Cellular localization of protoporphyrinogen-oxidizing activities of etiolated barley (*Hordeum vulgare* L.) leaves. Plant Physiology 102: 881-889.

Lermontova, I.; Kruse, E.; Mock, H.-P.; Grimm, B., 1997. Cloning and characterization of a plastidal and a mitochondrial isoform of tobacco protoporphyrinogen IX oxidase. Proceedings of the National Academy of Sciences, USA 94: 8895-8900.

Matringe, M.; Camadro, J.M.; Labbe, P.; Scalla, R., 1989. Protoporphyrinogen oxidase as a molecular target for diphenyl ether herbicides. Biochemical Journal 260: 231-235.

Moulin, M.; McCormac, A.C.; Terry, M.J.; Smith, A.G., 2008. Tetrapyrrole profiling in *Arabidopsis* seedlings reveals that retrograde plastid nuclear signaling is not due to Mg-protoporphyrin IX accumulation. Proceedings of the National Academy of Sciences, USA 105: 15178-15183.

Oliveira, I.C.; Brears, T.; Knight, T.J.; Clark, A.; Coruzzi, G.M., 2002. Overexpression of cytosolic glutamine synthetase. Relation to nitrogen, light, and photorespiration. Plant Physiology 129: 1170-1180.

Patzoldt, W.L.; Hager, A.G.; McCormick, J.S.; Tranel, P.J., 2006. A codon deletion confers resistance to herbicides inhibiting protoporphyrinogen oxidase. Proceedings of the National Academy of Sciences, USA 103: 12329-12334.

Sellers, B.A.; Smeda, R.J.; Johnson, W.G., 2003. Diurnal fluctuations and leaf angle reduce glufosinate efficacy. Weed Technology 17: 302-306.

Sørensen, H.; Cedergreen, N.; Skovgaard, I.M.; Streibig, J.C., 2007. An isobole-based statistical model and test for synergism/antagonism in binary mixture toxicity experiments. Environmental and Ecological Statistics 14: 383-397.

Steckel, G.J.; Wax, L.M.; Simmons, F.W.; Phillips, W.H., 1997. Glufosinate efficacy on annual weeds is influenced by rate and growth stage. Weed Technology 11: 484-488.

Strauch, E.; Wohlleben, W.; Pühler, A., 1988. Cloning of a phosphinothricin *N*-acetyltransferase gene from *Streptomyces viridochromogenes* Tü494 and its expression in *Streptomyces lividans* and *Escherichia coli*. Gene 63: 65-74.

Streibig, J.C.; Kudsk, P.; Jensen, J.E., 1998. A general joint action model for herbicide mixtures. Pesticide Science 53: 21-28.

Takano, H.K.; Beffa, R.; Preston, C.; Westra, P.; Dayan, F.E., 2019. Reactive oxygen species trigger the fast action of glufosinate. Planta 249: 1837–1849.

Winter, G.; Krömer, J.O., 2013. Fluxomics – connecting 'omics analysis and phenotypes. Environmental Microbiology 15: 1901-1916.

Zhang, J.; Hamill, A.S.; Weaver, S.E., 1995. Antagonism and synergism between herbicides: Trends from previous studies. Weed Technology 9: 86-90.

Appendix 1: Physiological Factors Affecting Glufosinate Uptake and Translocation
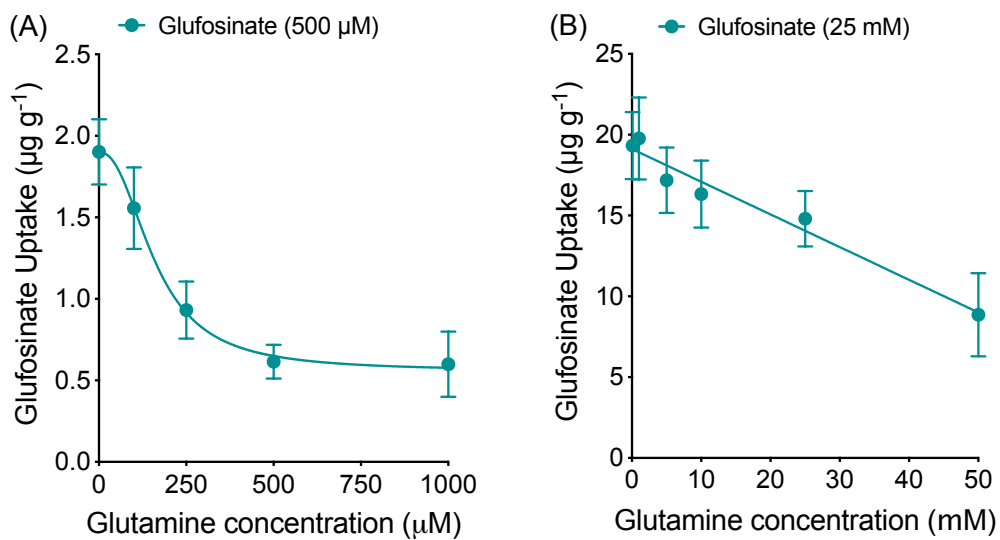
Figure A1.1: Glufosinate uptake in Palmer amaranth leaf discs over increasing µM concentrations of glutamine (A), or mM concentrations of glutamine (B). Data was pooled from two experiments with three replications (n = 6). *means are significantly different by t-test (p<0.05). Gln: glutamine.
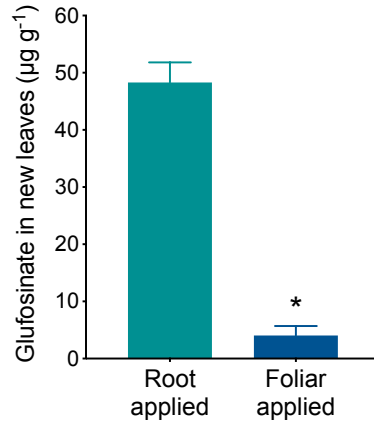
Figure A1.2: Glufosinate concentration in the apical meristem leaves when the herbicide was applied through roots or leaves. Root applied plants were hydroponically incubated in 20 mM glufosinate solution for one hour and then transferred to a solution of water. Foliar applied plants were sprayed with 560 g ha^{-1} glufosinate. Data was pooled from two experiments with three replications each (n = 6). *means are significantly different by t-test (p<0.05).
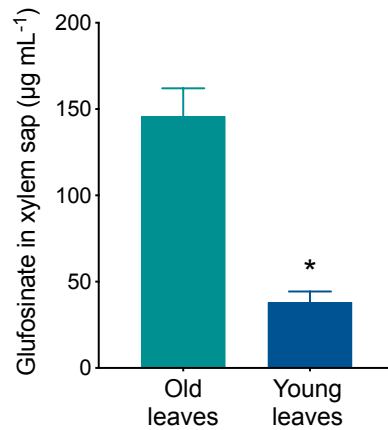
Figure A1.3: Glufosinate concentration in the xylem sap from old leaves compared to new leaves. Glufosinate was foliar applied at 560 g ha^{-1} and xylem sap was collected from old and new leaves using a pressure bomb. Data was pooled from two experiments with three replications each (n = 6). *means are significantly different by t-test (p<0.05).
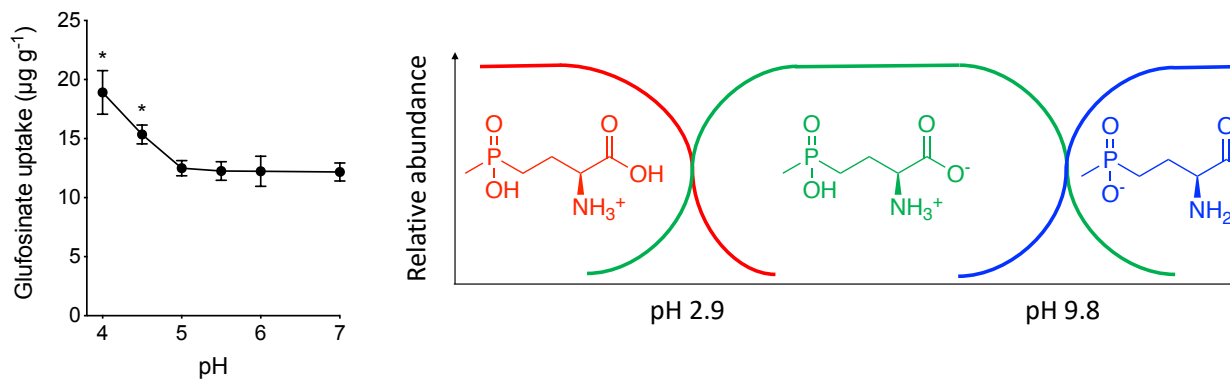
Figure A1.4: Effect of pH on glufosinate uptake in Palmer amaranth. Fifty 5-mm-diam leaf discs were incubated in 10 mM glufosinate solutions at different pH levels from 4 to 7 for 24 h. The solution pH was adjusted with hydrochloric acid before incubation. Data was pooled from two experiments with three replications ($n = 6$). *means are significantly different from control (pH 7) by t-test ($p < 0.05$).
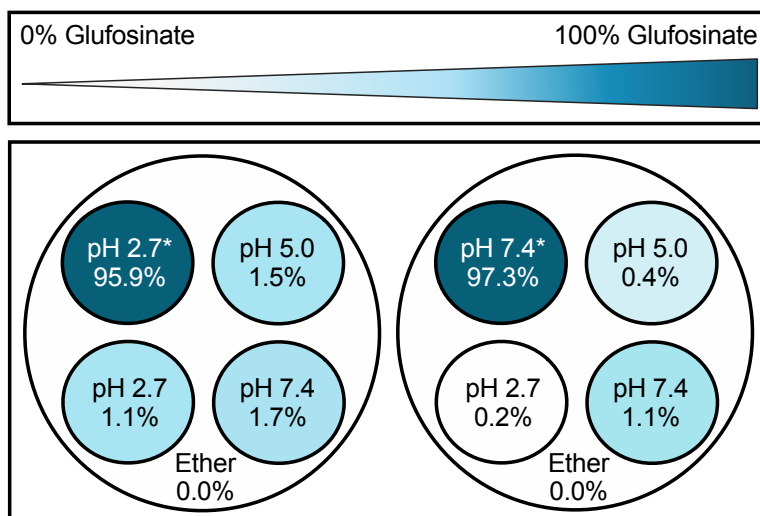
Figure A1.5. Glufosinate has very limited capacity to cross lipophilic membranes. An artificial apparatus to predict herbicide movement across lipophilic semipermeable membranes. Different cellular compartments with different pH levels are simulated floating on diethyl ether (lipophilic layer). Glufosinate is added to the membrane with an asterisk and let move for 24 h. Translocation is tracked by LCMS/MS.

Appendix 2: Reactive Oxygen Species Trigger the Fast Action of Glufosinate

Table A2.1: Dose for 50% response (I_{50}) in each experiment at 14 DAT for visual injury and 8 HAT for ammonia accumulation and GS activity. Glufosinate doses are represented in g ha^{-1} for visual phytotoxicity, ammonia accumulation and GS activity *in planta*, and in μM for ammonia accumulation in leaf discs and GS activity *in vitro*. GS, glutamine synthetase. Means of two experiments with three replications each (n=6) followed by standard error.

		Horseweed	Palmer amaranth	Kochia	Ryegrass	Johnsongrass
Visual injury		26.1±0.9	50.1±4.4	86.4±7.7	763.7±27.2	391.4±9.8
Ammonia[a]	Leaf disc	4.6±0.3	6.6±0.3	6.9±0.4	19.2±9.3	6.8±1.2
	in planta	14.0±0.4	30.6±1.0	55.9±2.2	468.7±38.5	123.2±5.4
GS activity[a]	*in vitro*	11.2±0.8	12.6±1.5	14.1±1.9	13.9±1.2	12.5±1.5
	in planta	61.1±5.3	58.3±4.4	151.8±33.9	1061.1±73.2	507.5±79.1

Table A2.2: Percentage of reduction (%) in glutamate, glutamine and carbon assimilation (CA) levels in five weed species after glufosinate treatment, relative to control. Control plants were sprayed with 2% ammonium sulfate, and treated plants were sprayed with 560 g ha^{-1} glufosinate + 2% ammonium sulfate. Data was calculated dividing the difference between treated and untreated means by the untreated mean. *, significant; [ns], not significant by t-test ($p<0.05$).

	Horseweed	Palmer amaranth	Kochia	Ryegrass	Johnsongrass
Glutamate	86±6.8*	82±5.3*	97±1.9*	49±5.2*	24±1.5*
Glutamine	99±4.0*	97±5.2*	98±4.8*	79±5.9*	94±4.3*
CA 30 min	40±3.0*	5±2.4*	18±2.5*	26±4.6*	1±0.5[ns]
CA 90 min	83±7.2*	38±1.4*	25±4.1*	61±4.5*	1±0.2[ns]
CA 150 min	98±2.8*	37±4.7*	55±7.9*	76±3.1*	2±0.6[ns]
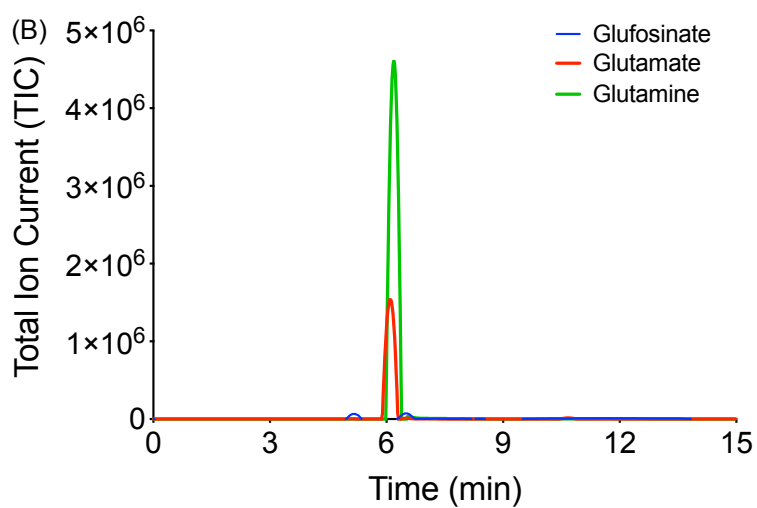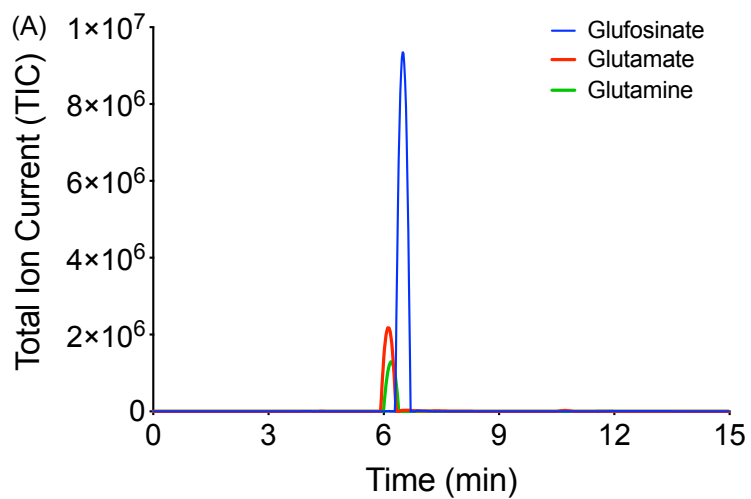
Figure A2.1: Total ion chromatogram from the LC-MS/MS analysis for glufosinate-treated (A) and glufosinate-untreated (B) Palmer amaranth plants.
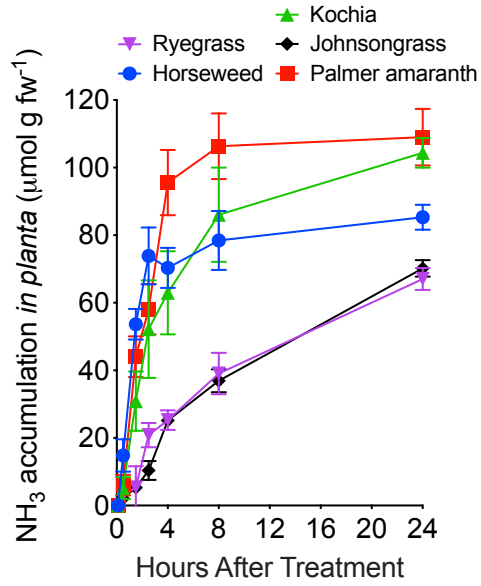
Figure A2.2: Ammonia accumulation overtime after glufosinate application in horseweed, Palmer amaranth, kochia, ryegrass and johnsongrass.
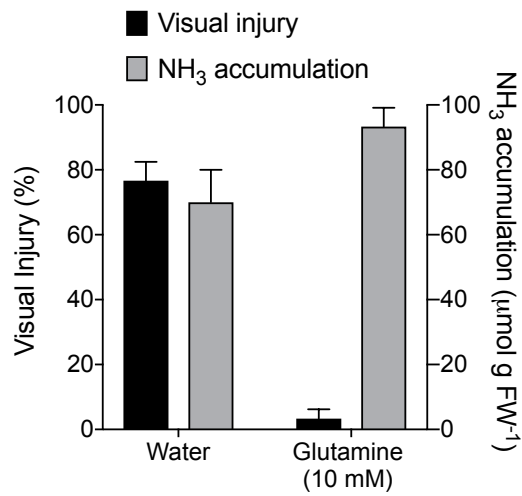
Figure A2.3: Visual injury and ammonia accumulation in glufosinate-treated plants growing in water or 10 mM glutamine at 8 HAT.

Appendix 3: The Sources of Reactive Oxygen Species in Glufosinate-Treated Plants
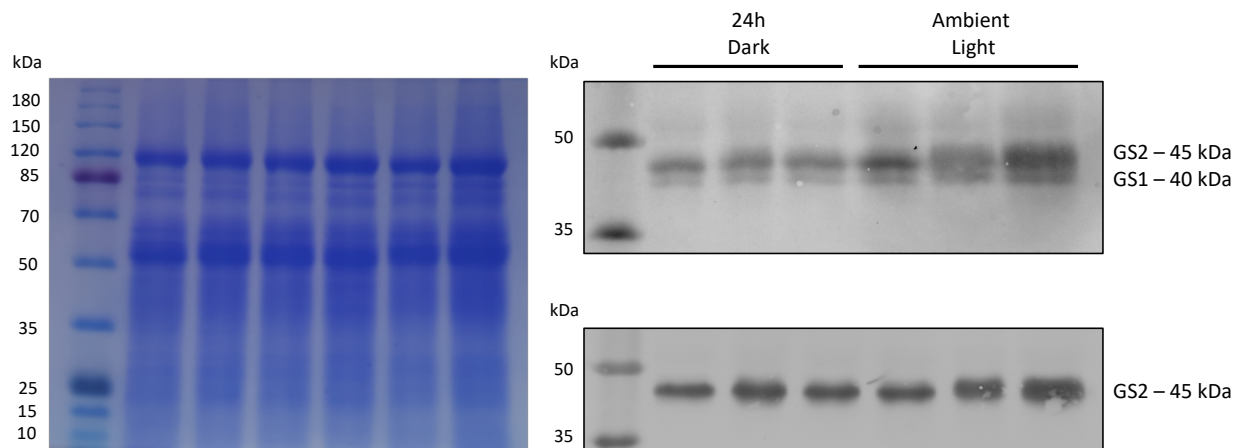
Figure A3.1: Commassie blue staining gel (on left) and western blot (on right) of protein extracts from Palmer amaranth (*A. palmeri*) plants under dark (24 h) or ambient light conditions.
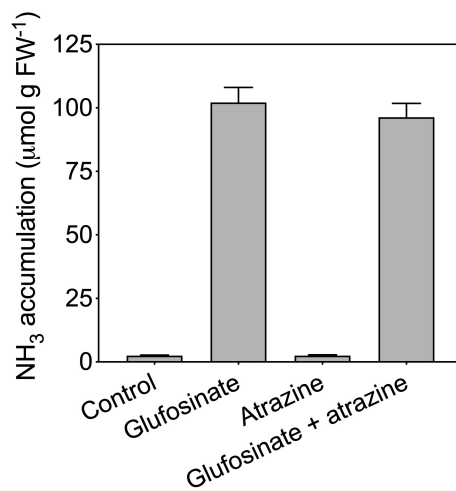
Figure A3.2: Ammonia accumulation in response to glufosinate (280 g ha^{-1}), atrazine (50 g ha^{-1}), and glufosinate + atrazine (280 + 50 g ha^{-1}). Measurements were taken at 8 HAT.
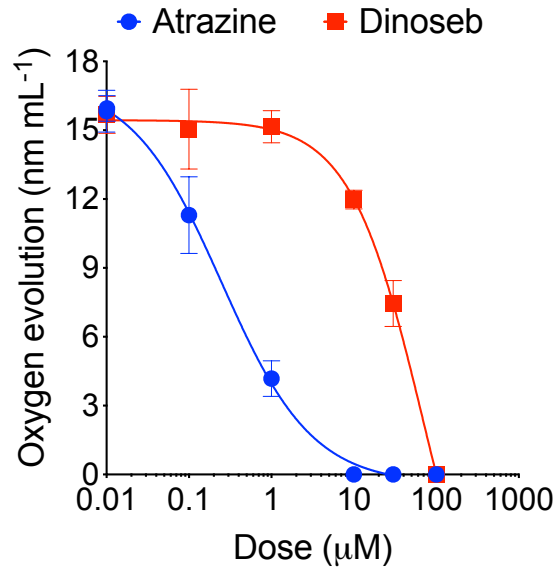
Figure A3.3: Oxygen evolution in Palmer amaranth (*A. palmeri*) chloroplasts over a dose response for atrazine and dinoseb.

Control   Water   10 mM Glycolate

Glufosinate (560 g ha^{-1})
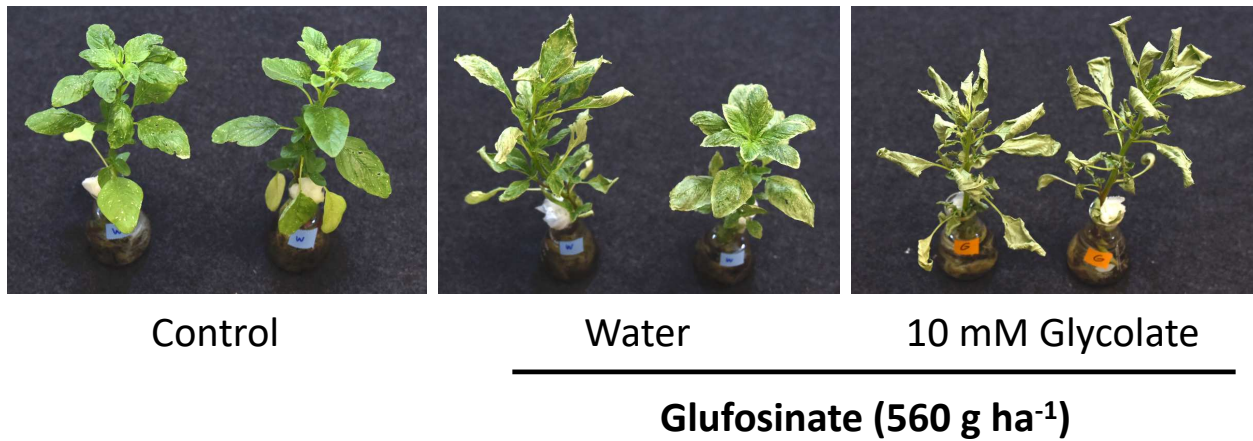
Figure A3.4: Visual after glufosinate application (560 g ha^{-1}) on Palmer amaranth (*A. palmeri*) growing in water or 10 mM glycolate solution.
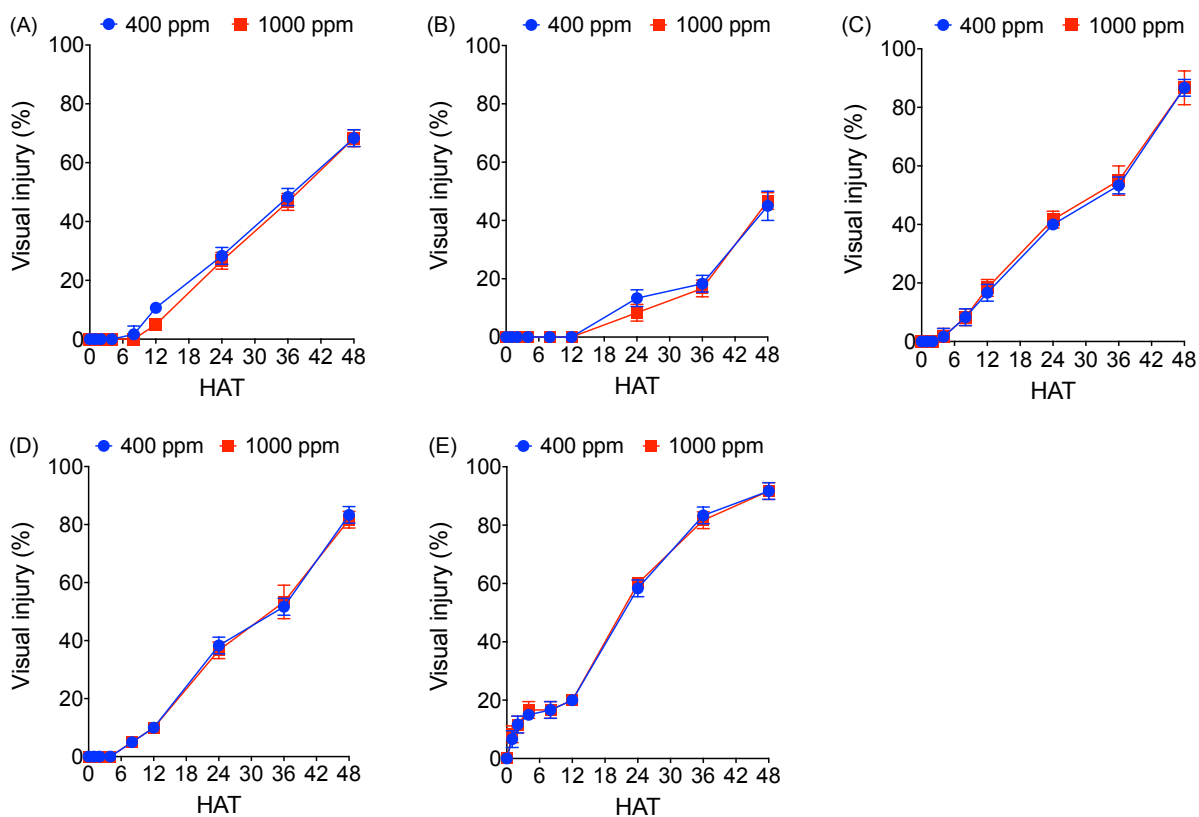
Figure A3.5: Visual injury (%) overtime after glufosinate application (560 g ha^{-1}) in whole-plant horseweed (A), ryegrass (B), kochia (C), johnsongrass (D), and Palmer amaranth (E) growing under ambient CO_2 levels (400 ppm) and enhanced CO_2 levels (1000 ppm).
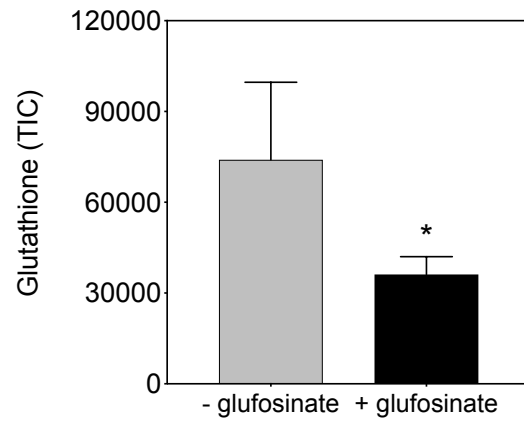
Figure A3.6: Levels of glutathione go down after glufosinate treatment (560 g ha^{-1}) in Palmer amaranth. *significant by t-test (p<0.05). TIC: total ion chromatogram.

Appendix 4: Glufosinate Enhances the Activity of Protoporphyrinogen Oxidase Inhibitors
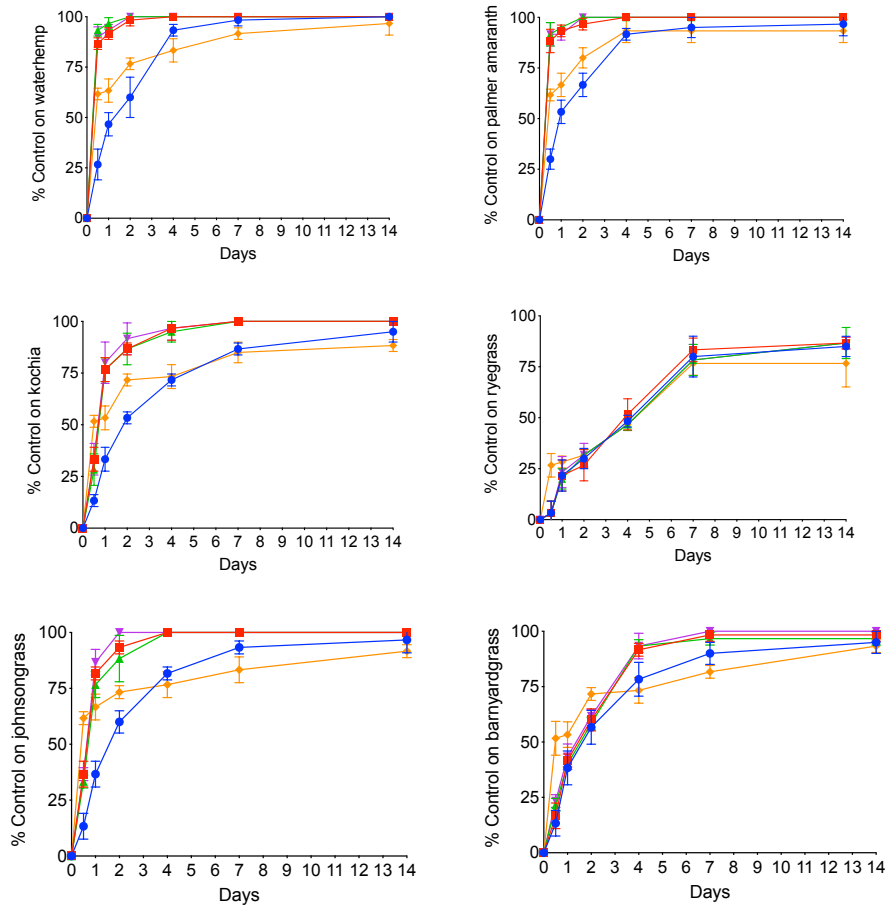
Figure A4.1. Visual control over time with (●) glufosinate (300 g ha^{-1}), (■) glufosinate + saflufenacil (300 + 1 g ha^{-1}), (▲) glufosinate + pyraflufen (300 + 0.17 g ha^{-1}), (▼) glufosinate + lactofen (300 + 5 g ha^{-1}), and (◆) glufosinate + paraquat (300 + 11) on waterhemp, Palmer amaranth, kochia, ryegrass, johnsongrass and barnyardgrass.
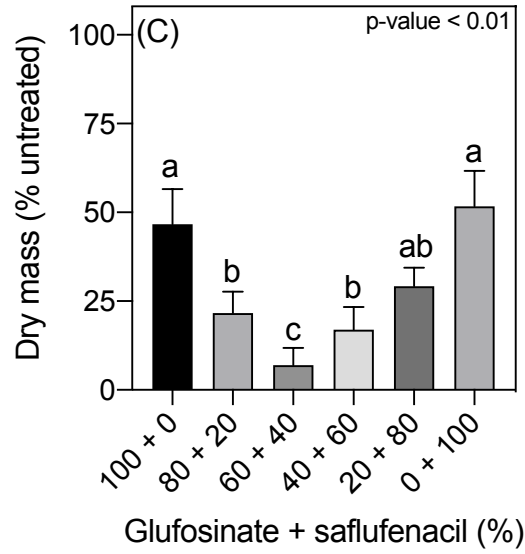
Figure A4.2. Dry mass of Palmer amaranth (*A. palmeri*) in response to different proportions of glufosinate (50 g ha^{-1}) and saflufenacil (2.5 g ha^{-1}) at 21 d after treatment. Means with the same letter do not differ by Tukey test ($p<0.05$).
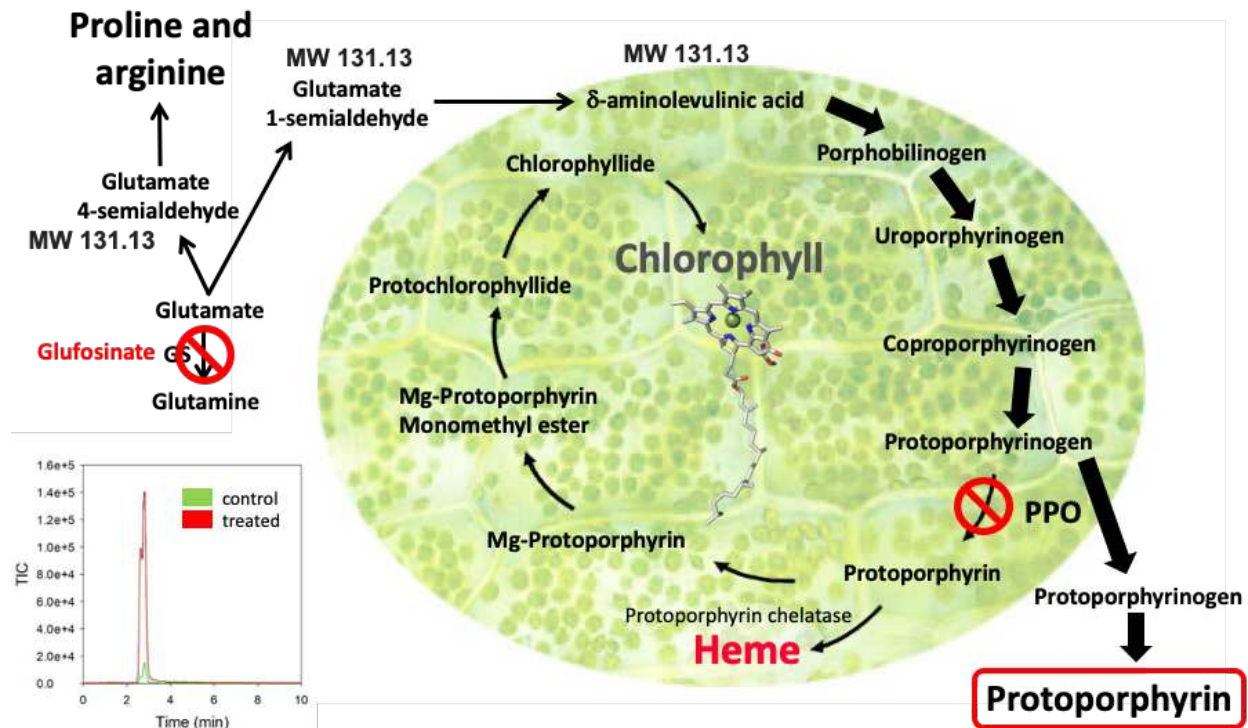
Figure A4.3. Inhibition of glutamine synthetase (GS) by glufosinate leads to proline and arginine accumulation and increased levels of protoporphyrin in the presence of protoporphyrinogen oxidase (PPO) inhibitors. An unknown compound with the same mass as aminolevulinic acid (131.13) accumulates in Palmer amaranth (*A. palmeri*) at 24 h after treatment with glufosinate (560 g ha^{-1}).
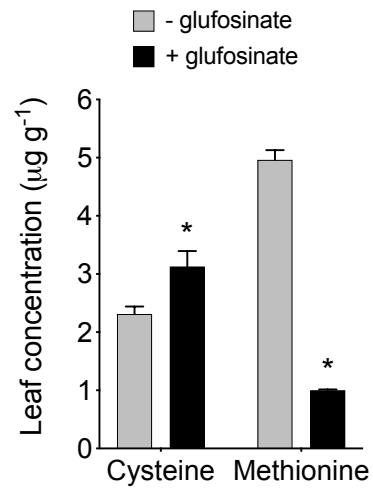
Figure A4.4: Levels of cysteine and methionine in glufosinate-treated and -untreated Palmer amaranth plants.